

Hypothalamic Glucocorticoid Action Regulates Lipid Metabolism

**by
Miguel Cardoso**

A thesis submitted in partial fulfillment of the requirements for the degree of

Master of Science

**Department of Physiology
University of Alberta**

© Miguel Cardoso, 2022

Abstract

Background: In metabolic disease states, such as diabetes and obesity, dyslipidemia is characterized by a dysregulation of lipid homeostasis, due in part to elevated triglyceride (TG)-rich very low-density lipoprotein (VLDL-TG) production and secretion by the liver. Further, these metabolic diseases are associated with excessive levels and/or actions of glucocorticoids (GCs), which may contribute to dyslipidemia. The dysregulation of VLDL-TG secretion, and particularly its hypersecretion in metabolic disease states, remains largely unknown. The brain, including the medial basal hypothalamus (MBH), senses circulating nutrients and hormones to regulate lipid metabolism and VLDL-TG secretion. Whereas the peripheral effects of GCs are well known, including the direct effect of GCs to stimulate hepatic VLDL-TG secretion, the central effects of GCs acting in the MBH to regulate lipid metabolism is unknown. Given the link between GCs and metabolic disease states, that GCs act in the periphery to effect lipid metabolism, and the fact that the brain is a hormone-responsive liporegulatory site, the aim of this study was to explore if GCs can act directly in the MBH to regulate liver VLDL-TG secretion to better understand mechanisms by which blood lipid levels may be lowered in those with dyslipidemia.

Hypothesis: (1) GCs act via the glucocorticoid receptors (GRs) in the MBH to modulate liver lipid homeostasis by increasing plasma TG and hepatic VLDL-TG secretion; (2) inhibition of MBH GC action (by blocking MBH GRs or downstream mediators of GC-GR action specifically within the MBH), will improve liver lipid metabolism in diet-induced hyperlipidemic rats.

Methods: Male Sprague Dawley rats underwent stereotaxic MBH bilateral cannulation and vascular catheterization to enable direct-continuous MBH infusion, intravenous infusion, and arterial blood sampling. Following MBH cannulation, a subset of rats received either a MBH

specific injection of a lentivirus containing a GRshRNA, to act as a GR knockdown, a heat shock protein 90 sh RNA (Hsp90 shRNA), to act as an Hsp90 knockdown, or a mismatch (MM) sequence to act as a control. A subset of rats were subjected to a 3-day high fat diet (HFD), as an acute model of diet-induced obesity. Following a 10-hour fast, free-moving, conscious rats were subjected to a direct, and continuous MBH infusion of a specific brain treatment (dexamethasone (DEX), as a synthetic GC, mifepristone, as a GR inhibitor, or a Hsp90 inhibitor) or saline paired with an intravenous poloxamer injection to inhibit lipoprotein lipase. Plasma samples were collected and TGs, glucose, and free fatty acids (FFAs) were quantified. Following experimentation rats were euthanized and brain and liver samples were collected for gene expression and protein level analysis.

Results: Direct MBH GC infusion, in the form of DEX, increased plasma VLDL-TG secretion compared to MBH vehicle-infused controls, and this effect was negated via the inhibition of the MBH GR. These changes occurred independent of changes in plasma apolipoprotein B (apoB)-48, apoB-100, glucose, FFAs, hepatic expression of *Srebf1c*, *Scd1*, *Dgat1/2*, *Fasn*, *Lpin2*, *Cideb*, *Nr1h3*, *Nr1h2*, *Arfl*, *Cpt1a*, *Ppara*, or hepatic protein levels of MTP, P-ACC/ACC, DGAT1, Arfl, or FAS relative to controls. In HFD-fed rats, which are characterized by elevated basal plasma GC and TGs, the chronic (13-day) inhibition of the GR via GRshRNA or the inhibition of Hsp90, in the MBH, significantly decreased plasma TGs and TG-rich lipoprotein secretion. The chronic (13-day) inhibition of Hsp90 in the MBH, using Hsp90 shRNA, in the 3-day HFD fed rats was associated with lower basal plasma FFAs, and lower plasma TG:apoB-100 ratio following experimentation compared to HFD controls.

Conclusion: The results of these studies provide evidence that MBH GC action alters fasting lipid metabolism, by increasing TG-rich lipoprotein secretion. Further, we show for the first time

that inhibition of GRs in the MBH negates diet-induced hypertriglyceridemia. The significance of this data is that it suggests that GC action in the hypothalamus may contribute to TG-rich lipoprotein overproduction and dysregulation of lipid homeostasis in diet-induced hypertriglyceridemia.

Preface

This thesis is an original work by Miguel Cardoso. The research project, of which this thesis is a part of, received research ethics approval from the University of Alberta Research Ethics Board, Project Name “CNS regulation of metabolic homeostasis”, number 1604. This project was funded by the Canadian Institute of Health Research (CIHR), the Natural Sciences Research Council of Canada (NSERC), and Diabetes Canada Scholar Award. Miguel Cardoso was funded the Faculty of Medicine & Dentistry (FOMD) 75th anniversary award for the final year of this project, as well as by the Graduate Students’ Association (GSA) and the Department of Physiology from the University of Alberta for conference travel funding.

In Chapter 1 of this thesis, in section ‘1.5. Central/ brain metabolic effects of glucocorticoid action’, Miguel Cardoso is a co-author of two articles published by Emilie Beaulieu-Bayne (EBB), who was a previous Master of Science student at the Yue laboratory. Miguel Cardoso assisted with general animal maintenance and care, as well as harvest plasma samples and tissue collection. Additionally, Miguel Cardoso has published an abstract from work from this project, which was not referenced in this thesis.

Lastly, in Chapter 1 of this thesis, in section ‘2.9. Liver mRNA expression’, the protocol and practices (lab equipment use and assistance with interpretation of data) of the quantitative real time polymerase chain reaction (qRT-PCR) was provided by Mr. Randal Nelson, a lab technician from the Dr. Richard Lehner laboratory at the university, as part of a collaboration with the Dr. Lehner and Dr. Yue laboratories.

Acknowledgements

I would firstly like to thank my supervisor, Dr. Jessica Yue, for taking me on for this project, her continuous patience, the opportunities she provided me with, and guidance during my graduate studies. To Bryan Lum, our lab manager, thank you for performing all the MBH cannulation surgeries and vascular catheterization surgeries (with the help of Dr. Yue). Additionally to Carrie-Lynn Soltys, our lab technician for the first two years of my studies, thank you for teaching all the molecular work you performed as well as all the molecular work you had taught me. To all the current and past undergraduate Yue lab members, thank you for all your help, teaching experience, and for creating a friendly working environment. A special thank you to Mark Wang, Eyram Asem, Emily J. Ling, and Hongju (Jennifer) Lee for being directly involved in this thesis project. Additionally, to the past and present graduate students, especially to Emilie Beaulieu-Bayne (EBB) and Hellen Veida da Silva, for not only putting up with me at the lab, but being my friend. Furthermore, a special thank you to EBB for also being directly involved in this project. Thank you to Dr. Robin Clugston, for welcoming me into your laboratory to use some of your lab equipment. I'd also like to thank my committee members, Dr. Donna Vine and Dr. Richard Lehner, for their contributions and time spent being part of this process. A special thank you to Dr. Lehner and his laboratory, especially Randal Nelson, for helping with my qRT-PCR work, I greatly appreciate it. To my friends, especially Samantha Cima, thank you for your support, understanding, countless long nights, and all the adventures we have been through during this experience. To my biggest supporters, my family, especially my parents, for helping me through this experience, endless love and support, and always being a phone call away. I cannot thank you enough. I could not have done any of this without the love and support of my friends and family. Lastly, I'd like to thank the rats, without them, none of this would be possible.

Table of contents

Chapter 1: Introduction	1
1.1. Obesity, Diabetes, and Insulin Resistance.....	2
1.1.1. Metabolic Characteristics of Obesity and Insulin Resistance.....	2
1.2. Lipids	3
1.2.1. Digestion of dietary lipids in the intestine.....	3
1.2.2. <i>De novo</i> lipogenesis	4
1.2.3. Triglyceride biosynthesis.....	6
1.2.3.1. The monoglyceride pathway.....	6
1.2.3.2. The glycerol-3-phosphate pathway	7
1.2.4. Triglyceride-rich lipoproteins: Chylomicrons and very-low density lipoproteins.....	7
1.2.4.1. Triglyceride-rich very-low density lipoprotein formation and secretion ...	8
1.2.5. Hepatic fatty acid β oxidation	9
1.2.6. Lipid storage and lipolysis	9
1.3. Glucocorticoids.....	11
1.3.1. Glucocorticoid synthesis and secretion	12
1.3.1.1. Glucocorticoid receptor and intracellular action	12
1.3.2. Glucocorticoid regulation: The hypothalamic-pituitary-adrenal axis.....	14
1.3.3. Non-metabolic peripheral actions of glucocorticoids	16
1.3.4. Metabolic actions of peripheral glucocorticoids	17
1.4. Hypothalamic sensing of peripheral nutrients and hormones and regulation of lipid metabolism	18
1.4.1. Nutrient sensing in the hypothalamus	19
1.4.2. Hormone sensing in the hypothalamus	20

1.5.	Central/ brain metabolic effects of glucocorticoid action.....	21
1.6.	Aim, hypothesis, and objectives	22
1.6.1.	Objective 1: To assess GC action and delineate GR requirements in the MBH in regulating hepatic VLDL-TG secretion in healthy rats.....	23
1.6.2.	Objective 2: To assess blocking GC action and delineate GR requirements in the MBH in regulating VLDL-TG secretion in diet-induced hyperlipidemic rats.....	24
Chapter 2: Methods		27
2.1.	Animal care, maintenance, and surgical procedures	28
2.1.1.	MBH stereotaxic bilateral cannulation surgery.....	28
2.1.2.	Vascular catheterization.....	29
2.2.	<i>In vivo</i> VLDL-TG secretion studies	29
2.3.	Plasma TG assay.....	31
2.4.	Hepatic TG content	33
2.5.	Plasma FFA assay.....	34
2.6.	Western blotting	35
2.6.1.	Tissue western blotting.....	35
2.6.2.	Plasma apoB western blotting.....	36
2.7.	Liver mRNA expression analysis.....	38
2.7.1.	RNA extraction	38
2.7.2.	cDNA synthesis.....	39
2.7.3.	qRT-PCR	39
2.8.	Statistical analysis	41
Chapter 3: Results.....		42
3.1.	Acute glucocorticoids act on glucocorticoid receptors in the medial basal hypothalamus to stimulate hepatic triglyceride secretion in regular chow-fed rats.....	43

3.1.1. Investigation of hepatic mechanisms involved in the medial basal hypothalamic glucocorticoid mediated increase in hepatic triglyceride-rich very-low density lipoprotein secretion.....	47
3.2. Medial basal hypothalamus-targeted glucocorticoid receptor knockdown negates the effects of medial basal hypothalamic glucocorticoid-stimulated hepatic triglyceride secretion in regular chow-fed rats	53
3.3. Medial basal hypothalamic heat shock protein 90 is required for medial basal hypothalamic glucocorticoid stimulation of triglyceride secretion in regular chow-fed rats	55
3.4. Three-day high fat diet feeding alters the metabolic profile independent of changes in body weight.....	57
3.5. Three-day high fat diet feeding elevates plasma triglycerides to a similar extent of glucocorticoids acting in the medial basal hypothalamus alone	60
3.6. Chronic inhibition of the medial basal hypothalamic glucocorticoid receptor lowers hepatic triglyceride-rich very low-density lipoprotein secretion in 3-day high fat diet fed rats	62
3.7. Both acute and pharmacological inhibition of heat shock protein 90 in the medial basal hypothalamus negates the hyperlipidemic effects of a 3-day high fat diet	68
Chapter 4: Discussion	73
4.1. Significance of results.....	74
4.2. Discussion of results	75
4.2.1. Glucocorticoids can act on glucocorticoid receptors in the medial basal hypothalamus to modulate liver lipid homeostasis in regular-chow fed rats.	75
4.2.2. Comparison of the physiological effects of a 3-day high fat diet feeding regimen to regular chow feeding with acute hypothalamic glucocorticoid infusions. ..	78
4.2.3. Inhibition of the glucocorticoid receptor, specifically within the medial basal hypothalamus, lowers plasma triglycerides in diet induced hyperlipidemic rodents. ..	81
4.3. Future directions	84

4.3.1. Further delineating mechanisms that underlie the lipostimulatory effects of glucocorticoid action in the medial basal hypothalamus.	84
4.3.2. Neural populations in hypothalamus that may be modulated by glucocorticoids	85
4.3.3. Brain-liver neurocircuitry.....	86
4.4. Limitations of the study.....	86
4.4.1. Medial basal hypothalamic glucocorticoid action was only investigated under fasted conditions	86
4.4.2. Limitations of pharmaceuticals used for medial basal hypothalamic treatments.....	87
4.4.3. High fat diet feeding studies.....	88
4.4.4. Apolipoprotein B assessments.....	89
4.4.5. Measurements of brain physiological concentrations of corticosterone	89
4.5. Conclusion.....	90
References	92

List of figures

Figure 1.1- Overview of hepatic lipid metabolism..	10
Figure 1.2- The glucocorticoid- glucocorticoid receptor complex..	13
Figure 1.3- The hypothalamic-pituitary-adrenal axis..	15
Figure 1.4- Schematic representation of overall working hypothesis.	26
Figure 2.1- Animal protocol and VLDL-TG secretion experiment.....	31
Figure 3.1- Acute glucocorticoid action in the medial basal hypothalamus stimulates hepatic plasma triglycerides and very-low density lipoprotein secretion in regular-chow fed rats.....	44
Figure 3.2- Acute glucocorticoid action in the medial basal hypothalamus does not alter hepatic triglyceride content in regular-chow fed rats.	45
Figure 3.3- Medial basal hypothalamic glucocorticoid induced triglyceride-rich, very-low density lipoprotein secretion occurs independent of changes in plasma free fatty acids and plasma glucose.....	46
Figure 3.4- Increased very-low density lipoprotein secretion was not due to changes in hepatic protein levels.	48
Figure 3.5- Medial basal hypothalamic glucocorticoid receptor activation does not alter hepatic <i>Srebf1c</i> , <i>Nr1h3</i> , or <i>Nr1h2</i> mRNA expression..	49
Figure 3.6- Changes in triglyceride-rich very-low density lipoprotein secretion associated with medial basal hypothalamic glucocorticoid action occurs independently of changes in hepatic lipogenic gene expression.....	50
Figure 3.7- Medial basal hypothalamic glucocorticoid induced increase of triglyceride-rich very-low density lipoprotein occurs independently from changes in liver mRNA expression of genes involved in fatty acid-oxidation.....	51
Figure 3.8- Plasma apolipoprotein B remained unchanged after medial basal hypothalamic glucocorticoid receptor activation relative to vehicle.....	52
Figure 3.9- Representative western blot confirming knockdown of glucocorticoid receptor in the medial basal hypothalamus.	53
Figure 3.10- Medial basal hypothalamic targeted glucocorticoid receptor knockdown negates the effects of medial basal hypothalamic stimulation in regular-chow fed rats.....	54

Figure 3.11- Acute heat shock protein 90 inhibition in the medial basal hypothalamus negates the effects of medial basal hypothalamic glucocorticoid stimulation in regular-chow fed rats.....	55
Figure 3.12- Genetic knockdown of heat shock protein 90 in the medial basal hypothalamus lowers the lipostimulatory effect of dexamethasone in regular-chow fed rats.....	57
Figure 3.13- Physiological effects of a 3-day high fat diet compared to regular chow.	58
Figure 3.14- Three-day high fat feeding elevates plasma triglycerides and triglyceride-rich very-low density lipoprotein secretion.	59
Figure 3.15- Three-day high fat diet fed rats have elevated basal plasma apolipoprotein B levels	60
Figure 3.16- Three-day high fat feeding elevates plasma triglycerides and triglyceride rich very-low density lipoprotein secretion to a similar extent as a direct medial basal hypothalamic infusion of dexamethasone rats fed a regular-chow diet.....	61
Figure 3.17- Three-day high fat feeding does not alter hepatic FAS, P-ACC:ACC, MTP, or DGAT1.	62
Figure 3.18- Chronic medial basal hypothalamus targeted glucocorticoid receptor knockdown lowers hepatic triglyceride-rich very-low density lipoprotein production and secretion in 3-day high fat diet fed rats.....	63
Figure 3.19- Chronic medial basal hypothalamus targeted glucocorticoid receptor knockdown lowers hepatic triglyceride content in 3-day high fat diet fed rats.	64
Figure 3.20- Decreased plasma triglycerides as a result of chronic medial basal hypothalamic glucocorticoid receptor inhibition in high fat diet fed rats occurred independently of changes in plasma substrates.	65
Figure 3.21- Medial basal hypothalamic targeted glucocorticoid knockdown did not change plasma apolipoprotein B in high fat diet fed rats.	66
Figure 3.22- Medial basal hypothalamic glucocorticoid receptor knockdown does not change hepatic FAS, MTP, or P-ACC: ACC protein levels.....	67
Figure 3.23- Acute inhibition of heat shock protein 90 in the medial basal hypothalamus lowers triglyceride-rich very-low density lipoprotein secretion in diet-induced hyperlipidemic rats.	68

Figure 3.24- Chronic knockdown of heat shock protein 90 in the medial basal hypothalamus lowers triglyceride-rich, very-low density lipoprotein secretion in rats fed a 3-day high fat diet.	69
Figure 3.25- The decrease in triglyceride-rich very-low density lipoprotein secretion in diet-induced hyperlipidemic rats subjected to acute inhibition of heat shock protein 90 in the medial basal occurs independently of changes in plasma free fatty acids and plasma glucose.	70
Figure 3.26- Chronic inhibition of medial basal hypothalamic heat shock protein 90 is associated with significantly lower plasma free fatty acids but not plasma glucose in rats fed a 3-day high fat diet.	71
Figure 3.27- Chronic inhibition of heat shock protein 90 in the medial basal hypothalamus does not alter hepatic MTP, FAS, or P-ACC: ACC protein levels in rats fed a 3-day high fat diet.	72

List of tables

Table 2.1- Primary antibodies used for western blotting.....	37
Table 2.2- Secondary antibodies used for western blotting	38
Table 2.3-TaqMan™ gene and probes used for gene expression analysis.....	40
Table 2.4-Custom primer sequences for gene expression analysis.....	40

List of abbreviations

11 β -HSD 1/2- 11 β -hydroxysteroid dehydrogenase 1/2

2-MG- 2-monoglyceride

ACC- Acetyl-CoA carboxylase

ACL- ATP-citrate lyase

ACTH- Adrenocorticotrophic hormone

AGPAT- Acylglycerol-phosphate acyltransferase

AgRP- Agouti-related protein

AMPK- AMP-activated protein kinase

ApoB-48/100- Apolipoprotein B-48/100

ARC- Arcuate nucleus

Arf1- ADP-ribosylation factor 1

ChREBP- Carbohydrate responsive element binding protein

CideB- Cell death-inducing DFF4-like effector B

CORT- Corticosterone

CPT-1 α - Carnitine palmitoyltransferase 1 α

CRH- Corticotrophin-releasing hormone

DEX- Dexamethasone

DG- Diglyceride

DGAT 1/2- Diacylglycerol acyltransferase 1/2

DHAP- Dihydroxyacetone- 3-phosphate

Elovl5- Elongases

FAS- Fatty acid synthase

FFA- Free fatty acids

GC- Glucocorticoid

GR- Glucocorticoid receptor

GRshRNA- Glucocorticoid receptor short hairpin RNA (GR knockdown)

GLUT4- Glucose transporter 4

GPAT- Glycerol-3-phosphate acyltransferase

GSK4- Glycogen synthase kinase 3

HFD- High-fat diet

HPA- Hypothalamic-pituitary-adrenal

Hsp90- Heat-shock protein 90

Hsp90i- Heat-shock protein 90 inhibitor (17-AAG)

Hsp90 shRNA- Heat-shock protein 90 short hairpin RNA (Hsp90 knockdown)

ICV- Intracerebroventricular

i.v.- Intravenous

LPA- Lysophosphatidate

Lpin2- Lipin-2

LPL- Lipoprotein lipase

LV- Lentivirus

LXR α/β - Liver x receptor α/β (gene names *Nr1h3* and *Nr1h2* respectively)

MBH- Medial basal hypothalamus

MGAT- Monoglyceride acyltransferase

MIF- Mifepristone

MM- Mismatch

MR- Mineralocorticoid receptor

MTP- Microsomal triglyceride transfer protein

NPY- Neuropeptide Y

PA- Phosphatidic acid

P-ACC- Phosphorylated acetyl-CoA carboxylase

PAP- Phosphatidic acid phosphatase

PKA- Protein Kinase A

Poloxamer- Poloxamer 407

POMC- Pro-opiomelanocortin

PPAR α - Peroxisome proliferator-activated receptor α

PVN- Paraventricular nucleus

R1/2- Reagent 1/2

RC- Regular chow

RIA- Radioimmunoassay

SCD1- Stearoyl-CoA desaturase 1

SREBP-1C- sterol regulatory element-binding protein 1C

TG- Triglyceride

TGH- Triglyceride hydrolase

VLDL-TG- Triglyceride-rich very-low density lipoprotein

WAT- White adipose tissue

Chapter 1: Introduction

1.1. Obesity, Diabetes, and Insulin Resistance

The metabolic syndrome, and metabolic disease states such as obesity and diabetes, are characterized by hyperlipidemia, due in part to elevated hepatic triglyceride (TG)-rich very-low-density lipoprotein (VLDL-TG)¹⁻⁵. Furthermore, excessive levels and/or actions of glucocorticoids (GCs) are associated with obesity, diabetes, insulin resistance, hyperglycemia, and dyslipidemia⁶⁻¹³. The WHO defines obesity as excessive fat accumulation that might impair health and is clinically diagnosed when one's body mass index exceeds 30 kg/m²¹⁴. Worldwide obesity has tripled since 1975, and as of 2016, 1.9 billion adults (39% global population) were overweight, and of these over 650 million were obese (13% global population)¹⁴. Furthermore, as of 2020, 39 million children under the age of 5 were considered overweight or obese¹⁴. In Canada alone, 36.3% of adults are considered overweight and 26.8% of adults are considered obese as of 2018¹⁵. Obesity is known to increase the risk of other metabolic diseases, such as type 2 diabetes and fatty liver disease, cardiovascular diseases, and musculoskeletal disease^{16,17}. Strikingly, most of the world's population live in countries where overweight and obesity kills more people than underweight¹⁴.

Similarly, the global prevalence of diabetes has been steadily increasing, as 422 million people had diabetes in 2014 (8.5% of global population) versus 108 million in 1980¹⁸. In Canada, 7.3% of individuals aged 12 and older were diagnosed with diabetes in 2017¹⁹. Importantly, individuals who were overweight or obese were more likely to be diagnosed with diabetes compared to normal weight individuals^{19,20}. Furthermore, diabetes is also associated with various comorbidities such as heart disease, stroke, and kidney disease¹⁹⁻²¹. Both diabetes and obesity carry a significant economic burden on the health-care system; thus, elucidating mechanisms to better understand, control, and regulate these metabolic diseases remains a priority.

1.1.1. Metabolic Characteristics of Obesity and Insulin Resistance

Dyslipidemia and insulin resistance play a key part in development of obesity and type 2 diabetes. Briefly, obesity is characterized by chronic and low grade inflammation which starts in the adipose tissue and liver due to lipid accumulation leading to the release of pro-inflammatory cytokines which cause systemic inflammation²²⁻²⁶. Chronic inflammation has been shown to induce insulin resistance in adipocytes and hepatocytes by inhibiting insulin signaling²²⁻²⁶. As insulin can no longer suppress lipolysis in the adipose tissue, there is an increased flux of free

fatty acids (FFAs) to the liver to stimulate VLDL-TG secretion and hepatic TG accumulation²²⁻²⁶. Further, hyperinsulinemia is associated with increased *de novo* lipogenesis, in part mediated by the activation of sterol regulatory element-binding protein 1C (SREBP-1C) (gene name: *Srebp1c*), which is considered the master regulator of lipogenic genes, which further stimulates TG production and subsequent VLDL-TG production and secretion^{23,25,27,28}.

Additionally, insulin resistance leads to a decrease in glucose uptake in muscle, as well as decreased FFA and glucose uptake in adipose tissue²⁸⁻³¹. Further, hepatic gluconeogenesis and glycogenolysis are not inhibited resulting in hyperglycemia²⁸⁻³⁰. The pancreas attempts to compensate by secreting more insulin, leading to a vicious cycle of insulin secretion in response to insulin resistance, which leads to hyperinsulinemia^{28,29,32}. The sustained stimulus for insulin secretion and, consequently, hyperinsulinemia, leads to pancreatic β -cell failure, characterizing type 2 diabetes^{28,29,32}. It should be noted however, that not all obese individuals develop dysregulated glucose homeostasis. Taken together, the physiological and economic costs of dyslipidemia, insulin resistance, and obesity are unquestionably high, and thus, delineating some of the mechanisms that may contribute to these metabolic disease states remains a priority.

1.2. Lipids

1.2.1. Digestion of dietary lipids in the intestine

Dietary fats, which consists mainly of TGs and cholesteryl esters, are digested in both the stomach and the intestine^{33,34}. The food is chewed in the mouth, which stimulates the release of lingual lipase from the von Ebner's glands on the tongue, and the food and lingual lipase are transported to the stomach³⁵⁻³⁸. In the stomach, lingual and gastric lipases, which is released from the gastric mucosa, hydrolyze TGs to form diglycerides (DGs) and fatty acids^{33-35,38}. Note however, rodents predominantly utilize high levels of lingual lipases, while humans and primates predominantly utilize gastric lipase for initial digestion of lipids³⁵. Gastric lipase activity is particularly important for infants, due to its specificity for fatty acids present in milk fat, and the lack of pancreatic lipase production and activity^{34,39,40}. The food bolus is then transported to the lumen of the small intestine, where the majority of the digestion occurs^{33,34}. Once food enters the intestine, gastrin and cholecystokinin are released from mucosal G cells and upper small intestinal I cells respectively^{33,34,41}. Cholecystokinin acts on the gallbladder to stimulate gallbladder emptying and acts on the pancreas to release pancreatic lipases^{33,34,41,42}.

Gallbladder emptying leads to the release of bile acids which emulsifies the dietary fats to enhance lipolysis via pancreatic lipases^{33,34,41,42}. Pancreatic lipases hydrolyze TGs to form 2-monoglyceride (2-MG), and eventually fatty acids and glycerol^{34,43}. Further, cholesterol esters are hydrolyzed by cholesterol esterase to form free cholesterol and fatty acids^{34,44}. The products of hydrolysis are incorporated into bile salt micelles, which are then transported from the intestinal lumen into the brush border of the enterocyte, where the cholesterol, 2-MG, and fatty acids are absorbed^{34,43}. Fatty acids and 2-MGs can either diffuse passively into the apical membrane when luminal concentrations are high, or, be transported into enterocyte by a variety of proteins, namely by CD36^{34,45-51}. Cholesterol uptake is mediated mainly by the Niemann-Pick C1- Like 1 protein³⁴.

Once absorbed, the fatty acids are then transported intracellularly, a mechanism mediated by the fatty acids binding onto various transport proteins, such as fatty acid binding protein 1 (FABP1) and FABP2^{34,52}, to either the mitochondria for fatty acid oxidation, or, to the endoplasmic reticulum to be synthesized into TGs, either via the MG pathway or via the glycerol-3- phosphate pathway³⁴. Similarly, the 2-MGs and other long chain fatty acids are sent to the endoplasmic reticulum where they are re-esterified to TGs via the MG pathway⁵³. The TGs, as well as cholesterol and phospholipids, are either packaged into chylomicrons in the jejunum and secreted from the enterocyte into circulation via the lymphatic system, or stored as lipid droplets in the cytosol^{34,54-56}. Briefly, secreted chylomicrons interact with lipoprotein lipase (LPL) that is secreted from muscle and adipose tissues and is found on the luminal surface of capillaries^{57,58}. This interaction leads to the hydrolysis of TGs stored in the chylomicrons, resulting in the formation of FFAs, which are then taken up by adjacent muscle cells and adipocytes for either storage or energy production^{57,58}. The remaining chylomicron remnant is cleared from the circulation by liver via receptor-mediated endocytosis⁵⁷. It should be noted that medium and short chain fatty acids are able to be absorbed directly into the portal circulation for transport to the liver for fatty acid oxidation or formation of VLDL-TGs^{34,59,60}.

1.2.2. *De novo* lipogenesis

The body is also capable of producing fatty acids *de novo* from dietary carbohydrates, a process known as *de novo* lipogenesis (Figure 1.1, pathway 1)^{29,61}. This process occurs predominantly in the liver, but can also occur in the adipose tissue⁶². In the fed state, glucose is

metabolized via the glycolytic pathway to produce citrate in the mitochondria, which is then converted to acetyl-CoA via ATP-citrate lyase (ACL) (gene name: *Acly*) in the cytosol^{29,63}. Subsequently, acetyl-CoA carboxylase (ACC) (gene names: *Acaca* and *Acacb*) converts acetyl-CoA to malonyl-CoA^{29,63-65}. In response to low intracellular energy stores, lipogenesis is inhibited by the inactivation of ACC via phosphorylation at various serine residues catalyzed by AMP-activated protein kinase (AMPK) and cAMP-dependent protein kinase (PKA) in response to low intracellular energy stores^{64,66}. Malonyl-CoA is used as a precursor for the synthesis of the fatty acids, mainly palmitic acid, via fatty acid synthase (FAS) (gene name: *Fasn*), which is the rate limiting step of *de novo* lipogenesis^{29,63}. Palmitic acid can then undergo elongation to form long chain fatty acids via various fatty acyl-CoA elongases (Elovl5) to yield stearate^{29,63,67}. The long chain fatty acids are then desaturated by stearoyl-CoA desaturase (SCD), of particular interest SCD1 which is the predominant isoform in the liver and adipose tissue, to form monounsaturated long chain fatty acids, namely oleate, which is the major fatty acid found in membrane phospholipids, TGs, and cholesterol esters^{29,63,67-70}. The resulting long chain fatty acids from *de novo* lipogenesis can then be converted to their acyl-CoA esters via various long chain acyl-CoA synthetases which can then be used for TG synthesis^{29,63}.

De novo lipogenesis is mediated by nutritional and hormonal regulation. Glucose not only provides the carbon source for fatty acid synthesis, but it also mediates various enzymes involved in the lipogenic pathway, mainly via the activation of carbohydrate responsive element binding protein (ChREBP)^{29,61,71,72}. ChREBP, found in liver, adipose tissue, and small intestine, stimulates the expression of *Acly*, *Acaca*, *Fasn*, *Scd1*, and *Elovl5* in response to glucose and is subsequently inhibited in states of low glucose where ChREBP is phosphorylated by PKA and AMPK^{71,73-75}. Further, glucose stimulates the release of insulin, which also stimulates *de novo* lipogenesis via activation of SREBP-1C, which is considered a master regulator of lipid metabolism⁷⁶. Of particular interest, SREBP-1C is abundantly found in the liver and adipose tissue and regulates expression of *Acly*, *Acaca*, *Acacb*, *Fasn*, and *Scd1*⁷⁶⁻⁷⁹. Similar to ChREBP, SREBP-1C is inhibited via phosphorylation mediated by AMPK⁸⁰. The SREBP-1C promoter is directly targeted to increase *Srebflc* expression by nuclear receptor liver x receptor (LXR)⁸¹. There are two LXR isotypes, LXR α (gene name: *Nr1h3*) and LXR β (gene name: *Nr1h2*), where LXR α is primarily expressed in metabolically active tissues, with the highest levels in the liver, while LXR β is expressed ubiquitously, and are activated by oxysterols or synthetic ligands^{82,83}.

Not only does LXR increase transcription of *Srebf1c*, but it also directly increases transcription of *Chrebp*, *Fasn*, and *Scd1*⁸⁴⁻⁸⁶. Obesity is linked to increased hepatic lipogenesis, due in part to insulin resistance leading to the dysregulation of SREBP-1C and ChREBP^{61,87}.

1.2.3. Triglyceride biosynthesis

TG synthesis is an acyl-CoA dependent mechanism, of which there are two main pathways aptly named based on the initial acyl acceptor; the MG pathway or the glycerol-3-phosphate pathway⁸⁸⁻⁹¹. Both pathways use fatty acyl-CoA thioesters as donors of acyl groups and they both converge on the final acylation step, which is mediated by diacylglycerol acyltransferase (DGAT), leading to the esterification of a DG to a TG^{63,92,93}. As this final step using DGATs is the only step committed to producing TGs, the DGAT enzymes is of particular importance.

DGATs are expressed in two isoforms that are part of two distinct gene families, *Dgat1* and *Dgat2*⁹⁴⁻⁹⁶. DGAT1 and 2 are expressed in many tissues in mammals, mostly in tissues that make large amounts of TG^{95,96}. In humans *DGAT1* mRNA levels are highest in the small intestine, and *DGAT2* mRNA is most abundant in the liver^{95,96}. In rodents, hepatic *Dgat1* mRNA levels are relatively low and *Dgat2* mRNA expression is in a broader range of tissues, with the highest levels being found in the adipose tissue followed by the liver^{95,96}. Further, DGAT2 has been found to be the dominant DGAT enzyme involved in *de novo* TG synthesis and DGAT1 is more involved in recycling hydrolyzed fatty acids^{68,97,98}. Oleic acid, the monounsaturated long chain fatty acid derived from the desaturation of fatty acids via SCD1, is the preferred substrate for DGAT1, while DGAT2 did not exhibit a preference of oleic acid compared to palmitoyl-CoA^{67,96}. DGAT activity is also mediated by carbohydrates and insulin, with glucose preferentially increasing *Dgat1* mRNA expression, and insulin increased *Dgat2* mRNA expression in adipocytes⁹⁹. Genetic- and diet-induced obesity models are associated with increased *Dgat2* and decreased *Dgat1* mRNA expression and protein levels in white adipose tissue (WAT) and liver^{100,101}. In the fasted state, *Dgat2* mRNA levels in WAT and in the liver are decreased, while *Dgat1* mRNA levels are increased^{63,94,99,102}.

1.2.3.1. The monoglyceride pathway

In brief, the MG pathway is the predominant pathway used to resynthesize TGs in the intestine in the fed state⁵³. The MG is initiated by the esterification of MGs with fatty acyl-

CoAs in the smooth endoplasmic reticulum of the enterocyte to form DGs, a reaction catalyzed by MG acyltransferase (MGAT)^{34,103}. The final step of TG synthesis using the MG pathway is mediated by DGAT, which catalyzed the esterification of DGs to TGs^{63,92}.

1.2.3.2. The glycerol-3-phosphate pathway

The glycerol-3-phosphate pathway is the main *de novo* TG synthesizing pathway that is conserved in all organisms^{104,105}. *De novo* lipogenesis occurs predominantly in the liver and adipose tissue⁹⁰. Similar to the MG pathway, the glycerol-3-phosphate pathway is characterized by a series of esterification steps in an acyl-CoA dependent manner within the endoplasmic reticulum^{88,89}. In the fed state, the initial substrate, glycerol-3-phosphate is initially synthesized via glucose via glycolysis^{63,92}. Glucose is converted to dihydroxyacetone-3P (DHAP), which is then further converted to glycerol-3-phosphate via glycerophosphate dehydrogenase^{63,92}. However, glycerol-3-phosphate can also be synthesized via non-carbohydrate substrates in the fasted state via glyceroneogenesis, in which DHAP is produced and converted to glycerol-3-phosphate^{29,89}. Alternatively, and preferentially, glycerol, can be phosphorylated via glycerol kinase in the liver (Figure 1.1, pathway 2)^{29,89}. In the liver, acylation of glycerol-3-phosphate occurs via glycerol-3-phosphate acyltransferase (GPAT), which catalyzes the synthesis of lysophosphatidate (LPA), which is again undergoes acylation via acylglycerol-P acyltransferase (AGPAT) to form phosphatidic acid (PA)^{89,90}. Phosphatidic acid can then be dephosphorylated to produce DGs via enzymes that have phosphatidic acid phosphatase (PAP) activity, such as the lipin protein family, with lipin-2 (gene name: *Lpin2*) being the most abundant in the liver^{89,90,106,107}. The DGs can then be esterified by DGAT to form TGs (Figure 1.1, pathway 3)^{63,92,93}.

1.2.4. Triglyceride-rich lipoproteins: Chylomicrons and very-low density lipoproteins

TGs, as well as other lipids, need to be packaged into proteins known as lipoproteins to be transported in the circulation. Chylomicrons and VLDLs are TG- rich lipoproteins which are secreted from the intestine in the post-prandial state, and from the liver in the fasted state respectively^{34,54,108}. They are composed of a hydrophilic monolayer membrane that consists of phospholipids, free cholesterol, and apolipoproteins, surrounding a hydrophobic core of neutral lipids, primarily TGs^{34,54,92,108}. Apolipoproteins not only play a role in the structure of the membrane of the lipoprotein, but they also play an important role the formation of lipoproteins,

the metabolism of lipoproteins, and they act as ligands for lipoprotein receptors^{109,110}. The primary apolipoproteins of both chylomicrons and VLDLs are apolipoproteins B (apoBs), with apoB-48 being the predominant apolipoprotein for chylomicrons and apoB-100 being the predominant apolipoprotein for VLDLs in humans, while apoB-48 is the predominant apolipoprotein for VLDLs in rats^{92,108,111–113}. Both apolipoproteins are derived from the same gene, and apoB-48 is the result of posttranscriptional mRNA editing of *Apob-100* by Apobec-1 in the intestine¹¹¹. Importantly, there is a single apoB molecule per VLDL or chylomicron particle. In humans, apoB-48 is produced exclusively in the small intestine, while apoB-100 is produced in the liver¹¹¹. Interestingly, in the rat, hepatocytes produce both apoB-100 and apoB-48^{113,114}.

1.2.4.1. Triglyceride-rich very-low density lipoprotein formation and secretion

Once the TGs have been synthesized in the liver, they can be packaged into VLDL-TGs. Hepatic VLDL-TG assembly, which occurs in the endoplasmic reticulum, is believed to occur in a two-step process (Figure 1.1, pathway 4)^{115,116}. In the first step, known as the co-translational step, *Apob* mRNA translation begins in the ribosome of the hepatocyte, and TGs are recruited and transferred to the apoB particle via microsomal triglyceride transfer protein (MTP), which yields a primordial TG-poor particle within the lumen of the endoplasmic reticulum known as a pre-VLDL^{115,117–121}. Further, an apoB-free luminal lipid droplet is formed containing other exchangeable apolipoproteins, which are also lipidated by MTP^{115,119,121,122}.

The second step of VLDL assembly, known as the post-translational step, a VLDL-TG is assembled by the transfer of core lipids from the primordial TG-poor, apoB-containing particle and the lipid droplet, leading to the bulk lipidation of the VLDL-TG particle^{115,119–121}. This second step is dependent on the activity of ADP-ribosylation factor 1 (Arf1), which activates phospholipase D, producing PA, which is required for the assembly of VLDLs^{123,124}. There is debate as to whether the second step of VLDL assembly occurs entirely in the endoplasmic reticulum^{115,125,126} or in a post-endoplasmic reticulum or Golgi apparatus compartment^{115,123,126–128}. Further, the lipidation of the pre-VLDL particle is mediated by cell death-inducing DFF4-like effector B (CideB), an endoplasmic reticulum and lipid droplet-localized protein, as it facilitates the transport of TGs synthesized in the ER or in cytosolic lipid droplets to pre-VLDL particles^{126,129}. The VLDL-TG particle is then transported to the Golgi apparatus via the

budding of transport vesicles from the endoplasmic reticulum to the Golgi apparatus, where the VLDL-TG can be secreted out into the periphery¹¹⁵. Arf1 participates in the formation of coatamer I secretory vesicles, which are important for the transport vesicles between the endoplasmic reticulum and Golgi apparatus^{123,130}.

1.2.5. Hepatic fatty acid β oxidation

In the fasted state, when energy levels are low, and AMPK levels are high, intracellular fatty acyl-CoAs are redirected towards fatty acid β -oxidation and away from glycerolipid biosynthesis (Figure 1.1, pathway 5)⁶³. In the liver, the fatty acids are targeted mainly towards ketogenesis, as ketone bodies can then be sent out from the liver to other tissues to be used for energy^{63,131}. The first, and rate-limiting step in fatty acid β oxidation is the translocation of fatty acyl-CoAs to the mitochondria via carnitine palmitoyltransferase 1a (CPT-1a), which catalyzes the production of acyl-carnitine^{63,131,132}. Acyl-carnitine is then transported to the mitochondrial matrix via a translocase enzyme, where acyl-CoA is regenerated via CPT-II^{63,131,132}. The acyl-CoA can then enter the β oxidation pathway^{63,131}. Fatty acid β oxidation is regulated at various steps, however notably, CPT-1a is inhibited by malonyl-CoA^{63,131,133}. Additionally, peroxisome proliferator-activated receptor α (PPAR α), which activated under conditions of energy deprivation, is required for the activation genes needed for fatty acid β oxidation, including CPT-1a^{63,134,135}.

1.2.6. Lipid storage and lipolysis

TGs that are not packaged into VLDL-TGs can be stored into lipid droplets. Lipid droplets are considered to be dynamic storage organelles with various function, but the main function is to store excess TGs¹³⁶. Once substrate is required, the TGs can undergo lipolysis to form fatty acids¹³⁷. Intestinal lipolysis has previously been outlined. Notably, in the liver, lipolysis of endoplasmic reticulum-localized luminal lipid droplets is regulated by triglyceride hydrolase (TGH), which has been shown to be integral for VLDL-TG secretion (Figure 1.1)^{122,138,139}. Hepatic VLDL-TG secretion has been shown to be regulated by FFA flux to the liver^{140,141}. In insulin-resistant states an increase in plasma FFA is observed due to the diminished inhibition of adipose tissue lipolysis^{142,143}. This can lead to increased lipid accumulation in hepatic lipid droplets, which contributes to the development hepatic steatosis and non-alcoholic fatty liver disease^{137,144–146}. Obesity and type 2 diabetes are major risk factors for the development of non-

alcoholic fatty liver disease, which is associated with numerous comorbidities, including cardiovascular disease, but additionally, non-alcoholic fatty liver disease is also a risk factor for the development of dyslipidemia and type 2 diabetes^{137,144,147–153}. Together, this highlights the tight association of lipid homeostasis (storage, secretion, and break-down of lipids) and the pathology of metabolic disease states.

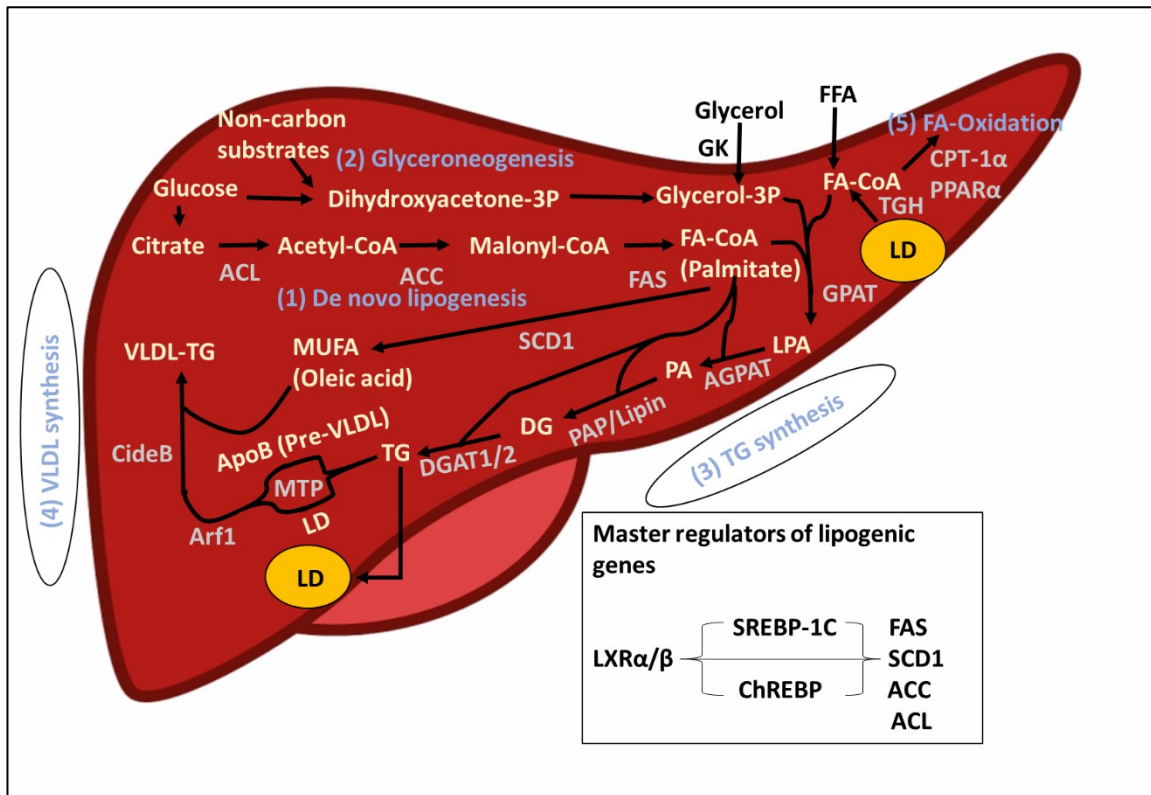


Figure 1.1- Overview of hepatic lipid metabolism. (1) *De novo lipogenesis*: In the fed state glucose is converted to citrate which can then be converted to acetyl-CoA via ATP-citrate lyase (ACL). Acetyl-CoA is converted to malonyl-CoA via acetyl-CoA carboxylase (ACC), which is subsequently converted to fatty acid (FA)-CoA (mainly palmitate) via fatty acid synthase (FAS). Palmitate can undergo elongation, then subsequently desaturation via stearoyl-CoA desaturase (SCD1) to yield monounsaturated fatty acids (MUFA), particularly oleic acid, which is preferentially used by diacylglycerol acyltransferase (DGAT) 1 when synthesizing triglycerides (TGs). (2) *Glyceroneogenesis*: In the fasted state, glycerol is preferentially used as a substrate for lipogenesis. Glycerol can be synthesized from glucose via glycolysis, or alternatively, from non-carbon substrates via glyceroneogenesis, which yields dihydroxyacetone-3P, which is converted to

glycerol-3P. Additionally, glycerol can be phosphorylated via glycerol kinase (GK). Many of the lipogenic genes are regulated by sterol regulatory element-binding protein 1C (SREBP-1C), carbohydrate responsive element binding protein (ChREBP), and liver X receptor (LXR) α and β . (3) *TG synthesis*. Glycerol-3P is acylated via glycerol-3-phosphate acyltransferase (GPAT) to synthesize of lysophosphatidate (LPA), which is undergoes acylation via acylglycerol-P acyltransferase (AGPAT) to form phosphatidic acid (PA). PA is dephosphorylated to form diglycerides (DGs) via enzymes that have phosphatidic acid phosphatase (PAP) activity, such as the lipin protein family. The DGs are then esterified to produce TGs via DGAT1 or DGAT2. Each of these steps are characterized by esterification in an acyl-CoA dependent manner. The acyl-CoA pool comes from de novo lipogenesis, incoming free fatty acids (FFA), and the lipolysis of stored hepatic lipids in lipid droplets (LD), which is in part mediated TG hydrolase (TGH) to drive TGs in luminal lipid droplets to pre-very-low density lipoproteins (VLDLs). (4) *VLDL synthesis*. TGs are packaged into TG rich very-low density lipoprotein (VLDL-TG) to be secreted out of the liver into the periphery. This occurs in a two-step process. The first step is the co-translation of an apolipoprotein B (apoB) containing molecule, yielding a pre-VLDL molecule, and a luminal lipid droplet, a process mediated by microsomal TG transfer protein (MTP). The second step, known as the post-translational step, requires the fusion of these two molecules, leading to bulk lipidation, which is facilitated by ADP-ribosylation factor 1 (Arf1) and cell death-inducing DFF4-like effector B (CideB). (5) *FA-Oxidation*. In the fasted state, intracellular FAs are directed to FA-oxidation to produce energy. This process is facilitated in part by carnitine palmitoyltransferase 1a (CPT-1a), which is subsequently mediated by peroxisome proliferator-activated receptor α (PPAR α). Imaged adapted from Saponaro et al., *Nutrients*¹⁵⁴.

1.3. Glucocorticoids

Glucocorticoids (GCs), are steroid hormones that play a fundamental role in whole body homeostasis and metabolism^{155,156}. Further, GCs are often using in clinical settings due to the anti-inflammatory and immunosuppressive effects^{155,156}. However, long-term GC-therapy and chronically elevated GCs, as observed in Cushings disease, is associated with the development of osteoporosis, hyperglycemia, cardiovascular disease, dyslipidemia, and insulin resistance¹⁵⁵⁻

¹⁵⁸. Additionally, excessive plasma concentrations and/ or actions of GCs are associated with obesity and diabetes^{6-10,12,159}.

1.3.1. Glucocorticoid synthesis and secretion

GCs, which include cortisol in humans and corticosterone (CORT) in rodents, are steroid hormones released from the adrenal glands upon stressor induced activation of the hypothalamic-pituitary-adrenal (HPA) axis, which is mediated via circadian and ultradian rhythms, to mobilize fuels (e.g., glucose and FFAs)^{160,161}. GCs are synthesized from cholesterol via steroidogenesis within the zona fasciculata of the adrenal glands. Cholesterol is transported from the outer mitochondrial membrane to the inner mitochondrial membrane via steroidogenic acute regulatory protein, a transport protein¹⁶²⁻¹⁶⁴. The rate limiting step in steroid hormone synthesis is the conversion of cholesterol to pregnenolone, a steroid precursor, via P450 side chain cleave enzyme¹⁶²⁻¹⁶⁴. CORT is then synthesized following a series of chemical reactions catalyzed by mitochondrial cytochrome P450 enzymes^{165,166}. Once GCs are secreted from the adrenal complex into peripheral circulation, GCs can passively diffuse into the plasma membrane of cells¹⁶⁷. However, the bioavailability of GCs depends not on the bioavailability of circulating levels, but also on cellular specific levels/ and or activity of one of two 11 β -hydroxysteroid dehydrogenases (11 β -HSDs)¹⁶⁸⁻¹⁷¹. 11 β -HSD1, which is highly expressed in the liver, adipose tissue, kidney, and brain, converts the inactive 11-dehydrocorticosterone to active CORT, while 11 β -HSD2, which is most abundant in the kidneys and salivary glands, performs the opposite reaction, such that CORT, but not synthetic GCs, is oxidized into its inactive form, 11-dehydrocorticosterone^{167-169,172}. GCs can act on two types of receptors- the mineralocorticoid receptor (MR) or the glucocorticoid receptor (GR)^{160,173,174}. GCs bind to MRs with a higher affinity, which means the MRs are occupied during basal levels, keeping plasma GC levels low during the normal daily circadian and ultradian rhythms^{160,174-176}. Only when GC levels are high, such as in response to stress or increases in the frequency or amplitude of GC secretory bursts from the circadian rhythm, do GCs bind to GRs^{160,174,177,178}.

1.3.1.1. Glucocorticoid receptor and intracellular action

When GCs enter the cell, typically, GCs can bind onto the cytosolic GR (Figure 1.2). GRs are found in the majority of the cells of the body, implicating their role in a variety of physiological processes^{167,179}. Specifically in the brain, GRs are highly expressed in the

paraventricular nucleus and the arcuate nucleus (ARC) of the hypothalamus¹⁸⁰⁻¹⁸³. Unbound GRs are found in the cytosol as part of a large multi-protein complex, which importantly includes heat-shock protein 90 (Hsp90), as well as other accessory proteins^{155,179,184}. Hsp90 is essential for the stability and biological function of the GR, as it is necessary for ligand binding and GR activation¹⁸⁵⁻¹⁸⁷. It has previously been reported that the absence or inhibition of Hsp90 resulted in the degradation of the GR^{185,188,189}. Upon GC-GR binding, GRs undergo a conformational change such that Hsp90, as well as the other accessory proteins, dissociate from the GR, allowing the GC-GR complex to translocate into the nucleus, where it is able to exert its effects in a genomic-fashion by binding onto GC response elements within the regulatory regions of target genes^{155,179,184}.

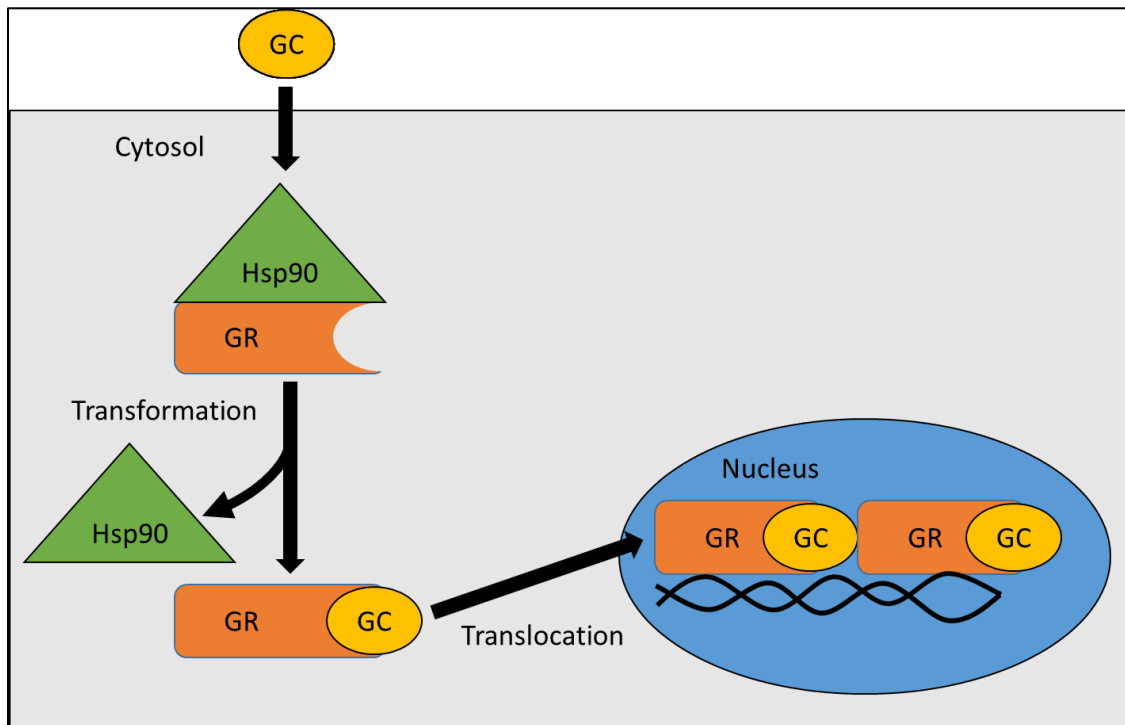


Figure 1.2- The glucocorticoid- glucocorticoid receptor complex. Typically, glucocorticoids (GCs) bind to the cytosolic glucocorticoid receptor (GR). Upon binding, heat shock protein 90 (Hsp90) as well as other accessory proteins dissociate from the GR complex. The GC-GR complex can then translocate into the nucleus where it exerts its effects in a genomic fashion.

1.3.2. Glucocorticoid regulation: The hypothalamic-pituitary-adrenal axis

GCs are secreted in response to stress-induced activation of the HPA axis to mobilize fuels (Figure 1.3)^{160,161,174}. The HPA axis is initiated upon the detection of a physiological stressor, in which neurons from the hypothalamic paraventricular nucleus (PVN) release corticotrophin-releasing hormone (CRH) into the median eminence, where it then travels via the hypophyseal portal circulation to the anterior pituitary gland and stimulates the production of adrenocorticotrophic hormone (ACTH)^{160,161,174}. ACTH is then released from the pituitary gland into the circulation and acts on the adrenal glands^{160,161,174}. ACTH acts on melanocortin 2 receptors in the zona fasciculata of the adrenal cortex, which leads to an increase in intracellular cAMP levels in an adenylate cyclase-dependent fashion, stimulating an increase cholesterol biosynthesis, which acts as the precursor for GC synthesis^{174,190,191}. Typically, negative feedback terminates the HPA stress response, where GCs act on the GRs at the level of the PVN and pituitary to inhibit further HPA activity^{160,161,192}. Importantly, in metabolic disease states, including diabetes and obesity, this negative feedback loop is attenuated and causes an elevation in plasma GCs^{6,9,10,12,13,159}.

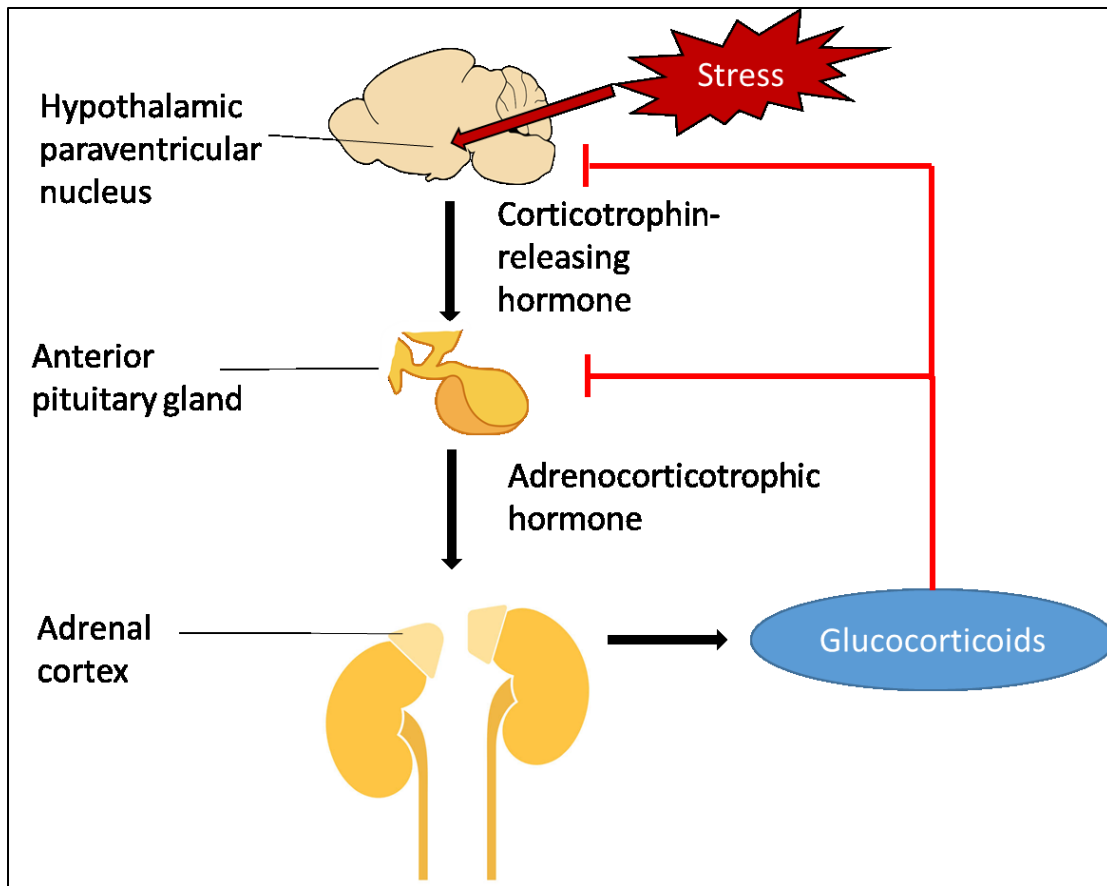


Figure 1.3- The hypothalamic-pituitary-adrenal axis. The hypothalamic-pituitary-adrenal axis is initiated upon detection of a stressor by the hypothalamic paraventricular nucleus, which leads to the release of corticotrophin-releasing hormone, which then acts on the anterior pituitary gland to release adrenocorticotrophic hormone, which subsequently acts on the adrenal glands to release glucocorticoids into the circulation. Typically, this is mediated by a negative feedback loop where glucocorticoids can act on the level of the hypothalamus and pituitary gland to inhibit further hypothalamic-pituitary-adrenal axis activity.

Further, GC secretion and release is regulated by circadian and ultradian rhythms^{160,161,193}. Typically, the diurnal GC secretion pattern is highest in the active state (upon awaking) and lowest during the inactive state (during rest), which is mirrored by plasma GC levels, and secretion continues with the ultradian rhythm, which is characterized by burst-like pulses within 1-2 hours¹⁹³⁻¹⁹⁷. It has been shown that chronic stress, long-term high-fat diet (HFD) feeding, and in metabolic disease states, such as obesity and diabetes, that are associated

with disrupted GC homeostasis, are also associated with disruptions in the circadian rhythm of GC regulation, such that the diurnal fluctuations of GC concentration are flattened, leading to elevated basal GCs compared to healthy conditions^{158,193,198–202}. Thus, with the association of metabolic disease states and GC-excess/dysregulation, GCs may play an important role in the progression of these disease states.

1.3.3. Non-metabolic peripheral actions of glucocorticoids

Due to the GRs being expressed in nearly all tissues types in the body, GCs action is involved in various physiological processes, including mediating the immune, respiratory, cardiovascular, musculoskeletal, and reproductive systems^{155,203}. Notably, synthetic GCs have been widely used in clinical settings due to their anti-inflammatory and immunosuppressive properties^{155,203}.

GCs can act on almost all immune cell types to mediate the immune response^{155,204}. Because of this, GCs can act on the GRs of these immune cells to alter the transcription of genes involved in the immune response^{155,157,204}. GC-GR action can lead to the transrepression of pro-inflammatory transcription factors, notably, nuclear factor κ B and activator protein-1^{205–208}. This leads to the repression of production and secretion of pro-inflammatory cytokines, chemokines, and cell adhesion molecules^{155,157,204}. Further, GCs can lead to the transactivation of various anti-inflammatory genes, such as interleukine 10, CD25, lipocortin 1, and inhibitory kinase B²⁰⁴. Thus, with the anti-inflammatory effects of GC-GR action, GCs have been used to treat inflammatory disorders such as asthma, arthritis, skin rashes, and chronic obstructive pulmonary disorder^{155–157,204}.

GC-GR action is essential for normal cardiac function and survival^{209,210}. In cardiomyocytes specifically, GC-GR action has been shown to have both antiapoptotic and anti-inflammatory effects^{155,211,212}. Additionally, GCs can help maintain blood pressure homeostasis via inhibiting the production of vasodilators^{155,211,212}. However, it should be noted that increased concentrations of GCs, due to either endogenous production or exogenous administration, is associated with a greater risk of developing cardiovascular disease^{155,211–213}.

Though therapeutic GC therapy is considered the gold standard for treating musculoskeletal disorders due to the anti-inflammatory effects of GCs in the joints of surrounding tissues, long-term GC treatment is also associated with the development of

osteoporosis^{155,214}. This is due in part to GCs inducing apoptosis of osteoblasts and osteocytes, inhibition of osteoblast function, and induction of osteoclastogenesis^{155,215}. These effects may be also be due to GCs increasing renal calcium elimination, decreasing intestinal calcium absorption, increases in parathyroid hormone synthesis and secretion, and decreases in the synthesis and secretion of sex hormones²¹⁴.

1.3.4. Metabolic actions of peripheral glucocorticoids

As mentioned, during situations of stress, GCs are required to mobilize fuels throughout the body to provide substrate to tissues for utilization to cope with increased metabolic demands. Thus, GCs have been shown to effect substrate output and utilization in muscle, adipose tissue, and liver.

In the muscles, GCs metabolic effects mostly occur via the antagonism of the insulin signaling cascade, leading to a decrease in glucose uptake, utilization, and glycogen synthesis^{216,217}. GCs have been shown to inhibit AKT phosphorylation, decrease insulin receptor tyrosine phosphorylation, and reduce PI3 kinase activity²¹⁸⁻²²¹. GCs decrease insulin-stimulated glucose uptake and utilization by inhibiting translocation of glucose transporter 4 (GLUT4) into the cellmembrane²²²⁻²²⁶. Further, GCs decrease the phosphorylation of glycogen synthase kinase 3 (GSK3), which is needed to activate glycogen synthase, resulting in a decrease in glycogen synthesis²²⁶⁻²²⁹. With regard to lipid homeostasis, GC treatment has been associated with increased intramuscular DG and TG accumulation, which may also contribute to insulin resistance^{230,231}. AMPK activity in skeletal muscle is decreased as a result of GC exposure, which is associated with an increase in malonyl-CoA²³¹⁻²³³. Interestingly, treating mice with 11 β -HSD1 inhibitors reduces lipogenic gene expression (ACC, FAS, and DGAT) and increased FFA utilization²²⁶.

Similar to muscle, GC action in adipose tissue inhibits insulin-stimulated glucose uptake via decreasing translocation of GLUT4, reducing insulin receptor expression, and decreasing insulin receptor affinity²³⁴⁻²³⁶. Further, GCs directly stimulate lipolysis by increasing transcription and expression of lipase proteins ATGL and HSL, as well as impair the ability of insulin to suppress lipolysis, which contribute to hyperlipidemia²³⁷⁻²⁴⁰. This also leads to a significant rise in plasma FFAs, which can contribute to insulin resistance in adipocytes^{241,242}. However, paradoxically, GCs also stimulate lipogenesis and visceral adipogenesis in the fed

state²³⁸. This effect to induce both breakdown and synthesis of lipids may be due to localized GC excess and increased activity due to 11 β HSD1 in adipocytes^{238,243}. Additionally, GCs have been shown to alter the activity and expression of adipokines, such as adiponectin and leptin^{244–248}.

Importantly in the liver, GCs directly increase gluconeogenesis, lipogenesis, and VLDL-TG secretion^{249–251}. Notably, it has been observed that GR ligand binding directly activates the transcription of phosphoenolpyruvate carboxykinase and glucose-6-phosphatase, which are required for gluconeogenesis²¹⁶. Similar to muscle and adipose tissue, hepatic GC action antagonizes the actions of insulin by indirectly inhibiting AKT phosphorylation, which contributes to hyperglycemia and insulin resistance²⁵². In regards to lipid homeostasis, GCs directly stimulates hepatic *Acaca*, *Acacb*, *Fasn*, *Dgat1*, and *Dgat2* gene expression, which contribute to increased TG synthesis^{232,251,253,254}. Further, GCs have also been shown to increase PAP activity of lipin-1, which may also contribute to hepatic TG synthesis^{255–257}. Additionally TGH, which is a lipase required for the hydrolysis of intracellular TGs, decreases as a result of GC treatment, suggesting that GCs decrease hepatic lipolysis and increases *de novo* lipogenesis, which may contribute to increased hepatic TG content²⁵¹. Further, hepatic GC-GR action increases plasma TGs, cholesterol, and VLDL-TG secretion^{249,250,258}. This may be due in part to increased synthesis and decreased degradation of hepatic apoB-48 and apoB-100, as observed in cultured rat hepatocytes treated with dexamethasone (DEX), a synthetic GC²⁵⁹.

Taken together, GC excess greatly alters the metabolic profile, namely by contributing to hyperglycemia, hyperlipidemia, and insulin resistance. With the association of metabolic disease states, such as diabetes and obesity, having excessive levels and/or actions of GCs, GC excess may contribute to the aberrant lipid homeostasis as observed in these disease states.

1.4. Hypothalamic sensing of peripheral nutrients and hormones and regulation of lipid metabolism

The hypothalamus, specifically the medial basal hypothalamus (MBH), has been shown to detect and respond to peripheral nutrients and hormones to modulate lipid and glucose metabolism^{112,260–268}. The MBH, which includes the ARC and minor medial aspects of the ventromedial hypothalamus, is a key region of the brain that is involved in various neuroendocrine and physiological functions^{265–267,269–271}. Neurons in the MBH are able to sense circulating hormones and nutrients in the blood due in part to being near the median eminence,

the third ventricle, and a leaky region of the blood-brain barrier^{265–267,269–271}. In response to changes in the peripheral nutrient and hormone status, the hypothalamus can modulate food intake, energy expenditure, and glucose and lipid metabolism^{265–267,271}.

1.4.1. Nutrient sensing in the hypothalamus

The concept that the brain can sense and respond to peripheral nutrients has been studied since the 19th century, with Claude Bernard's work involving lesioning the fourth ventricle of rabbits, which lead to altered glucose homeostasis, ultimately resulting in hyperglycemia²⁷². It is now generally accepted that the brain is integral to maintaining whole body homeostasis via the detection of changes in nutrients and mediating a physiological response^{112,265–269,271,273–275}. Glucose detection in the brain has been shown in various regions of the brain, and can lead to peripheral changes in glucose production and food intake^{268,269,274–280}. Notably, direct infusions of glucose into the hypothalamus of rats via a intracerebroventricular (ICV) infusion targeting the third ventricle of the brain, is associated with a decrease body weight, food intake, hepatic gluconeogenesis and glycogenolysis, and this decrease in glucose output was associated with the inhibition of hepatic glucose-6-phosphatase flux and mRNA expression, resulting in a decrease in hepatic glucose production^{278,281}. Additionally, the ICV infusion of glucose and/or lactate into the third ventricle of rats also lead to a reduction in hepatic VLDL-TG secretion, increase in hepatic TG content, and a decrease in peripheral TGs, an effect mediated by decreased hepatic SCD1 activity, which in turn decreased hepatic oleic acid content²⁶¹. Interestingly, the infusion of a lactate dehydrogenase inhibitor specifically into the MBH negated the lipo-inhibitory effects lactate, implicating the role of the MBH in whole body metabolism²⁶¹. However, in HFD conditions, the ability of brain glucose to lower hepatic VLDL-TG secretion was abolished, indicating a potential defect in brain-glucose sensing²⁶¹. Thus, a defect in the ability of the brain to detect and respond to glucose, which mediates food intake, hepatic glucose production, and hepatic VLDL-TG secretion, contributes to multiple facets of the metabolic syndrome, including obesity, insulin resistance, and dyslipidemia^{261,278,281}.

Further, FFA acids can be detected by the brain and lead to changes in peripheral metabolism. MBH target oleic acid infusion, ICV infusion of oleic acid targeting the third ventricle in conscious rats, or inhibiting hypothalamic β -oxidation via inhibiting hypothalamic CPT1 α , thus increasing hypothalamic fatty acid availability, inhibited glucose production and

food intake^{282–285}. The decrease in food intake was associated with a decrease in hypothalamic expression of neuropeptide Y (NPY), a orexigenic neuropeptide, as well as hepatic glucose-6-phosphatase expression in the liver^{282,283,286}. However, the central infusion of oleic acid is unable to decrease food intake, NPY, and glucose production in 3-day HFD induced, hyperlipidemic rats, though the inhibition of hypothalamic CPT1a, specifically in the MBH, was able to normalize food intake, NPY expression, glucose homeostasis in hyperlipidemic rats^{285,286}. Subsequently, chronic degradation of hypothalamic malonyl-CoA, which inhibits CPT1 α , via the overexpression of malonyl-CoA decarboxylase induces hyperphagia obesity^{287,288}. In terms of lipid homeostasis, similarly, central actions of fatty acids inhibit VLDL-TG secretion. It was observed that an infusion of oleic acid directly into the MBH of fasted rats led a decrease in hepatic VLDL-TG secretion, an effect mediated by decreased hepatic *Scd1* mRNA expression¹¹². Similar to the aforementioned results in reference to glucose metabolism, the negative-feed effect of elevated FFAs acting in the MBH to lower peripheral VLDL-TG secretion was negated in diet induced hyperlipidemic rats¹¹².

1.4.2. Hormone sensing in the hypothalamus

The hypothalamus indeed detects various hormones to regulate glucose production and lipid homeostasis. Insulin, which has been implicated in the regulation of both glucose and lipid homeostasis, has been shown to also be involved in these processes via action in the brain alone. ICV administration of insulin targeting the third ventricle, or the MBH directly, led to decreases feeding, body weight, *Npy* expression, and hepatic glucose production in animal models^{289–295}. Insulin action in the brain has been shown to promote both WAT and hepatic lipogenesis, due to increased fat mass, adipocyte size, adipose tissue lipoprotein lipase (LPL) expression, hepatic VLDL-TG secretion and decrease hepatic lipid levels^{260,296}. Administration of glucagon, glucagon-like peptide-1 (gut- derived incretin hormone) or glucagon-like peptide-1 receptor agonists to the hypothalamus have been shown to lower hepatic glucose production and VLDL-TG secretion^{297–302}.

It is well known that leptin, an adipokine secreted from adipocytes, helps regulate energy balance via inhibiting hunger, thus inhibiting NPY neurons, and upregulating energy expenditure by acting in various brain regions, including the MBH^{303–306}. Briefly, ICV infusion of leptin stimulates hepatic gluconeogenesis but does not alter glucose production due to the

compensatory decrease in glycogenolysis³⁰⁷⁻³⁰⁹. Importantly, ICV infusion of leptin normalizes blood glucose levels in diabetic rodents and reverses insulin resistance in HFD –fed rodents^{307,310-313}. Direct leptin infusion into the MBH of rats inhibits WAT *de novo* lipogenesis³¹⁴. Similarly, ICV delivery of leptin targeting the third ventricle of rats, leads to an increase in hepatic VLDL-TG secretion and a decrease in hepatic *de novo* lipogenesis³¹⁵. Leptin action in the brain is associated with a changes in liporegulatory genes and proteins, namely, decreases in hepatic FAS and SCD1 protein and mRNA expression³¹⁵⁻³¹⁷.

In parallel to the previously stated effects of nutrients and hormones in the brain suppressing the activity of hypothalamic NPY, direct hypothalamic infusions of NPY also mediates glucose and lipid metabolism. An ICV infusion of NPY targeting the third ventricle of rats stimulates hepatic VLDL-TG secretion, due in part to an increase in hepatic SCD1, ARF-1, and lipin-1 mRNA expression and protein levels^{263,318-320}. Chronic ICV administration of NPY leads to alters whole body homeostasis, characterized by dyslipidemia, hyperinsulinemia, and hypercorticosteronemia³²¹. Furthermore, central NPY signaling is able to negate the inhibitory effect of insulin on VLDL-TG secretion³²².

Taken together, the hypothalamus, specifically the MBH, can detect and respond to peripheral nutrients and hormones that are involved in glucose and lipid metabolism. However in metabolic disease states, as observed in diet-induced hyperlipidemic models and obesity, the sensing of the nutrients and hormones can be defective, which can contribute to a disruption of metabolic homeostasis^{265,267,287}.

1.5. Central/ brain metabolic effects of glucocorticoid action

Although the peripheral effects of GCs are well known, and the hypothalamus has been shown to be a hormone-responsive site, less is known about the brain mechanisms of GC action to modulate homeostasis. Previous literature has shown that a single ICV injection of DEX, a synthetic GC, into adrenalectomized genetically obese mice leads to a significant increase in plasma insulin, decreased brown adipose tissue thermogenesis, increased hypothalamic NPY secretion, and food intake 24h post-GC injection³²³⁻³²⁵. Furthermore, a 2-3 day chronic ICV GC infusion into healthy rodents induced obesity, marked by weight gain, hyperphagia, hypertriglyceridemia, hyperinsulinemia, hyperleptinemia, increased glucose uptake but no change in glucose production, and increased NPY levels³²⁶⁻³²⁸. Additionally, 2-3 day ICV GC

infusions has adipose-tissue specific effects, namely an increase in adipose 11 β -HSD1, increased expression of key lipogenic enzymes (ACC and FAS), and decreased *Hsl* and *Cpt1* mRNA expression³²⁸. Moreover, GC infusion directly into the MBH decreased hepatic insulin sensitivity, and this effect was negated via the inhibition of NPY, implicating MBH-GC action in regulating whole body energy homeostasis³²⁹. Recent evidence has confirmed that chronic CORT treatment via CORT delivery in drinking water of rodents, increased peripheral CORT, which can act on GRs in the MBH to contribute to hyperphagia, hyperinsulinemia, and obesity^{330–332}. The Yue laboratory has already provided evidence that acute GC action, specifically in the MBH, increases hepatic glucose production in healthy and pre-obese rats with elevated plasma GCs, and this effect can be negated via the inhibition of MBH GRs, illustrating that GC-GR action in the MBH modulates hepatic glucose metabolism, and that the inhibition of GRs can normalize peripheral metabolisms in models with elevated GCs to maintain euglycemia^{333,334}. With evidence to demonstrate that hypothalamic GC action contributes to metabolic disturbances, there remains a gap in the literature with reference to if hypothalamic GCs alter hepatic lipid metabolism in healthy and pre/obese states.

1.6. Aim, hypothesis, and objectives

The aim of this project is to explore if GCs directly act in the MBH to regulate liver VLDL-TG secretion to better understand mechanisms by which blood lipid levels may be lowered in diet-induced hyperlipidemia. With the association between GCs and dyslipidemia, and evidence illustrating the MBH being a hormone-responsive liporegulatory site, I hypothesize that (1) GCs act via GRs in the MBH to modulate liver lipid homeostasis by increasing plasma TGs and hepatic VLDL-TG secretion, and (2) inhibition of MBH GC action (by blocking MBH GRs or downstream mediators of GC-GR action specifically within the MBH) would improve liver lipid metabolism in diet-induced hypertriglyceridemic rats (Figure 1.4).

Thus, the objectives of this project were broken into two parts, which are associated with the two parts of the hypothesis. The conducted *in vivo* experiments delineate molecular and physiological mechanisms of MBH GC action that modulate lipid homeostasis in normal and diet-induced hyperlipidemic rats. Further, protein and gene expression analysis of various hepatic liporegulatory enzymes would provide understanding on how brain GC action may affect the liver to modulate hepatic lipid homeostasis.

1.6.1. Objective 1: To assess GC action and delineate GR requirements in the MBH in regulating hepatic VLDL-TG secretion in healthy rats

These studies assess for the first time the effects of acute GC infusion into the MBH on plasma TG secretion and test the requirements of MBH GRs in mediating the MBH GC liporegulatory effect in healthy 10-hour fasted rats fed a regular-chow (RC) diet. It was assumed that the TG-rich lipoproteins that appear in circulation are liver derived VLDL-TG particles, as previous literature has shown that rats fasted for as little as 4-hours resulted in nearly undetectable levels of chylomicrons compared to fed controls, suggesting that chylomicrons do not contribute to the observed changes in VLDL-TG secretion in the current study^{112,263}. Thus, hepatic VLDL-TG secretion was assessed based on the rate of appearance of plasma TGs over time. It was anticipated that GCs, in the form of synthetic GC, DEX, (widely used synthetic GC to study GC-mediated GR signaling^{157,335}), can act on MBH GRs to lead to an increase in VLDL-TG secretion and plasma TGs. However, if the MBH GRs were antagonized either pharmacologically via mifepristone (MIF) (a known GR antagonist³³⁶), genetically via MBH specific injections of a lentivirus (LV) to deliver GR shRNA, or by targeting Hsp90 (acutely via pharmacological inhibition with known Hsp90 inhibitor, 17-AAG (Hsp90i)³³⁷⁻³³⁹, or chronic loss of function via MBH-specific injections of a LV expressing Hsp90 shRNA), the lipostimulatory effects of MBH DEX should be blocked (Figure 1.4, pathway 1).

The chemical and genetic loss-of-function approaches targeting the GR in MBH were used to evaluate the requirement of the GR in the MBH to mediate MBH GC mediated liporegulatory action. Pharmacological inhibition of MBH GRs via MIF was co-administered with and without DEX to assess the requirement of MBH GRs to mediate the lipostimulatory effects of MBH GC. To alternatively test the requirement of GRs to mediate MBH GCs, genetic loss-of-function techniques was used to evaluate whether MBH GRs are necessary for MBH GC liporegulatory action. Evaluation of GRs was achieved via MBH targeted injections of LVs to deliver GR shRNA, or a mismatch sequence (MM) as a control and rats were treated with and without DEX infusions into the MBH.

To further implicate the necessity of GRs, Hsp90 was investigated. Hsp90 is required for the biological function and stability of the GR complex and biological function, thus the inhibition of the Hsp90 in the MBH would negate the effect of MBH GCs acting on GRs to

stimulate hepatic VLDL-TG secretion¹⁸⁵⁻¹⁸⁹. Thus, pharmacological and genetic loss-of-function of MBH Hsp90 via Hsp90i and LV Hsp90shRNA respectively, with and without DEX infusions into the MBH on the day of the experiment, was used to assess the requirement of functional MBH GRs in regulating the MBH GC-mediated effects on lipid homeostasis.

To begin revealing some of the underlying hepatic mechanisms to explain the lipostimulatory effects of MBH DEX, plasma and livers of the RC-fed rats were obtained following experimentation and was assessed for hepatic regulators of lipid metabolism. Proteins and genes involved in lipogenesis, VLDL secretion, and fatty acid oxidation were assessed via western blotting and/or quantitative real time polymerase chain reaction (qRT-PCR). Plasma concentrations of apoB-48 and apoB-100 were also be assessed via western blotting. It is anticipated that as plasma TG levels increase, plasma apoB-48 and apoB-100 similarly increase regardless of treatment group. Plasma was analyzed for TG and FFA content. Plasma TGs will increase over the duration of the experiment due to an intravenous injection of poloxamer, a lipoprotein lipase inhibitor at the beginning of the experiment. It is anticipated that the increase in plasma TGs is independent of changes in plasma FFAs.

1.6.2. Objective 2: To assess blocking GC action and delineate GR requirements in the MBH in regulating VLDL-TG secretion in diet-induced hyperlipidemic rats

Previous literature has clearly shown that 3-day HFD feeding leads to a pre-obese model that shows signs of early onset metabolic disease via various changes in the metabolic profile, including disrupted hypothalamic nutrient sensing, hyperinsulinemia, hyperglycemia, hypertriglyceridemia, and increased VLDL-TG secretion independent of changes in body weight^{112,264,297,340,341}. Moreover, long-term (12 weeks) HFD-feeding is associated with altered HPA activity and increased basal plasma GCs¹⁹⁸. Further, Yue et al., has previously demonstrated that in this 3-day HFD feeding model, there is a significant increase in basal plasma GCs^{333,334}. Thus, it was hypothesized that the increase in plasma GCs, as a result of HFD feeding, could act in the MBH on the GRs and contribute to the dyslipidemia observed in these models. Further, it was anticipated that the antagonism of the GRs within the MBH should lower VLDL-TG secretion in 3-day HFD fed hypertriglyceridemic rats (Figure 1.4, pathway 2).

Genetic knockdown of the GR in the MBH to assess whether blocking MBH GRs would lead to improved lipid profiles in diet-induced hyperlipidemic rats was achieved via MBH

specific GR shRNA in pre-obese rats. These experiments tested whether MBH GC action contributes to the aberrant lipid metabolism observed in HFD-feeding. Further, once increased GC action in the MBH has been implicated in the dysregulation of lipid metabolism in the 3-day HFD rodents, Hsp90 was investigated. Again, this was to further implicate the necessity of GRs as Hsp90 is necessary for the biological function and stability of the GR¹⁸⁵⁻¹⁸⁹. The effects of chemical and genetic knockdown of Hsp90 in pre-obese on lipid metabolism was assessed.

Comparison of hepatic proteins and genes involved in hepatic lipid homeostasis will be assessed in different HFD treatment groups and compared to RC-fed rats via western blotting and/or qRT-PCR. This will help delineate some of the underlying hepatic mechanisms responsible for the changes observed in hepatic lipid homeostasis. Again, it is anticipated that the changes in plasma TGs are specifically from liver derived VLDL-TGs and not chylomicrons due to previous literature demonstrating nearly undetectable amounts of chylomicrons in 4-hour fasted rats^{112,263}. Plasma analysis for TGs, apoB-48, apoB-100, and FFAs will also be assessed. It is anticipated that as plasma TG levels increase following an intravenous injection of poloxamer, plasma apoB-48 and apoB-100 would similarly increase regardless of treatment group. It is anticipated that the increase in plasma TGs over time is independent of changes in plasma FFAs.

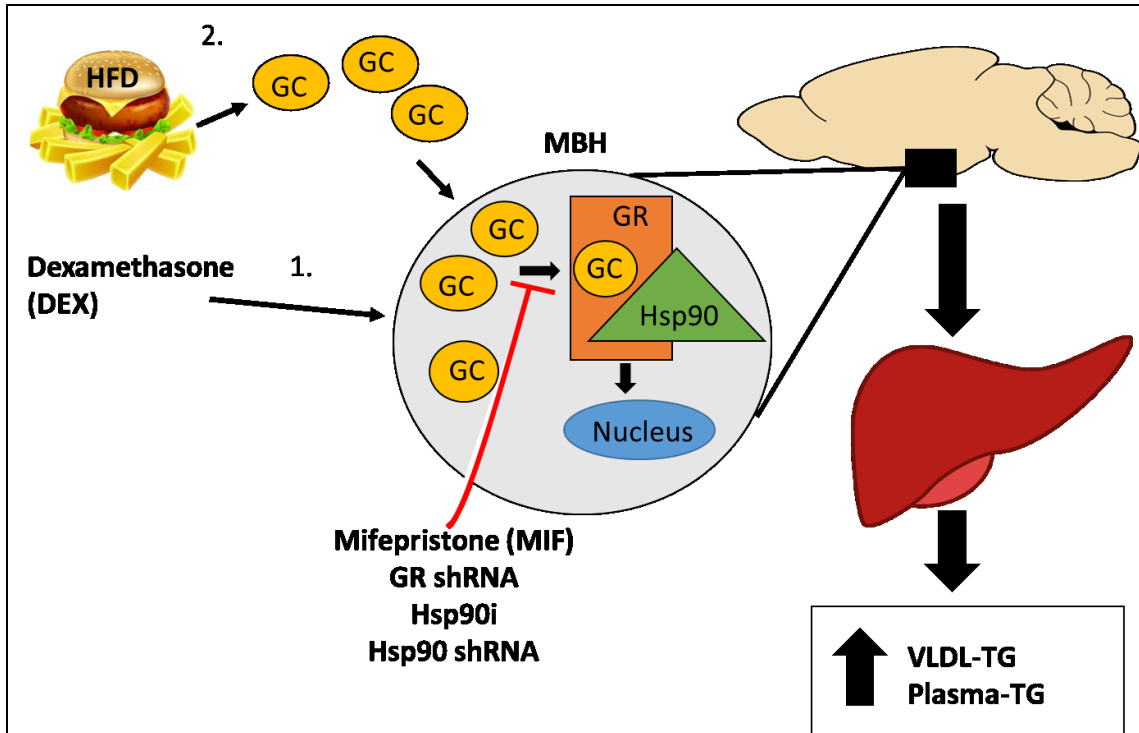


Figure 1.4- Schematic representation of overall working hypothesis. (1)

Glucocorticoids (GC) act via glucocorticoid receptors (GRs) in the medial basal hypothalamus (MBH) MBH to modulate liver lipid homeostasis by increasing plasma triglycerides (TGs) and hepatic TG rich very-low density lipoprotein (VLDL-TG) secretion.

GCs, in the form of synthetic GC dexamethasone (DEX) can act on MBH GRs to lead to increased VLDL-TG secretion and plasma TGs. However if the GRs are antagonized, either pharmaceutically via mifepristone (MIF), genetically via GR shRNA, or by targeting downstream targets such as heat shock protein 90 (Hsp90)

(pharmacologically with Hsp90 inhibitor (Hsp90i) or genetically with Hsp90shRNA), we should block the lipostimulatory effects of DEX. (2) The inhibition of MBH GC action

(by blocking MBH GRs or downstream mediators of GC-GR action specifically within the MBH) will improve liver lipid metabolism in diet-induced hyperlipidemic rats.

High fat diet (HFD) feeding- induced hyperlipidemia has been shown to increase peripheral GCs, which could act in the MBH to contribute to hyperlipidemia. It is expected that antagonizing GRs, either, genetically via GR shRNA, or by targeting downstream targets such as Hsp90 should lower VLDL-TG secretion in HFD fed rats.

Chapter 2: Methods

2.1. Animal care, maintenance, and surgical procedures

All procedures and protocols for animal care and experiments were approved by the University of Alberta Animal Care and Use Committee (protocol N°1604) in accordance with regulations set forth by the Canadian Council for Animal Care. Male Sprague Dawley (SD) (Charles River Laboratories, Montreal, QC) rats were used for *in vivo* experimentation. Male rats SD were used as previous literature has shown that male SD rats fed a 10% lard-oil enriched diet for as little as 3 days develop a pre-obese phenotype (hypertriglyceridemia, hyperinsulinemia, hyperglycemia, insulin resistance, and increased hepatic triglyceride (TG)-rich very-low density lipoprotein (VLDL-TG) secretion) with brain hormone sensing defects that dysregulate lipid and glucose metabolism^{112,264,297,340,341}. Eight-week-old rats arrived weighing 190-200g and were individually housed in individual cages on a standard 12-12h light-dark cycle and given ad libitum access to water and standard regular chow (RC) (LabDiet PicoLab[®] Laboratory Rodent Diet, 5LOD; 60% cal. from carbohydrate, 28% cal. from protein, and 12% cal. from fat; 3.0 kcal/g of total metabolized energy). A subset of rats were subjected to a 3-day 10% lard oil enriched high fat diet (HFD) (HFD is comprised of 90% RC combined with 10% saturated fat (lard oil)) (TestDiet Modified LabDiet[®] Laboratory Rodent Diet, 5001; 44% cal. from carbohydrate, 22% cal. from protein, and 34% cal. from fat; 3.9 kcal/g of total metabolized energy) following vascular catheterization surgery (described below).

2.1.1. MBH stereotaxic bilateral cannulation surgery

Rats were acclimated for one-week following delivery, followed by being subjected to bilateral stereotaxic cannulation under anesthesia (intraperitoneal administration of 60mg/kg ketamine (Ketalean, Bimeda-MTC), 8mg/kg xylazine (Rompun, Bayer)). Medial basal hypothalamic (MBH) bilateral cannulation enabled direct MBH infusions of various brain treatments on experimentation day, such as dexamethasone (DEX) (Sigma, D1756; 100ng/ μ l) a synthetic glucocorticoid (GC), mifepristone (MIF) (Tocris #1479; 25nM) a GC receptor (GR) antagonist, heat-shock protein 90 inhibitor (Hsp90i) (Tocris #1515; 0.606nmol/ μ l) an acute inhibitor of Hsp90, which is required for GR function and stability, or 0.9% saline vehicle (Veh). Stereotaxic implantation of 26-gauge, stainless steel bilateral guide cannula (C235G, Plastics One Inc.) into the MBH occurred in rats following the coordinates 3.1mm posterior to bregma, 0.4mm lateral to midline, 9.6mm below the cranial surface^{112,297,333,334}. Immediately after cannulation, a subset of rats received a 3 μ l injection in each cannula of a lentivirus (LV) that

expressed GR shRNA (Santa Cruz Biotechnology, sc-35506-V), Hsp90 shRNA (Santa Cruz Biotechnology, sc-156099-V), or a control mismatch (MM) sequence (Santa Cruz Biotechnology, sc-108080). MBH cannulation placement confirmation, and to confirm the localization of brain infusions to the MBH, 3 μ l of bromophenol blue dye was injected into the bilateral cannula at the end of the *in vivo* experimentation.

2.1.2. Vascular catheterization

Eight days following brain cannula implantation, rats were subjected to vascular catheterization surgery to enable for intravenous (i.v.) infusions and repeated arterial blood sampling without stressing the rat during experimentation. The left carotid artery and right jugular vein were catheterized while the rats anaesthetized (intraperitoneal administration of 90mg/kg ketamine, 10mg/kg xylazine) using catheters consisting of polyethylene (PE-50) (ID: 0.58mm, OD: 0.965mm; Becton, Dickinson and Company) and silastic tubing (Jugular: ID 0.64mm, OD: 1.19mm; Carotid: ID: 0.51mm, OD: 0.94mm; Dow Corning Corporation)^{112,297,333,334}. Catheters were filled with 10% heparinized saline following surgery to maintain patency and were sealed with a metal pin. Additionally, rats were treated with analgesic (2mg/kg Metcam) for 2 days postoperatively. Again, a subset of rats were subjected to 3-day HFD feeding following vascular catheterization. Body weight and food intake was assessed daily following surgery to ensure animal welfare and recovery of all rats. Only rats that attained a minimum of 90% of their pre-vascular body weight were used for the *in vivo* studies.

2.2. *In vivo* VLDL-TG secretion studies

Approximately 13 days post-MBH cannulation, 10-hour fasted, freely moving, conscious rats were subjected to a pre-infusion of continuous MBH infusions of specific brain treatments (saline, DEX, MIF, MIF+DEX, Hsp90i, or Hsp90i+DEX) (0.0055 μ L/min infusion) followed by a i.v. injection of poloxamer (Poloxamer 407) (Sigma, #16758, 600 mg/kg, dissolved in saline)^{112,264}. Poloxamer inhibits endogenous lipoprotein lipase (LPL), and thus blocks the clearance of TG-rich lipoprotein particles, therefore, the rate of appearance of plasma TGs as a function of time will yield the rate of TG-rich lipoprotein secretion^{112,261,264,342}. Due to the rats being fasted for 10-hours, TG-rich lipoprotein secretion will most likely be derived from liver derived VLDL-TGs, and not from gut derived chylomicrons. Previous literature has shown that following a 4 hour fast in a similar rat model, chylomicron-TGs were barely detectable compared

to ad-libitum fed controls, suggesting that chylomicrons do not contribute to the observed changes in TG-rich lipoprotein secretion in the current study^{112,263}. Thus, all reports of VLDL-TG secretion in this thesis are based on the assumption that in this particular 10-hour fasted model chylomicrons do not play a significant role in TG-rich lipoprotein secretion. However, we cannot definitively say that chylomicrons did not play a role in this study as lipid fractions were not assessed. Following the pre-infusion and i.v. injection of poloxamer, which is considered time (t) 0 of the experiment, or the beginning of the experiment, intra-arterial plasma samples (~350µl) were collected over 300 minutes at half hour increments. Plasma was separated via centrifugation and immediately analyzed for glucose concentration via the glucose oxidase method (Glucose Analyzer GM9, Analox Instruments). Briefly, the reagent solution used in the apparatus contains glucose oxidase, which catalyzes the oxidation of glucose in the plasma sample to gluconic acid and hydrogen peroxide, and the rate of oxygen consumption by the sample is directly related to glucose concentration. The Clark-type amperometric oxygen electrode within the analyzer measures oxygen concentration in the plasma. Plasma was then treated with heparin or protease inhibitor (Roche, #11836170001) and stored at -20°C for analysis of TGs, FFAs, apoB-48, and apoB-100. The packed red blood cells were resuspended in 0.2% heparinized saline and reinfused into the rat to prevent hypovolemia and anemia. Following experimentation (t=300min) rats were anesthetized with a 50µl i.v. injection of ketamine and euthanized via decapitation. Brain (MBH wedges) and liver samples were collected immediately, flash frozen in liquid nitrogen, and stored at -80°C for future analysis of gene or protein expression (Figure 2.1).

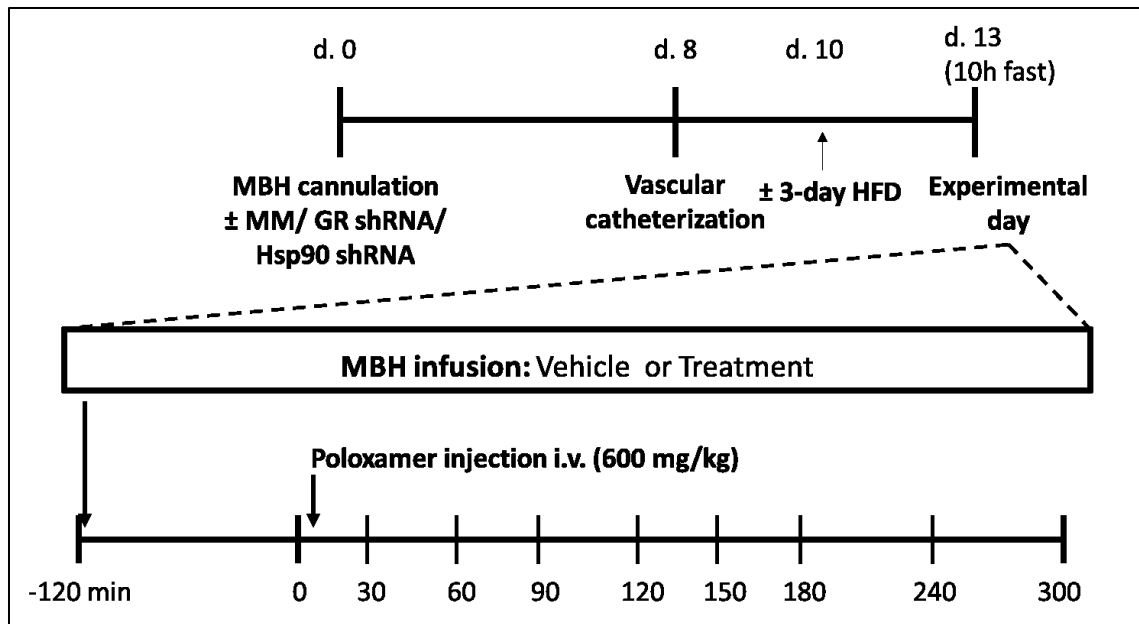


Figure 2.1- Animal protocol and VLDL-TG secretion experiment. Male Sprague Dawley rats received stereotaxic medial basal hypothalamus (MBH) bilateral cannulation. During MBH cannulation, some rats were subjected to MBH specific lentivirus-either glucocorticoid receptor (GR) shRNA, which acted as a GR knockdown, heat shock protein 90 (Hsp90) shRNA which knocks down Hsp90, or a mismatch (MM) sequence to act as a control. Following cannulation, vascular catheterization surgery was performed to enable intravenous (i.v.) injections, and blood sampling. Some rats were subjected to 3-day high fat diet (HFD) feeding on day 10. Following 13 days post MBH cannulation, rats were subjected to a 10-hour fast. On the day of experimentation, rats were subject to a pre-infusion of brain treatments, followed by an i.v. injection of poloxamer, a lipoprotein lipase inhibitor. Blood samples (~350 μ l) were collected every half hour for a total of 300 minutes. Rats were then euthanized via decapitation for tissue collection.

2.3. Plasma TG assay

Plasma TG levels were quantified via enzymatic colorimetric analysis using commercial assay kits that are specific for plasma TGs and not total lipids (Roche Diagnostics, #11877771216 (discontinued in 2020) and Fujifilm Wako Chemicals Lab, #994-02891, 990-02991, 992-02892, 998-02992, and 464-01601). Both commercial assay kits follow the same principles and were compared to ensure comparable data. The principle of this two-step assay is

based on the elimination of free glycerol of a plasma sample, followed by the hydrolysis of TGs to glycerol which is then oxidized to generate a product that reacts with peroxidase and generates a colour that can then be measured on a microplate spectrophotometer reading the correct absorbance at different wavelengths (540nm for the Roche kit and 600nm and 700nm for the Wako kit). The TG concentration of each plasma sample is obtained by interpolating the absorbance of each sample to a standard curve of known concentration values.

Though the two commercial assay kits use slightly different protocols, the individual steps remain the same. The individual protocol for each assay kit was used as follows. A glycerol standard curve (Sigma, G7793, for the Roche kit and Fujifilm Wako #464-01601 (reconstituted in distilled water) for the Wako kit) of known TG concentrations was loaded in duplicate onto sterile, non-treated polystyrene 96-well assay plate (Corning, 9017). Plasma samples were centrifuged at 2500rpm at 4°C for 30 seconds then placed on ice. Plasma samples collected from each time point were then added to individual wells (10µl of 5x diluted plasma sample for Roche kit, 4µl of undiluted plasma for Wako kit). The first reagent (R1) is then added to each well (100µl for Roche kit, note for Roche protocol R1 is added before plasma samples are loaded, or 90µl for Wako kit). R1 decomposes free glycerol via glycerol kinase, glycerol-3-phosphate oxidase, and catalase to produce an oxidation product which does not contribute to the colorimetric reaction. The Wako kit requires an incubation step of the plate at 37°C for 5 minutes. The 96-well plates were then placed in the microplate reader (Epoch, BioTek) for measurement of absorbance at wavelengths of 540nm for the Roche kit and 600nm and 700nm for the Wako kit. For the Wako kit, the difference of the 600nm and 700nm absorbances was then quantifying to obtain concentration values. Following the initial read, reagent 2 (R2) was added to each well (100µl for Roche kit, 30µl for Wako kit). R2, which contains LPL, glycerol kinase, and glycerol-3-phosphate oxidase, hydrolyses the TGs in the plasma sample to glycerol, which after a series of enzymatic reactions yields hydrogen peroxide, which contributes to the oxidative condensation of various enzymes, catalyzed by peroxidase, which produces colour change of each sample based on the availability of glycerol. Again, following this step, the Wako kit requires an incubation step at 37°C for 5 minutes, while the Roche kit requires a 1-hour incubation at room temperature. The plate is again placed into the microplate reader (Epoch, BioTek) for measurement of absorbance at wavelengths of 540nm for the Roche kit and 600nm and 700nm for the Wako kit. When quantifying the data, the sample background controls (first

read after R1) were subtracted from the sample reading, and the absorbance values of these corrected values were plotted against the reference curve from the known standard to determine the amount of TG per well (mM).

2.4. Hepatic TG content

Hepatic TG content was quantified using a modified version of the Folch method³⁴³. The principle of this procedure is that the initial step, which is homogenized liver tissue samples in a 2:1 mixture of chloroform (Fisher chemical, C298-1) and methanol (Sigma-Aldrich, 34860-4L-R) results in non-extractable residue and one liquid phase which contains an array of small biomolecules³⁴⁴. When a buffer is added to the mixture a new aqueous phase is formed³⁴⁴. The upper phase is predominantly methanol, water, hydrophilic components, and salts³⁴⁴. The lower phase is mostly chloroform, which retains lipids. The lower phase is washed with water or buffer to minimize the amount of non-lipid components³⁴⁴.

The protocol is as follows. Approximately 50mg of frozen liver samples were obtained and placed in a 12x75mm glass tube (Fisher Scientific, 14-961-26). Actual weights of liver samples were recorded so that TG concentration could be accurately assessed following the TG assay (μg of TGs per mg of liver). The liver was homogenized in 5ml of a 2:1 chloroform: methanol solution. The tubes were wrapped in parafilm and left overnight. The following day the parafilm was removed from the glass tubes, and the solution was filtered through #1 Whatman[®] paper (4.25cm, #1001 042) into 13x100mm glass tubes (Fisher Scientific, 14-961-27). 2ml of 2:1 chloroform: methanol solution was added to the initial 12x75mm glass tube and then poured through the Whatman paper to extract all TG from the solution. An acidified saline solution was prepared with 100ml of 0.9% saline solution and 1ml of 1N HCl (Fisher Scientific, SA48B-1). 1.25ml of acidified saline solution was added to the filtrate, which was then vortexed. The vortexed solution sat at room temperature for 5 minutes and was then centrifuged at 1000rpm for 15 minutes. The upper phase of the solution was removed via Pasteur pipette (Fisher Scientific, 13-678-20C) and disposed. The above process of adding acidified saline, centrifuging the sample, and removing the top layer was then repeated. Additionally, a 'upper phase solution' was prepared, which consists of methanol (480ml/L), water (470ml/L), chloroform (30ml/L) and calcium chloride dihydrate (400ml/L) (Fisher Scientific, BP5100500). Similar to previous steps, 1.25ml of this upper phase solution was added to the precipitate, which was vortexed,

centrifuged, and the top layer was removed. This step was also repeated. Following these steps the samples were then dried down using nitrogen gas. The remaining pellet was then resuspended and dissolved with 100 μ l of 100% ethanol (Commercial Alcohols, Greenfield Global, P016EAAN). The sample was diluted at a 1:5 ratio and was then used in the previously mentioned 'Plasma TG assay' protocol. The Roche Diagnostics Kit (see above for details) was used when quantified hepatic TG content, which is again specific to TGs.

2.5. Plasma FFA assay

Plasma free fatty acids (FFAs) was quantified were measured via enzymatic colorimetric analysis using a commercial assay kit (Fujifilm Wako Chemicals Lab #999-34691, 995-34791, 991-34891, 993-35191, and 276-76491). The principle of this two-step assay is that plasma FFAs can form acyl-CoAs when treated with acyl-CoA synthetase, which can then be oxidized to produce hydrogen peroxide which in the presence of peroxidase allows for various oxidative condensation reactions to form a colour which can then be measured on a microplate spectrophotometer at optimal density. The FFA concentration of each plasma sample is obtained by comparing the absorbance of each sample to a standard curve of known concentration values.

The protocol provided by the manufacturer with the assay kit was used as follows, and the samples were assayed in duplicate. The standard curve, using the nonesterified fatty acid C standard (1.0mM oleic acid) (0, 0.1, 0.2, 0.3, 0.4, 0.5, 0.7, 1.0 mM) was prepared with double distilled water. Additionally reagent 1 (R1) and reagent 2 (R2) were prepared by reconstituting the applicable solvent to the applicable solute and stored on ice. Plasma samples from $t=0$ mins (beginning of experiment) and $t=300$ mins (end of experiment) were centrifuged at 2500rpm at 4°C for 30 seconds then placed on ice. In a sterile non-treated polystyrene 96 well assay plate (Corning, 9017), 5 μ l of each standard and sample in duplicate was added to the appropriate well, followed by 200 μ l of R1. The plate then sat in an incubation over at 37°C for 5 minutes. R1 is required as it contains acyl-CoA synthetases and adenosine triphosphate and CoA, which reacts with the FFA in the serum to produce acyl-CoA. Following this step, 100 μ l of R2 was added to all the wells, and the plate was incubated at 37°C for 5 minutes. R2, which contains acyl-CoA oxidase and peroxidase, catalyzes the enzymatic colorimetric reaction, leading to a coloured end product with an absorption maximum at 550nm. Therefore, the concentration of FFAs in the

sample can be determined from the optical density measured at 550nm relative to known concentrations from the standard curve.

2.6. Western blotting

Both tissue samples (liver and MBH) and plasma (for plasma apoB) were used for protein analysis via western blotting. Both tissue and plasma follow similar core procedures for western blotting, with slight variations, as described below.

2.6.1. Tissue western blotting

Proteins of interest from frozen liver tissue and MBH wedges that were obtained after experimentation were analyzed via western blotting. Liver tissue (~20mg) and MBH wedges (~10mg) were homogenized with a Dounce homogenizer at a dilution factor of 1:10 in 1% NP-40 lysis buffer (20mM Tris-HCl (pH 7.4), 5mM EDTA, 1% (w/v) Nonidet P-40, 2mM sodium orthovanadate, 5mM sodium pyrophosphate tetrabasic, 100mM sodium fluoride, phosphatase, and protease inhibitor). Homogenized samples sat on ice for 30 minutes, followed by centrifugation at 1200xg for 30 minutes at 4°C. The supernatant was collected and transferred into a new tube on ice. Protein concentration of the lysate, as well as the concentration of sample to be used to prepare a loading sample for loading onto a gel for western blotting was determined using the Pierce™ BCA Protein Assay Kit (Thermo Scientific, 23225). Lysate samples were diluted with double distilled water at a 1:20 ratio for liver and 1:10 ratio for MBH and the microplate protocol provided with the assay kit was used.

Liver and MBH loading samples with a final concentration of 1.67µg/µl (25µg of protein/lane and 15µl of volume of load sample per lane), were loaded onto a polyacrylamide gel (5%, 8%, 12%, 15%, depending on the molecular weight (MW) of the protein of interest) and were subjected to gel electrophoresis (Mini-PROTEAN® Tetra Vertical Electrophoresis Cell, Bio-Rad) and were transferred (90V for 2 hours and 30 minutes at 4°C) to nitrocellulose membranes (0.45 µm, Bio-Rad, #1620115). To confirm the efficiency of protein transfer, Membranes were stained and destained (MemCode™ Reversible Protein Stain Kit, Thermo Scientific; #24580, or Ponceau S Solution, Abcam, ab270042 (destained blocking buffer)). Membranes were then incubated in blocking buffer (5% milk in Tris-buffered saline containing 0.2% Tween-20 (TBST) (Sigma, P1379)) for 1 hour at room temperature on a rotary platform and rinsed with 1xTBST. Membranes were then incubated overnight at 4°C in primary antibody solutions diluted

as shown in table 2.1 for liver samples (FAS, MTP, DGAT1, P-ACC, ACC, Arf1), and for MBH tissue (GR). Tubulin, β -actin, and GAPDH were used as loading controls (table 1.1). Membranes were then washed three times with 1x TBST for 5 minutes following primary antibody dilution, then incubated in horseradish peroxidase-linked secondary antibody (table 1.2) solution diluted 1:1000 in blocking buffer for 1 hour at room temperature on a rotating platform. Following incubation, the membranes were washed three times with 1x TBST for 10 minutes and protein expression was enhanced using a chemoluminescence reagent (Western Lighting[®] Plus-ECL, PerkinElmer; NEL105001EA, or, Clarity[™] Western ECL Substrate, Bio-Rad, 170-5061, or, Pierce[™] ECL Western Blotting Substrate, thermo scientific, 32106). Immunoblots were detected via chemiluminescent imaging system (Bio-Rad ChemiDoc), quantified by densitometry with ImageJ image analysis software, and normalized for the total protein using loading controls.

2.6.2. Plasma apoB western blotting

Plasma that was treated with protease inhibitor was diluted by 1:50 via adding 2 μ l of plasma in 98 μ l of double distilled water, plus 100 μ l of 2x Laemmli Sample Buffer (Bio-Rad, 1610737). The diluted samples were then boiled for 5 minutes. On a 4-15% gradient gel (4-15% Mini-PROTEAN[®] TGX[™] Precast Protein Gels, Bio-Rad, #4561086), 10 μ l of diluted sample was added, and was subject to gel electrophoresis with a constant current for approximately 3 hours to let the gradient run out. Following this step, the gel was transferred (90V for 2 hours and 30 minutes) onto a nitrocellulose membrane (0.45 μ m, Bio-Rad, #1620115). Again, membrane was stained and destained (MemCode[™] Reversible Protein Stain Kit, Thermo Scientific; #24580) to confirm efficacy of transfer. Membranes were then incubated in blocking buffer for 1 hour at room temperature on a rotary platform and rinsed with 1x TBST. Membranes were then incubated overnight at 4°C in primary antibody solutions diluted as shown in Table 2.1 (apoB-48, apoB-100). The membranes were then washed in 1x TBST and incubated in horseradish peroxidase-linked secondary antibody (Table 2.2) solution diluted 1:1000 in blocking buffer for 1 hour at room temperature. Similar to westerns with tissues, the membrane was washed with 1xTBST, protein expression was enhanced with using a chemiluminescence reagent (Western Lighting[®] Plus-ECL, PerkinElmer; NEL105001EA), imaged using a chemiluminescent imaging system, and quantified by densitometry via ImageJ image analysis software.

Table 2.1- Primary antibodies used for western blotting

Antibody and molecular weight	Company name and catalog number	Dilution	Secondary antibody
Anti- Fatty acid synthase (A-5) (FAS)- 270kDa	Santa Cruz #sc-55580	1:1000	GAM
Anti-MTP (MTP)- 97kDa	BD Transduction Laboratories #612022	1:1000	GAM
Anti-DGAT1 (DGAT1)-55kDa	Novus Biologicals #NB110-41487SS	1:500	GAR
Anti-P-ACC (Ser79) (P-ACC)-265, 280kDa	Cell Signaling #3661	1:1000	GAR
Anti-ACC (ACC)-265, 280kDa	Cell Signaling #3662	1:1000	GAR
Anti-Arf1 (Arfs 1A9/5) (Arf1)-~20kDa	Santa Cruz #sc-53168	1:1000	GAM
Anti-apoB (A-6) (apoB-48)-250kDa, (apoB-100)-500kDa	Santa Cruz #sc-393636	1:500	GAM
Anti-Glucocorticoid Receptor (D8H2) (GR)-94kDa	Cell signaling #3660	1:1000	GAR
Anti- β -actin (C4) (β-actin)- 43kDa	Santa Cruz #sc-47778	1:1000	GAM
Anti-GAPDH (A-3) (GAPDH)-37kDa	Santa Cruz #sc-137179	1:1000	GAM
Anti- α -Tubulin (Tubulin)-52kDa	Cell Signaling #2144	1:1000	GAR

Table 2.2- Secondary antibodies used for western blotting

Secondary antibody	Company name and catalog number	Dilution
Anti-mouse IgG, HRP-linked Antibody (GAM)	Cell Signaling #7076	1:1000
Anti-rabbit IgG, HRP-linked Antibody (GAR)	Cell Signaling #7074	1:1000

2.7. Liver mRNA expression analysis

The mRNA expression of liver liporegulatory genes involved in *de novo* lipogenesis (*Srebf1c*, *Fasn*, *Nr1h3*, *Nr1h2*), VLDL-TG production and secretion (*Scd1*, *Cideb*, *Lpin2*, *Dgat1*, *Dgat2*, *Arfl*) and fatty acid oxidation (*Cpt1a*, *Ppara*, *Ampk*) were analyzed using two-step qRT-PCR.

2.7.1. RNA extraction

First, RNA was extracted from homogenized liver using Trizol (Ambion[®], 15596026) and quantified using a Nanodrop spectrophotometer (260/280nm). In sterol microtubes, ~35-50mg of liver tissue was homogenized in 1ml of ice cold Trizol. This sample was centrifuged at 8700 rpm for 10 minutes at 4°C. The supernatant was transferred to a new sterile tube and 200µl of chloroform was added to the solution, which will lead to a phase separation where protein is extracted to the organic phase and RNA remains in the aqueous phase. The solution sat at room temperature for 2-3 minutes followed by centrifugation at 8700 rpm for 15 minutes at 4°C. The upper phase was then transferred to a new sterile microtube, where 500µl of isopropanol (Sigma-Aldrich, 439207) was added. The samples were mixed via inverted samples several times, and then incubated overnight at -20°C.

The following day the samples were centrifuged at 12,000xg for 10 minutes at 4°C. Following this step, the supernatant was removed and discarded. 1ml of 75% ethanol was added to the solution, which was then centrifuged at 7500xg for 5 minutes. Following centrifugation, the supernatant was removed. This step of adding ethanol, centrifuging, and discarding the supernatant was repeated 2-3 times in attempt to remove any remaining Trizol contamination.

The samples then air dried at room temperature for 30 minutes. Pellets were resuspended in 100µl of RNase free water.

Quantification of RNA content was performed by measuring the optical density at 260 and 280nm using 1.5µl of sample with a NanoDrop 1000 spectrophotometer (Thermo Fisher). As a quality control step for RNA, the ratio of 260/280 should be between 1.8 and 2. Any samples not within this threshold were not used.

2.7.2. cDNA synthesis

After RNA extraction, first-strand complementary DNA (cDNA) was synthesized using Superscript IITM IV VILO Master Mix kit (Invitrogen, #11756050). Using the concentration of RNA determined by the NanoDrop, the volume of sample needed to make a sample with exactly 2µg of total RNA in 9µl of RNase free water (Invitrogen, #10977-015) was determined. Following this step, the samples were primed by adding 2µl of Random Hexamer Primers (1µg/µl) (Invitrogen, #48190011) to each sample and ran through a PCR program (Eppendorf, Mastercycler gradient) to be denatured (70°C for 10 minutes). A master mix was prepared using Superscript IITM IV VILO Master Mix kit (Invitrogen, #11756050), and 9µl was added to each sample, yielding a final volume of 20µl per sample. The sample was then ran through a PCR program for cDNA transcription at 40°C for 1 hour to yield cDNA at a concentration of 100ng/µl. cDNA was then diluted to a ratio of 1:100 using RNase-free water for a final concentration of 1.0ng/µl, except for cDNA used for *srebflc*, which was diluted to a ratio of 1:10 for a final concentration of 10.0ng/µl.

2.7.3. qRT-PCR

Quantification of qRT-PCR was performed in a StepOneTM Real-Time PCR Systems (Applied BiosystemsTM) in duplicates. Initial qRT-PCR work, which assessed mRNA expression of *Srebflc*, *18s*, and *Scd1*, was performed on MicroAmpTM 48-Well Reaction Plates (Applied BiosystemsTM, #4375816) using TaqManTM Gene Expression Assays (Table 2.3) and TaqManTM Universal PCR Master Mix (Applied BiosystemsTM, #4304437) per the manufacturer's instructions.

In collaboration with the Dr. Richard Lehner laboratory, the rest of the genes of interest were analyzed on MicroAmpTM 96-Well Reaction Plate with Barcode (Applied Biosystems, #4346906) using POWER SYBR Master Mix (Applied Biosystems, #4367659) and custom

designed primers (Table 2.4), developed by Integrated DNA Technologies. Expression values were normalized to the internal control gene, Cyclophilin (gene name: *Ppia*) or *18s* for the efficiency of amplification and quantified via the $2^{-\Delta\Delta C_t}$ method³⁴⁵. The expression values of *Ppia* or *18s* did not vary between experimental groups, thus, they are considered suitable controls.

Table 2.3-TaqMan™ gene and probes used for gene expression analysis

Gene name	Company name and catalog number
Sterol regulatory element binding transcription factor 1 (<i>Srebflc</i>)	Applied Biosystems #Rn01495769_m1
Stearoyl-Coenzyme A desaturase 1 (<i>Scd1</i>)	Applied Biosystems Rn00594894_g1
Ribosomal protein s18-like (<i>18s</i>)	Applied Biosystems Rn01428915_g1

Table 2.4-Custom primer sequences for gene expression analysis

Gene name	Forward primer sequence	Reverse primer sequence
<i>Cideb</i>	GAG CTG GAG CCC AAA GAG T	GGC GAT GTC CTT GCT ATG TT
<i>Nr1h3</i>	GCA GTG CCT GAT GTT TCT CC	CAG TTG ATT GGG GCA TCC T
<i>Nr1h2</i>	TCC AGC TCT GCC TAC ATC GT	GGA CCC TTC TTC CGC TTG
<i>Ampk</i>	CCG TCT GAT ATT TTC ATG GTC A	ACT CTC CTT TTC GTC CAA CCT
<i>Arfl</i>	TGG CGC CAC TAC TTC CAG	TCG TTC ACA CGC TCT CTG TC
<i>Dgat1</i>	TAC GGC GGG TTC TTG AGA T	CGT GAA TAG TCC ATG TCC TTG A
<i>Dgat2</i>	GTG TGG CGC TAT TTT CGA G	GGT CAG CAG GTT GTG TGT CTT

<i>Fasn</i>	GTG GAC ATG GTC ACA GAC GA	CGC TTA GGC AAC CCA TAG AG
<i>Lpin2</i>	AAG ATG CCG AAG AAA TCT GG	CTT GGT CTC CGG CAA CTG
<i>Cpt1a</i>	ACA ATG GGA CAT TCC AGG AG	AAA GAC TGG CGC TGC TCA
<i>Ppara</i>	TGC GGA CTA CCA GTA CTT AGG G	GGA AGC TGG AGA GAG GGT GT
<i>Ppia</i>	TCC AAA GAC AGC AGA AAA CTT TCG	TCT TCT TGC TGG TCT TGC CAT TCC
<i>I8s</i>	TTC GAA CGT CTG CCC TAT CAA C	GAA CCC TGA TTC CCC CGT CAC

2.8. Statistical analysis

Statistical analyses were calculated with GraphPad Prism software. In statistical analysis of two groups, unpaired Student's t-tests were performed. For comparisons of more than two groups, analysis of variance (ANOVA) was performed assuming unequal standard deviation, and if significant, was followed by Dunnett's or Tukey's post-hoc tests when appropriate. Repeated measures ANOVA will compare measurements taken repeatedly over time, assuming unequal standard deviation. If the time and treatment interaction between groups was found to be significant, multiple t-tests were used to determine the statistical significance at specific time points between groups. The P value lower than 0.05 was considered statistically significant.

Chapter 3: Results

All surgeries performed on rats prior to experimentation were performed by Bryan Lum and Dr. Jessica Yue. Some VLDL-TG secretion studies were performed by undergraduate students Mark Wang, Emily Ling, Hongju (Jennifer) Lee, Bethany Chan, and Eyram Asem. Plasma and hypothalamic western blotting was performed by Carrie-Lynn Soltys. Plasma corticosterone and plasma insulin radioimmunoassays were performed by Emilie Beaulieu-Bayne.

3.1. Acute glucocorticoids act on glucocorticoid receptors in the medial basal hypothalamus to stimulate hepatic triglyceride secretion in regular chow-fed rats.

To assess whether glucocorticoid (GC) action in the medial basal hypothalamus (MBH) regulates triglyceride (TG)-rich very-low density lipoprotein (VLDL-TG) secretion *in vivo*, we first tested the effect of direct MBH GC infusion on 10-h fasted, conscious, freely moving Sprague Dawley (SD) rats on a regular chow (RC)-diet. Note that VLDL-TG secretion rate is based on the rate of appearance of TGs in the plasma over the duration of the experiment. It is assumed that the TG-rich lipoproteins are liver derived VLDL-TGs based on the assumption that chylomicrons do not significantly contribute to TG-rich lipoprotein secretion in 4-hour fasted rat models^{112,263}. However, lipid fraction assessment is required to confirm the contribution of gut-derived chylomicrons.

The MBH infusion of dexamethasone (DEX), a synthetic GC, significantly increased plasma TG (Figure 3.1a), and VLDL-TG secretion (Figure 3.1b), compared to vehicle (Veh). The MBH infusion of mifepristone (MIF), a GC receptor (GR) antagonist, had no effect on plasma TGs, similar to that of the Veh group, suggesting that the inhibition of GRs in the MBH does not have an effect on plasma TGs. Importantly, the co-infusion of MIF+DEX into the MBH saw the lipostimulatory effects of DEX diminished (Figure 3.1a-b), suggesting that DEX can act on GRs in the MBH to increase plasma TGs and VLDL-TG secretion and this effect can be negated via the co-infusion of MIF+DEX. However, there was no significant change in hepatic TG content between the four groups (Figure 3.2). Though, MBH DEX and MBH MIF+DEX both decreased hepatic TG content relative to controls, however this may be due to the sample-size variability (Figure 3.2). As plasma glucose and FFAs can be used as substrates for TG synthesis, plasma glucose and FFAs were assessed^{29,63,140,141}. There was no change in basal (time=0 min) or end of experiment (t=300 min) plasma free fatty acids (FFAs) (Figure 3.3a) or plasma glucose (Figure 3.3b), suggesting that the increase in VLDL-TG secretion induced by DEX in the MBH was independent of changes in plasma FFAs and glucose. Thus, DEX was able to stimulate VLDL-TG production by acting on GRs within the MBH, and this hyperlipidemic effect can be negated by blocking GRs with MIF within the MBH, an effect independent of changes in hepatic TG storage and levels of FFAs and glucose.

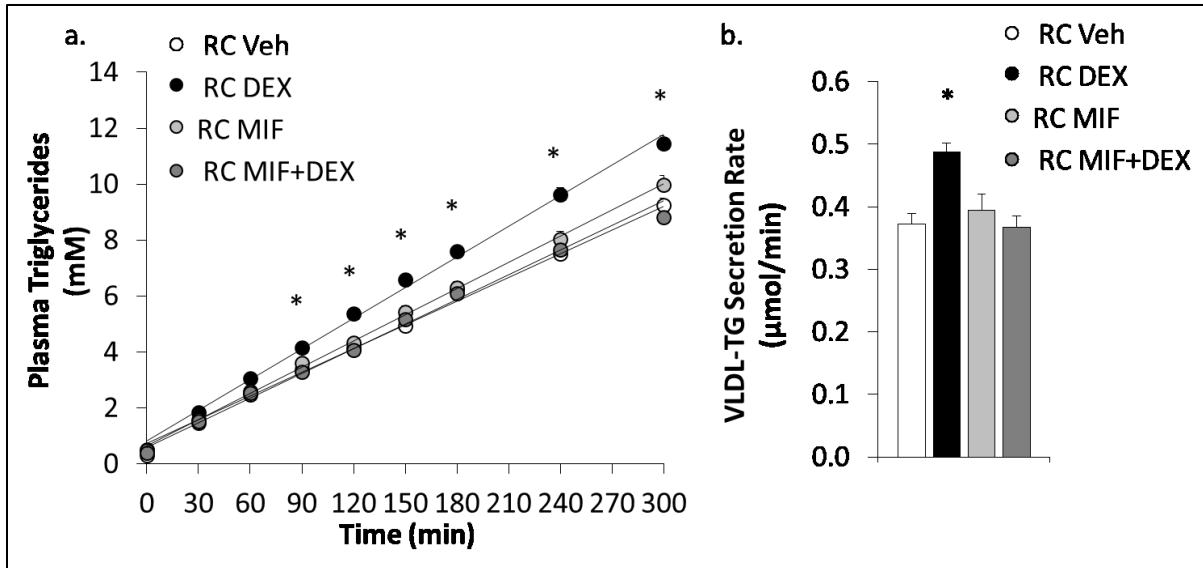


Figure 3.1- Acute glucocorticoid action in the medial basal hypothalamus stimulates hepatic plasma triglycerides and very-low density lipoprotein secretion in regular-chow fed rats. (a) Plasma triglycerides (TG) and (b) TG-rich, very-low density lipoprotein (VLDL-TG) secretion rates of poloxamer-injected rats on a regular chow (RC) diet that were subjected to a continuous MBH infusion of either saline (RC Veh) (n=13, white circle or bar), dexamethasone (RC DEX) (n=29, black circle or bar), mifepristone (RC MIF) (n=20, light grey circle or bar), or a co-infusion of MIF and DEX (RC MIF+DEX) (n=10, dark grey circle or bar). *P<0.05 for RC DEX versus all groups.

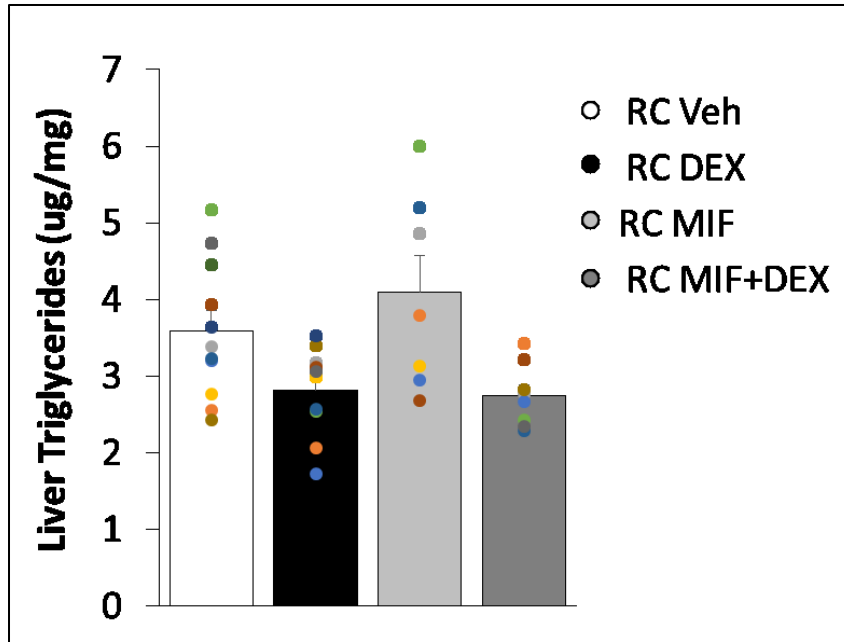


Figure 3.2- Acute glucocorticoid action in the medial basal hypothalamus does not alter hepatic triglyceride content in regular-chow fed rats. Hepatic triglyceride content was assessed in rats fed a regular-chow (RC) diet following continuous medial basal hypothalamic infusions of saline (RC Veh) (n=11, white bar), dexamethasone (RC DEX) (n=10, black bar), mifepristone (RC MIF) (n=7, light grey bar), or a co-infusion of MIF and DEX (RC MIF+DEX) (n=8, dark grey bar) Units are reported as mean μg of TG per mg of liver weight.

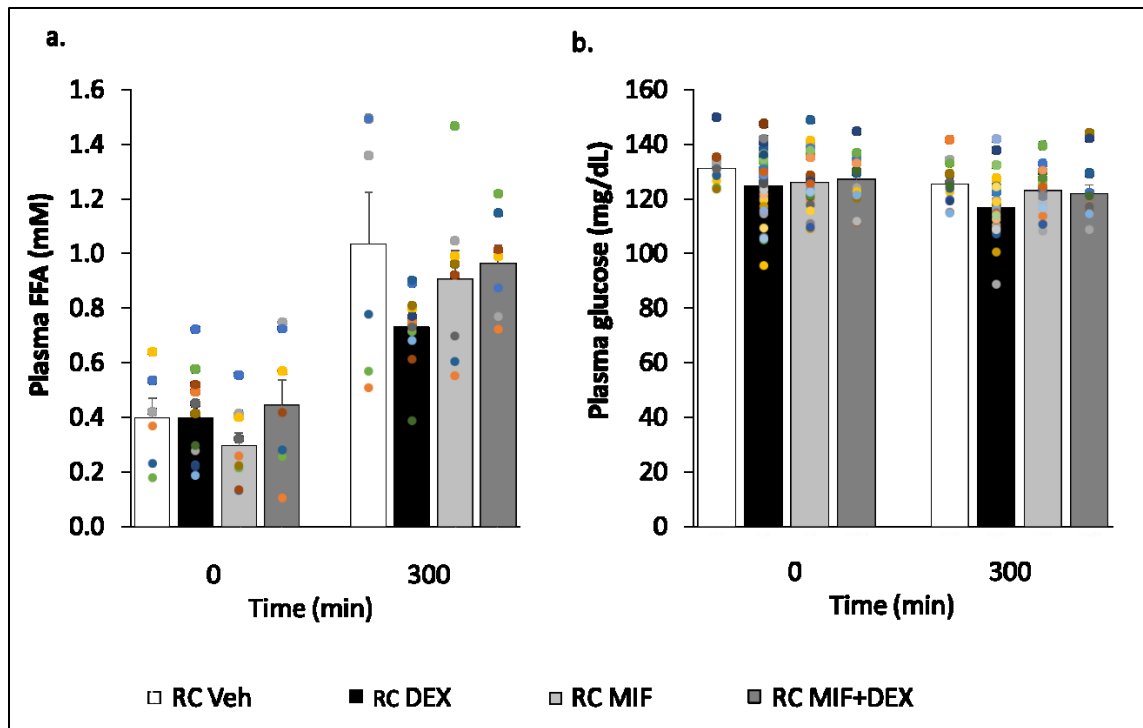


Figure 3.3- Medial basal hypothalamic glucocorticoid induced triglyceride-rich, very-low density lipoprotein secretion occurs independent of changes in plasma free fatty acids and plasma glucose. (a) Plasma free fatty acids (FFAs) from time (t)=0 and time=300 for rats fed a regular-chow diet (RC) treated with a continuous medial basal hypothalamic infusion of either saline (RC Veh) (n=6 at t=0 mins and t=300 mins, white bar), dexamethasone (RC DEX) (n=11 at t=0 mins and at t=300 mins, black bar), mifepristone (RC MIF) (n=9 at t=0 mins, n=8 at t=300 mins, light grey bar), and the co-infusion of MIF and DEX (RC MIF+DEX) (n=7 at t=0 and 300, dark grey bar). (b) Plasma glucose from time (t)=0 mins and t=300 mins for rats fed a regular-chow diet (RC) treated with a continuous medial basal hypothalamic infusion of either saline (RC Veh) (n=10 at t=0 mins, n=12 at t=300 mins, white bar), dexamethasone (RC DEX) (n=32 at t=0 mins, n=29 at t=300 mins, black bar), mifepristone (RC MIF) (n=24 at t=0 mins and 300 mins, light grey bar), and the co-infusion of MIF and DEX (RC MIF+DEX) (n=13 at t=0 mins and t=300 mins, dark grey bar).

3.1.1. Investigation of hepatic mechanisms involved in the medial basal hypothalamic glucocorticoid mediated increase in hepatic triglyceride-rich very-low density lipoprotein secretion.

To begin revealing some of the underlying mechanisms related to hepatic contribution to increase plasma TGs following MBH GC treatment hepatic regulators of lipid metabolism were investigated. These proteins and genes of interest are related to hepatic lipogenesis, VLDL-TG secretion, and fatty acid oxidation.

RC DEX's effect to increase plasma TGs and potentially VLDL-TG secretion was independent of changes in hepatic fatty acid synthase (FAS), phosphorylated-acetyl CoA carboxylase (P-ACC) to total acetyl-CoA carboxylase (ACC), microsomal triglyceride transfer protein (MTP), diacylglycerol acyltransferase 1 (DGAT1), or ADP-ribosylation factor 1 (Arf1) protein levels (Figure 3.4a-f) which are involved in hepatic TG production and VLDL-TG synthesis. Additionally, there was no significant change in hepatic sterol regulatory element-binding protein 1c (*Srebf1c*), liver x receptor α (*Nr1h3*), or liver x receptor β (*Nr1h2*) mRNA expression between groups, which are considered master regulators of gene expression for genes involved in lipid homeostasis, in part by increasing hepatic TG synthesis (Figure 3.5a-c). This finding was associated with a lack of change in hepatic *Dgat1*, *Dgat2*, *Fasn*, stearoyl-CoA desaturase 1 (*Scd1*), lipin 2 (*Lpin2*), cell death-inducing DFF4-like effector B (*Cideb*), or ADP-ribosylation factor 1 (*Arf1*) mRNA expression between the groups, which are genes involved in the regulation of TG synthesis and VLDL production and secretion (Figure 3.6a-g). There was also no significant change in hepatic mRNA expression in genes involved in fatty acid oxidation (carnitine palmitoyltransferase 1a (*Cpt1a*), peroxisome proliferator-activated receptor α (*Ppara*), and AMP-activated protein kinase (*Ampk*)) between treatment groups (Figure 3.7a-c). A change in fatty acid oxidation could suggest a change in hepatic fatty acid utilization, which in turn would contribute to altered hepatic lipid storage, utilization, and/ or VLDL-TG assembly^{63,144}. Together, this suggests that the change in plasma TGs and VLDL-TG secretion following MBH GC treatment was independent of changes in lipogenic genes involved in TG synthesis, VLDL-TG assembly, and fatty acid oxidation.

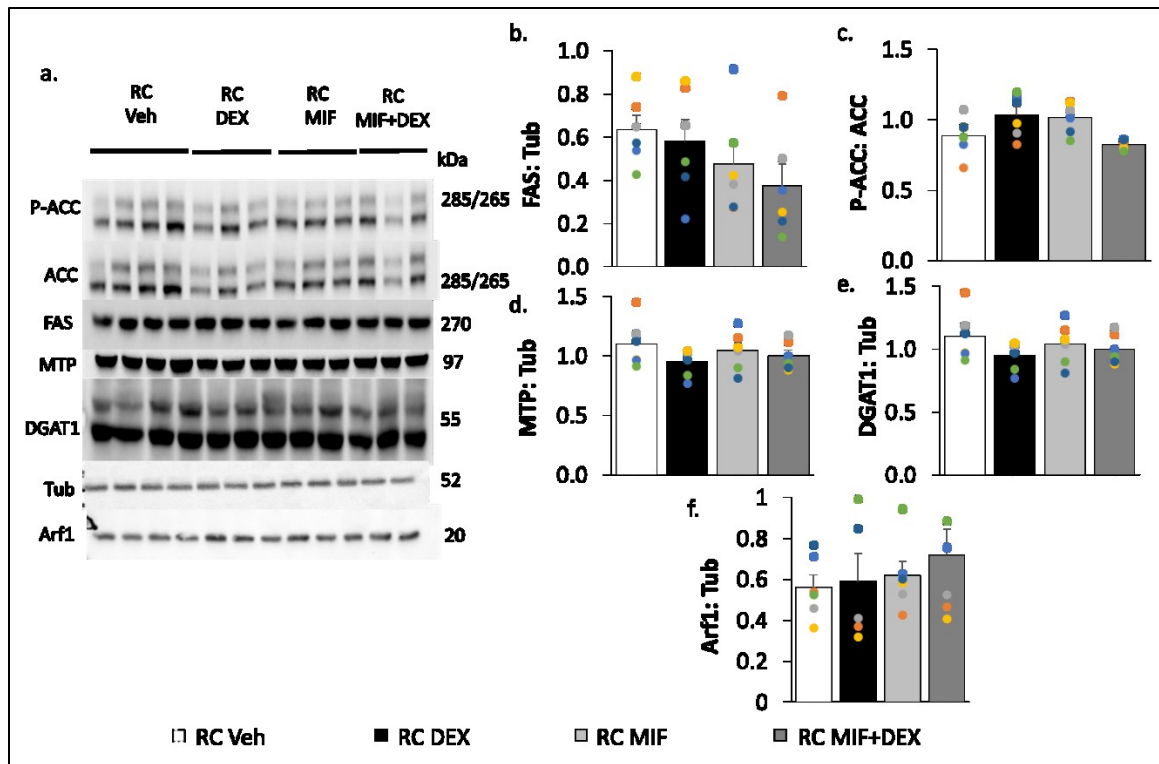


Figure 3.4- Increased very-low density lipoprotein secretion was not due to changes in hepatic protein levels. (a) Representative western blot images from liver samples obtain from rats on a regular-chow (RC) diet that received continuous medial basal hypothalamic infusions of saline (RC Veh) (white bars), dexamethasone (RC DEX) (black bars), mifepristone (RC MIF) (light grey bars), and the co-infusion of MIF and DEX (RC MIF+DEX) (dark grey bars). Protein molecular weight is indicated in kilodaltons (kDa). Western blots were quantified and expressed relative to a control. Shown are hepatic protein levels of (b) fatty acid synthase (FAS) relative to loading control tubulin (Tub), (c) phosphorylated-acetyl CoA carboxylase (P-ACC) to total acetyl-CoA carboxylase (ACC), (d) microsomal triglyceride transfer protein (MTP) to Tub, (e) diacylglycerol acyltransferase 1 (DGAT1) to Tub, and (f) ADP-ribosylation factor 1 (Arf1) to Tub. For all groups there is an n=6, except for an n=5 for RC DEX when assessing for protein levels of Arf1.

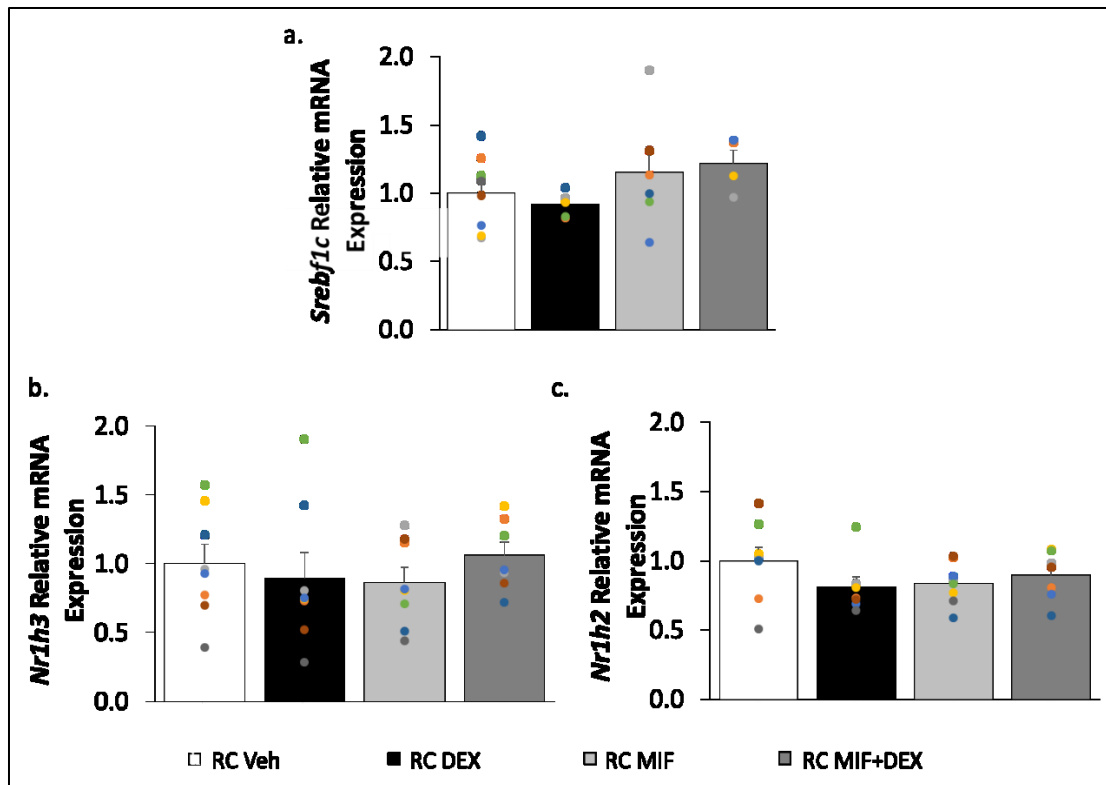


Figure 3.5- Medial basal hypothalamic glucocorticoid receptor activation does not alter hepatic *Srebf1c*, *Nr1h3*, or *Nr1h2* mRNA expression. Liver samples were obtained from rats, that were fed a regular chow diet (RC), after medial basal hypothalamic infusions of saline (RC Veh, white bars), dexamethasone (RC DEX, black bars), mifepristone (RC MIF, light grey bars), or a co-infusion of MIF and DEX (RC MIF+DEX, dark grey bars). Samples were assessed for relative hepatic mRNA expression of (a) sterol regulatory element-binding protein 1c (*Srebf1c*) (RC Veh n=8, RC DEX n=5, RC MIF n=6, RC MIF+DEX n=4), and (b) liver x receptor α (*Nr1h3*) (RC Veh n=8, RC DEX n=8, RC MIF n=8, RC MIF+DEX n=7) and (c) β (*Nr1h2*) (RC Veh n=8, RC DEX n=7, RC MIF n=8, RC MIF+DEX n=7). RC Veh normalized to 1.0. *18s* was used as a housekeeper gene for *Srebf1c*, and *Ppia* was used as a housekeeper gene for *Nr1h3* and *Nr1h2*.

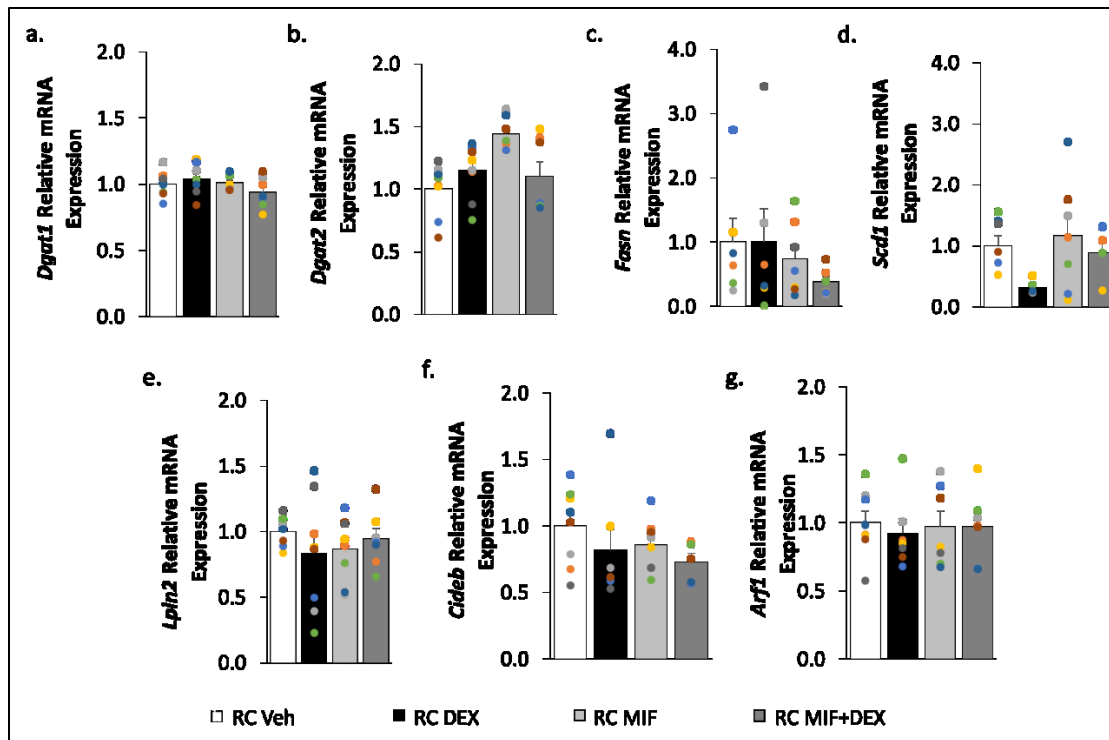


Figure 3.6- Changes in triglyceride-rich very-low density lipoprotein secretion associated with medial basal hypothalamic glucocorticoid action occurs independently of changes in hepatic lipogenic gene expression.

Liver samples were obtained from rats, that were fed a regular chow diet (RC), after medial basal hypothalamic infusions of saline (RC Veh, white bars), dexamethasone (RC DEX, black bars), mifepristone (RC MIF, light grey bars), or a co-infusion of MIF and DEX (RC MIF+DEX, dark grey bars). Samples were assessed for relative hepatic mRNA expression of (a) diacylglycerol acyltransferase 1 (*Dgat1*) (RC Veh n=8, RC DEX n=7, RC MIF n=7, RC MIF+DEX n=7), (b) diacylglycerol acyltransferase 2 (*Dgat2*) (RC Veh n=8, RC DEX n=8, RC MIF n=8, RC MIF+DEX n=7), (c) fatty acid synthase (*Fasn*) (RC Veh n=6, RC DEX n=6, RC MIF n=8, RC MIF+DEX n=7), (d) stearoyl-CoA desaturase 1 (*Scd1*) (RC Veh n=7, RC DEX n=5, RC MIF n=7, RC MIF+DEX n=4), (e) lipin-2 (*Lpin2*) (RC Veh n=7, RC DEX n=8, RC MIF n=8, RC MIF+DEX n=7), (f) cell death-inducing DFF4-like effector B (*Cideb*) (RC Veh n=8, RC DEX n=7, RC MIF n=8, RC MIF+DEX n=5), and (g) ADP-ribosylation factor 1 (*Arf1*) (RC Veh n=8, RC DEX n=7, RC MIF n=7, RC MIF+DEX n=7). RC Veh normalized to 1.0. *Ppia* was used as a housekeeper gene for all genes of interest except for *Scd1*, which used *18s*.

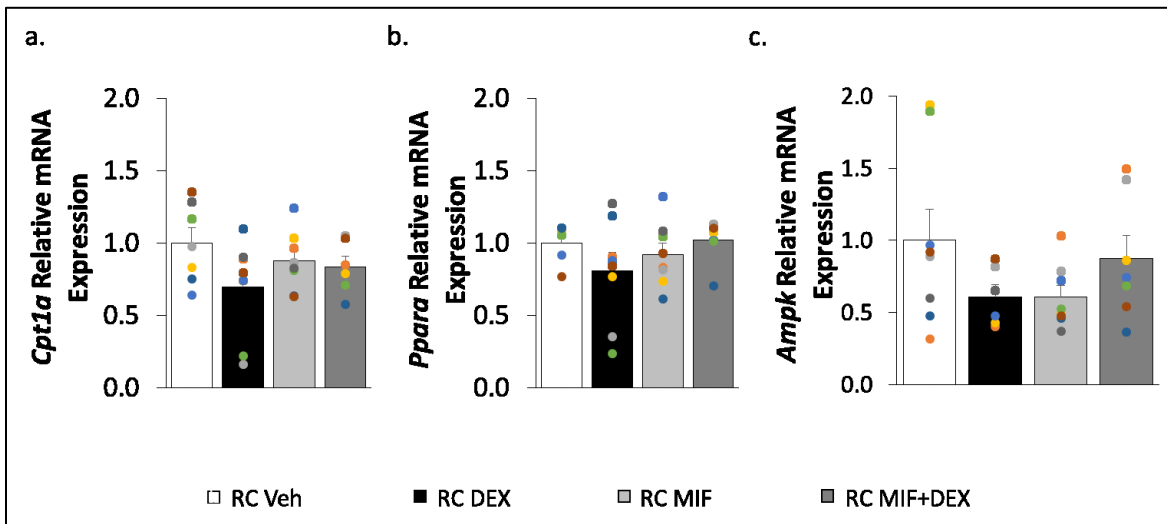


Figure 3.7- Medial basal hypothalamic glucocorticoid induced increase of triglyceride-rich very-low density lipoprotein occurs independently from changes in liver mRNA expression of genes involved in fatty acid-oxidation. Liver samples were obtained from rats, that were fed a regular chow diet (RC), after medial basal hypothalamic infusions of saline (RC Veh, white bars), dexamethasone (RC DEX, black bars), mifepristone (RC MIF, light grey bars), or a co-infusion of MIF and DEX (RC MIF+DEX, dark grey bars). Samples were assessed for relative hepatic mRNA expression of (a) carnitine palmitoyltransferase 1a (*Cpt1a*) (RC Veh n=7, RC DEX n=8, RC MIF n=8, RC MIF+DEX n=6), (b) peroxisome proliferator-activated receptor α (*Ppara*) (RC Veh n=8, RC DEX n=8, RC MIF n=8, RC MIF+DEX n=7), and (c) AMP-activated protein kinase (*Ampk*) (RC Veh n=8, RC DEX n=6, RC MIF n=8, RC MIF+DEX n=7). RC Veh normalized to 1.0. *Ppia* was used as a housekeeper gene.

As each VLDL-TG particle has a single apoB attached¹¹¹ and both apoB-48 and apoB-100 are produced in rodent hepatocytes^{113,114}, plasma apoB-48 and apoB-100 concentrations were determined between the RC Veh group and RC DEX group at t=0 mins (basal) and t=300 mins (end of experimentation) (Figure 3.8a). RC MBH DEX treatment had no effect on basal apoB-48 relative to RC Veh (Figure 3.8b), but RC MBH DEX had significantly higher basal plasma apoB-100 (Figure 3.8c) relative to RC Veh. Additionally, there was an expected increase

in plasma apoB-48 and plasma apoB-100 following experimentation (at t=300 mins), however no effect of MBH DEX was observed compared to the Veh group. (Figure 3.8a-c). Further, there was no significant difference in the ratio of plasma TGs to plasma apoBs between the two groups, which may suggest that there are similar levels of TGs per apoB particle (Figure 3.8d-e).

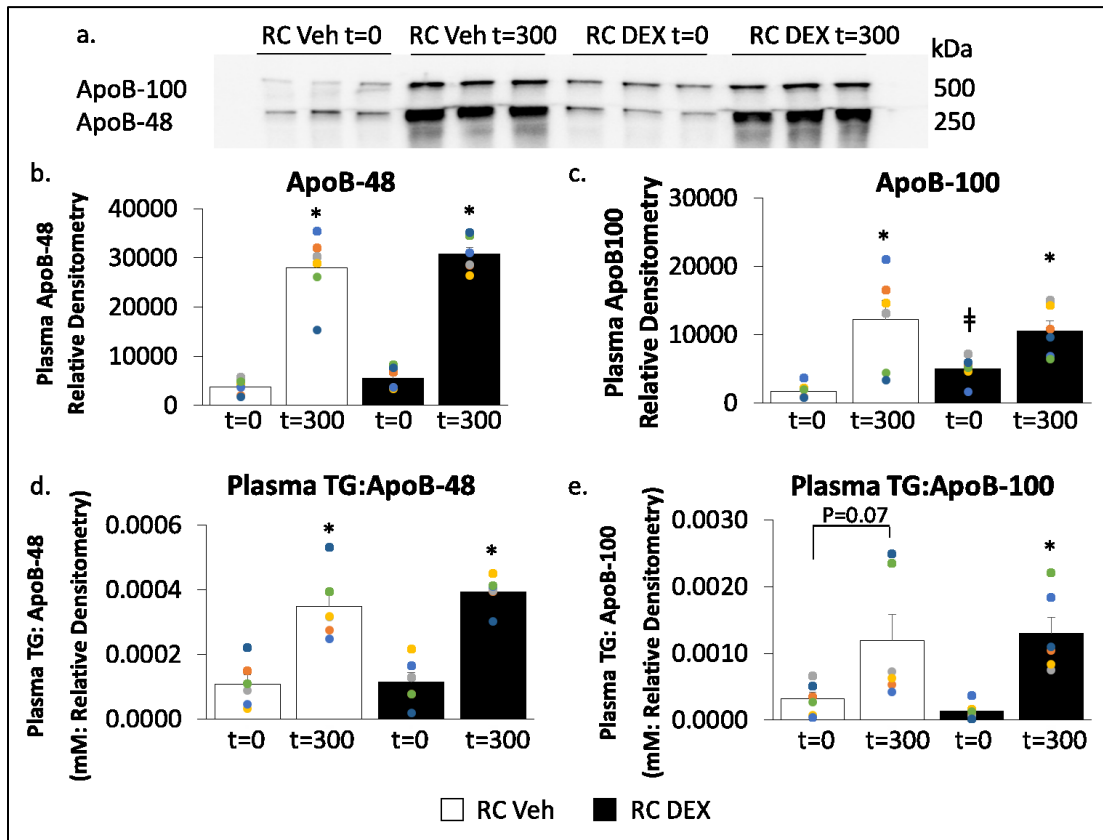


Figure 3.8- Plasma apoB remained unchanged after medial basal hypothalamic glucocorticoid receptor activation relative to vehicle. Plasma samples from the beginning of the experiment (t=0 mins) and after experiment (t=300 mins) were obtained from rats fed a regular-chow (RC) diet that were subject to continuous medial basal hypothalamic infusions of either saline (RC Veh) (n=6, white bars) or dexamethasone (RC DEX) (n=6, black bars) and were assessed for plasma apoB-48 or apoB-100. (a) A representative western blot of the plasma samples from t=0 mins and t=300 mins assessing protein levels of apoB-100 and apoB-48 via relative densitometry. (b) Plasma apoB-48 and (c) plasma apoB-100 were assessed. The average ratio of plasma triglycerides (TGs) to (d) apoB-48 or (e) apoB-100 for each sample for each time was

also assessed. †P<0.05 for RC DEX t=0 mins versus RC Veh t=0 mins. *P<0.05 for t=300 mins versus t=0 mins within each treatment group.

3.2. Medial basal hypothalamus-targeted glucocorticoid receptor knockdown negates the effects of medial basal hypothalamic glucocorticoid-stimulated hepatic triglyceride secretion in regular chow-fed rats

To alternatively test the requirement of MBH GRs to mediate MBH GCs, chronic inhibition of MBH GRs was investigated using rats that received a MBH specific LV containing GRshRNA compared to rats that received MBH MM as a control. These genetic loss-of-function techniques were used to evaluate whether MBH GRs are necessary for MBH GC liporegulatory action. A significant knockdown of MBH GR protein levels in RC GRshRNA rats compared to RC MM was confirmed via western blotting (Figure 3.9a-b).

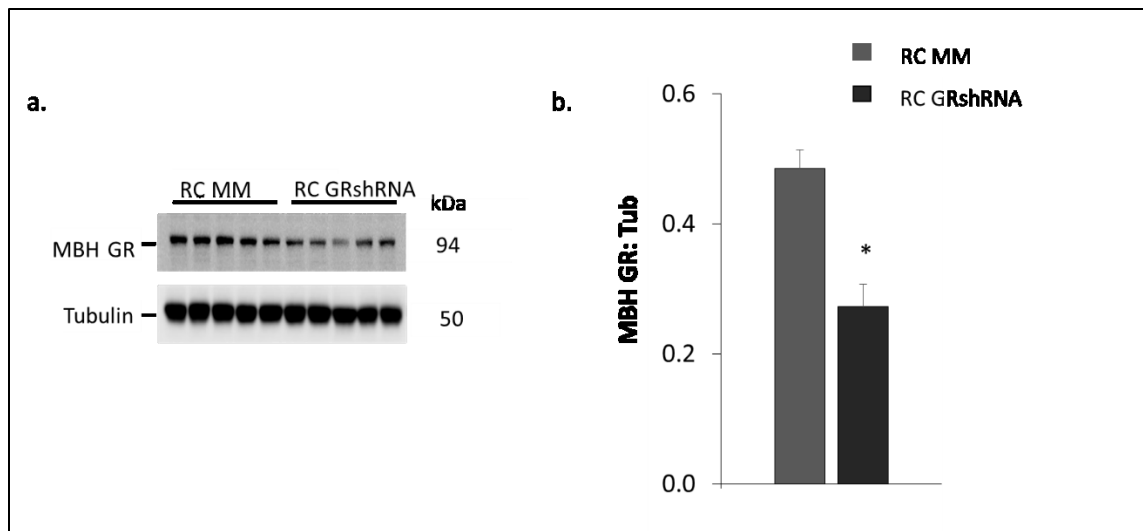


Figure 3.9- Representative western blot confirming knockdown of glucocorticoid receptor in the medial basal hypothalamus. (a) The medial basal hypothalamus (MBH) of rats fed a regular-chow (RC) diet that were subjected to either a lentivirus injection containing a glucocorticoid receptor (GR) knockdown, GRshRNA, or a mismatch sequence (MM) as a control, specifically in the MBH, were obtained after experimentation for analysis via western blotting. (b) Western blot analysis of MBH wedges from RC MM (n=5, dark grey) and RC GRshRNA (n=5, black) for protein levels of GR relative to tubulin (Tub). *P=0.001 for RC GRshRNA versus RC MM.

RC MM rats had plasma TGs and VLDL-TG secretion rates similar to that of the RC Veh, suggesting that the MM sequence injected into the MBH did not alter hepatic lipid metabolism. RC MM rats treated with DEX (RC MM DEX) had significantly higher plasma TGs and VLDL-TG secretion rates compared to RC MM rats, which is a similar effect observed in RC DEX vs RC Veh. Whereas MBH GRshRNA alone did not have an effect, suggesting that basal hypothalamic GCs do not have a role in the RC model in modulating hepatic lipid metabolism, MBH GR knockdown was able to negate the lipostimulatory effects of MBH DEX, as seen in RC GRshRNA DEX (Figure 3.10a-b). This data suggests that chronic knockdown of MBH GRs is capable of blocking MBH GC-stimulated hepatic TG secretion in RC rats, illustrating that MBH GCs require MBH GRs for the liporegulatory effects.

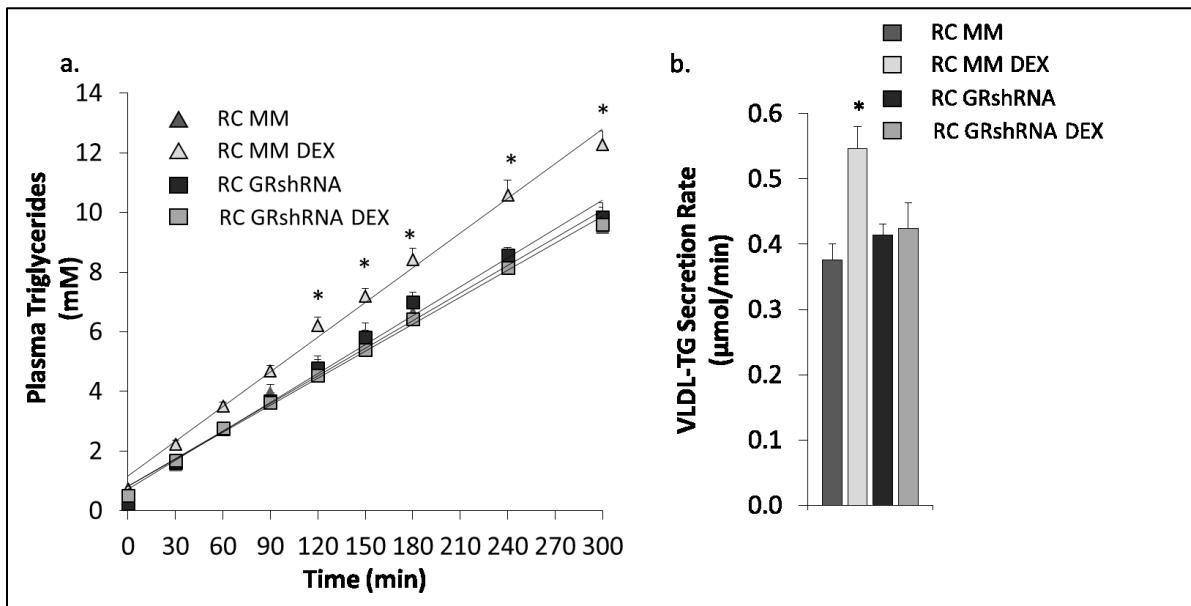


Figure 3.10- Medial basal hypothalamic targeted glucocorticoid receptor knockdown negates the effects of medial basal hypothalamic stimulation in regular-chow fed rats. (a) Plasma triglyceride (TG) and (b) TG-rich very low density lipoprotein (VLDL-TG) secretion rate was measured from rats on a regular-chow (RC) diet subjected that were subjected to a medial basal hypothalamic (MBH) injection containing a mismatch (MM) sequence, or a lentivirus containing a glucocorticoid receptor knockdown (GRshRNA) approximately 13 days prior to experimentation. The rats were subjected to an acute continuous MBH directed infusion of saline (RC MM, n=6, light black triangle or bar, and RC GRshRNA, n=6, black square or bar) or dexamethasone

(DEX) (RC MM DEX, n=10, light grey triangle or bar, and RC GRshRNA DEX, n=7, dark grey square or bar). RC MM (saline infusion) was used the control to RC MM DEX. *P<0.05 for RC MM DEX versus all groups.

3.3. Medial basal hypothalamic heat shock protein 90 is required for medial basal hypothalamic glucocorticoid stimulation of triglyceride secretion in regular chow-fed rats

To further implicate the necessity of MBH GRs, heat shock protein 90 (Hsp90) was investigated. This is again due to the fact that Hsp90 is required for the stability of the GR complex and biological function¹⁸⁵⁻¹⁸⁷. Thus, it was postulated that the inhibition of Hsp90 in the MBH would negate the effect of MBH GCs acting on MBH GRs to stimulate hepatic VLDL-TG secretion.

The effects of acute Hsp90 inhibition were first tested on SD rats fed a RC-diet that received a continuous MBH infusion of Hsp90i, a pharmacological Hsp90 inhibitor, directly into the MBH. RC Hsp90i alone did not significantly change plasma TGs (Figure 3.11a) or VLDL-TG secretion rate (Figure 3.11b) relative to RC Veh. However, we show that acute pharmacological inhibition of Hsp90 in the MBH, using Hsp90i co-infused with DEX (RC Hsp90i+DEX), lowers plasma TGs and VLDL-TG secretion rates compared to RC DEX (Figure 3.11a-b).

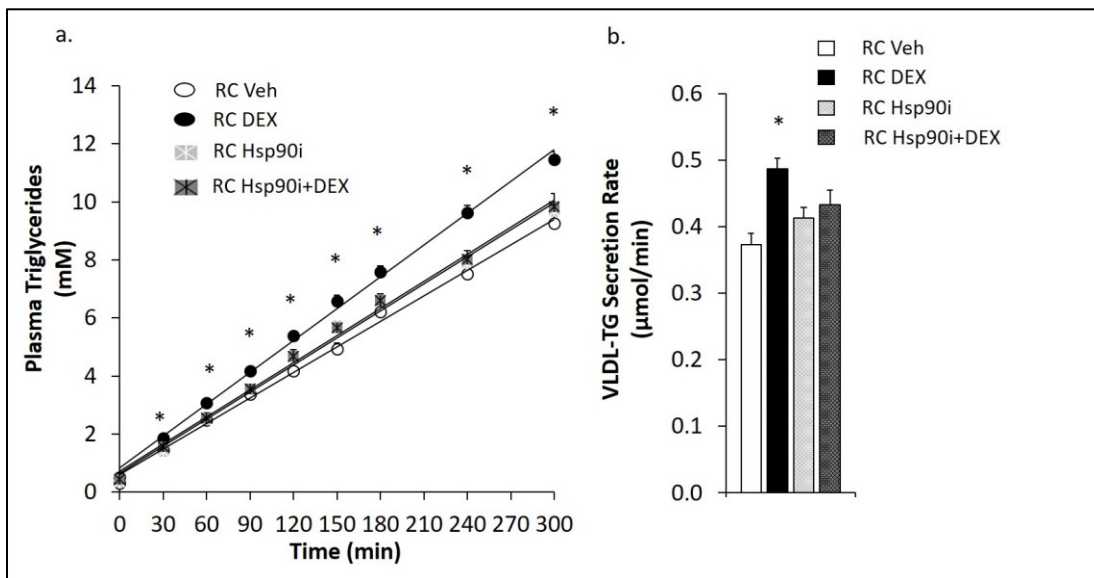


Figure 3.11- Acute heat shock protein 90 inhibition in the medial basal hypothalamus negates the effects of medial basal hypothalamic glucocorticoid

stimulation in regular-chow fed rats. (a) Plasma triglycerides (TG) and (b) TG-rich very low density lipoprotein (VLDL-TG) secretion rate were measured in rats fed a regular-chow (RC) that were subjected to direct medial basal hypothalamic infusions of either saline (RC Veh) (n=13, white circle or bar), dexamethasone (RC DEX) (n=29, black circle or bar), heat shock protein 90 inhibitor (RC Hsp90i) (n=13, light grey squares with white asterisk, or light grey hashed bars), or a co infusion of Hsp90i and DEX (RC Hsp90i+DEX) (n=12, dark grey squares with black asterisk, or dark grey hashed bars). *P<0.05 for RC DEX versus all groups.

Further, to implicate the necessity of Hsp90, the effects of Hsp90 knockdown was investigated in rats treated with a MBH specific LV which contained Hsp90 shRNA, compared to MM controls. SD rats that received MBH specific Hsp90shRNA (RC Hsp90 shRNA) had a lipid profile similar to that of RC MM (Figure 3.12 a-b), indicating that Hsp90 knockdown alone in the MBH in the RC-model does not alter lipid homeostasis relative to RC MM. Importantly, chronically knocking down Hsp90 in the MBH negated the lipostimulatory effects of DEX as observed with RC Hsp90 shRNA+DEX (Figure 3.12a-b). Furthermore, the culmination of data thus far illustrates that both pharmacological inhibition (using MIF and Hsp90i) and genetic knockdown (using GRshRNA and Hsp90 shRNA) of GRs are able to abate the lipostimulatory of MBH GR stimulation in a RC-model. This data supports the claim of that GC act directly on GRs within the MBH, and this GC-GR function is mediated by Hsp90, to regulate hepatic lipid metabolism in a RC model.

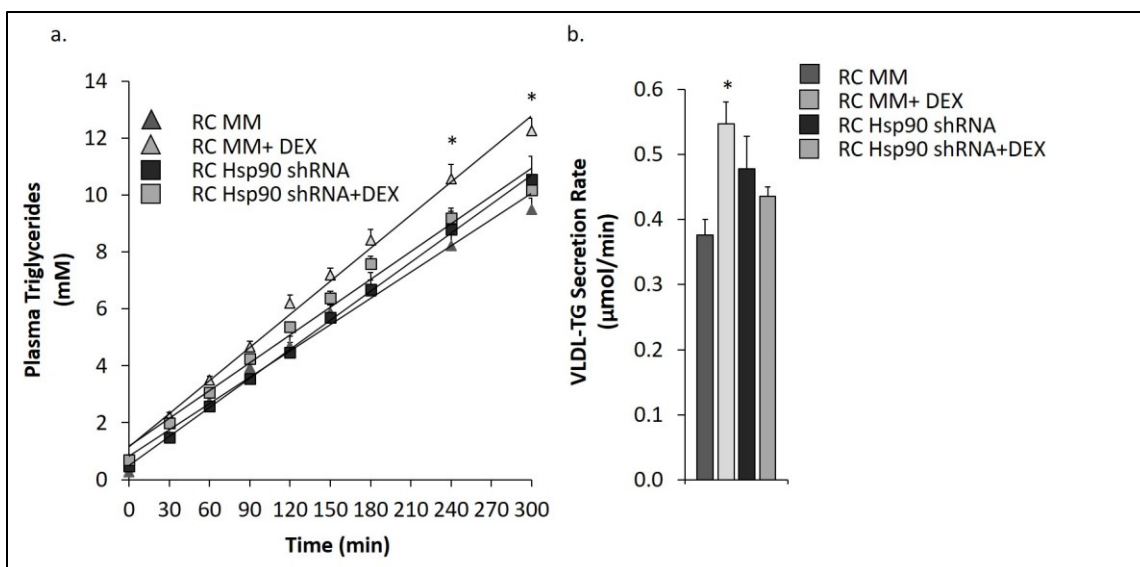


Figure 3.12- Genetic knockdown of heat shock protein 90 in the medial basal hypothalamus lowers the lipostimulatory effect of dexamethasone in regular-chow fed rats. (a) Plasma triglyceride (TG) and (b) TG-rich very low density lipoprotein (VLDL-TG) secretion rate was measured from rats on a regular-chow (RC) diet subjected that were subjected to a medial basal hypothalamic (MBH) injection containing a mismatch (MM) sequence, or a lentivirus containing a heat shock protein 90 knockdown (Hsp90 shRNA) approximately 13 days prior to experimentation. The rats were subjected to an acute continuous MBH directed infusion of saline (RC MM, n=6, light black triangle or bar, and RC Hsp90 shRNA, n=7, black square or bar) or dexamethasone (DEX) (RC MM DEX, n=10, light grey triangle or bar, and RC Hsp90 shRNA DEX, n=10, dark grey square or bar). RC MM (saline) was used as a control for RC MM DEX. *P<0.05 for RC MM DEX versus RC MM and RC Hsp90 shRNA+DEX.

3.4. Three-day high fat diet feeding alters the metabolic profile independent of changes in body weight

As we have shown that MBH GC-GR action plays a role in TG metabolism in the RC model, we next addressed MBH GC action in a pre-obese 3-d high fat diet (HFD) model that shows signs of early onset metabolic disease. Previous literature has shown that a 3-d HFD is capable of changing the metabolic profile via inducing mild hyperglycemia, mild hyperinsulinemia, as well as increased basal plasma TG and hepatic VLDL-TG secretion^{112,264,297,340,341}. Comparing the RC Veh to the HFD Veh group, indeed, HFD feeding led

to a significant increase in basal plasma glucose and TGs and significantly higher hepatic TG content, independent of changes in body weight (Figure 3.13a-d). This same model has previously been shown to increase plasma insulin levels^{333,334}. Importantly, Yue et al., has shown that 3-d HFD feeding leads to elevated plasma CORT levels compared to RC fed rats^{333,334}. Thus, it was hypothesized that the elevated GCs, that are associated with HFD feeding, can act in the MBH to contribute to the hypertriglyceridemic profile that is associated with HFD feeding.

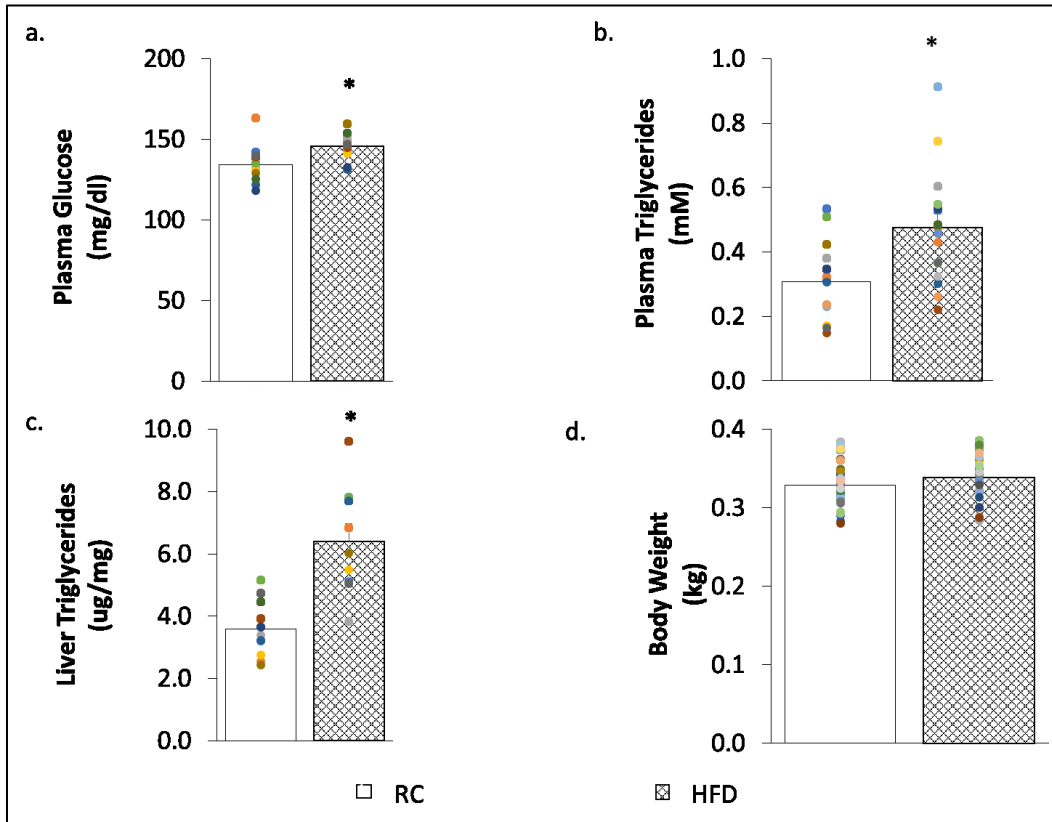


Figure 3.13- Physiological effects of a 3-day high fat diet compared to regular chow. A comparison of the metabolic effects a regular-chow (RC, white bars) diet has compared to a 3-day high fat diet (HFD, black and white hashed bars) on rats. (a) Basal plasma glucose, RC n= 11, HFD n=11, (b) basal plasma triglycerides RC n=13, HFD n=17, (c) liver triglyceride content RC n=11, HFD n=9 (liver TG content is reported as μg of TG per mg of liver weight), and (d) body weight, RC n=49, HFD n=32. * $P < 0.05$ for HFD versus RC. Note, body weight data is pooled from multiple treatment groups.

The HFD Veh group had expectedly significantly higher plasma TGs and VLDL-TG secretion rats (Figure 3.14a-b). HFD-fed rats had significantly higher basal (t=0 mins) plasma

apoB-48 and apoB-100 levels, as well as a significant increase in both apoBs following experimentation (t=300 mins), but no significant difference in plasma apoB-48 or apoB-100 between the RC Veh and HFD Veh groups at t=300 mins (Figure 3.15a-c). No change in the ratio of plasma TGs: plasma apoBs at t=300 between the RC Veh group and HFD group was observed, indicating there was no significant change in the amount of TGs per apoB particle following HFD feeding (Figure 3.15d-e). Notably, these results are similar to what was observed in the RC Veh and RC DEX model.

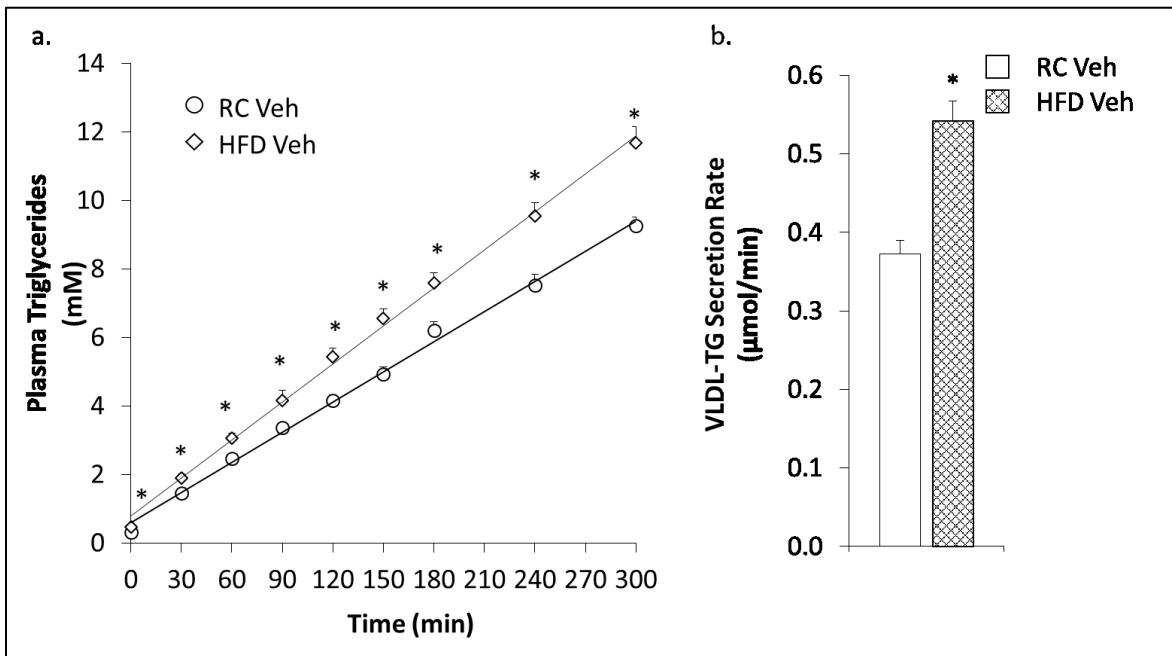


Figure 3.14- Three-day high fat feeding elevates plasma triglycerides and triglyceride-rich very-low density lipoprotein secretion. (a) Plasma triglycerides (TG) and (b) TG-rich very low density lipoprotein (VLDL-TG) secretion rate was assessed from rats following an intravenous injection of poloxamer. Rats were subjected to either a regular-chow (RC Veh) (n=13, white circle or bar), or a 3-day high fat diet (HFD Veh) (n=17, white diamond or hashed bar). *P<0.05 for HFD Veh versus RC Veh.

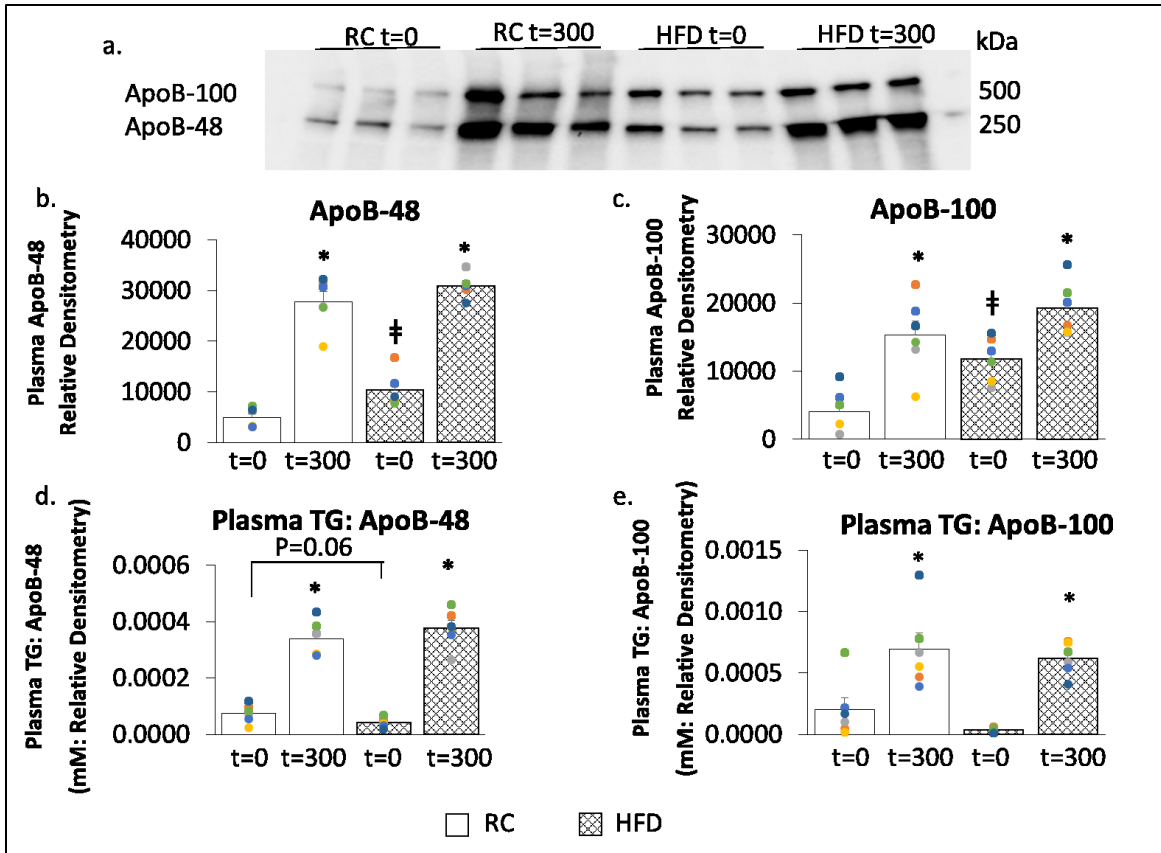


Figure 3.15- Three-day high fat diet fed rats have elevated basal plasma apoB levels.

Plasma samples from the beginning of the experiment (t=0 mins) and after experiment (t=300 mins) were obtained from rats fed either a regular-chow (RC) (n=6, white bar) diet or a 3-day high fat diet (HFD) (n=6, black and white hashed bar) and were assessed for plasma apoB-48 or apoB-100. (a) A representative western blot of the plasma samples from t=0 mins and t=300 mins assessing protein levels of apoB-100 and apoB-48 via relative densitometry. (b) Plasma apoB-48 and (c) plasma apoB-100 were assessed. The average ratio of plasma triglycerides (TGs) to (d) apoB-48 or (e) apoB-100 for each sample for each time was also assessed. *P<0.05 for t=300 mins versus t=0 mins within each treatment group. #P<0.05 for HFD t=0 mins versus RC t=0 mins.

3.5. Three-day high fat diet feeding elevates plasma triglycerides to a similar extent as glucocorticoid treatment in the medial basal hypothalamus

Given there are similar effects between the HFD group and the RC Dex versus the RC Veh group, this led us back to the hypothesis that the elevated GCs that are associated with HFD feeding could act in the MBH to increase plasma TGs via increased VLDL-TG secretion. Thus,

some comparisons of the HFD Veh group, RC Veh and RC DEX group were made. RC MBH DEX treatment had a similar effect compared to the HFD group with an increase in plasma TGs and VLDL-TG secretion, compared to the RC Veh group (Figure 3.16a-b). These findings were not associated with changes in hepatic FAS, P-ACC:ACC, MTP, or DGAT1 protein levels between RC Veh, RC DEX, and HFD Veh groups (Figure 3.17a-e). This provides further support to the hypothesis that increased GC action in the MBH may be stimulating VLDL-TG secretion. However, the mechanism remains unclear as the lipostimulatory effects of GCs in the hypothalamus were not associated with changes in liporegulatory protein levels.

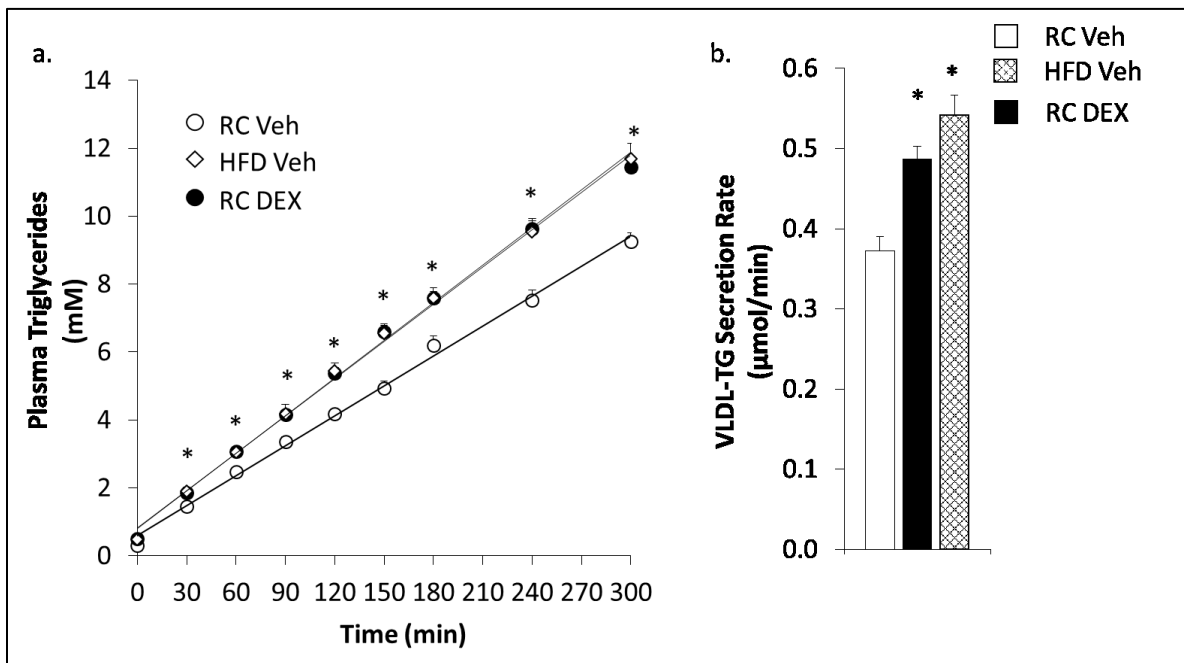


Figure 3.16- Three-day high fat feeding elevates plasma triglycerides and triglyceride rich very-low density lipoprotein secretion to a similar extent as a direct medial basal hypothalamic infusion of dexamethasone rats fed a regular-chow diet.

(a) Plasma triglycerides (TG) and (b) TG-rich very low density lipoprotein (VLDL-TG) secretion rate was assessed from rats following an intravenous injection of poloxamer. Rats were given either a regular-chow (RC) (white circle or bar), or a 3-day high fat diet (HFD Veh) (white diamond or hashed bar). Rats were subjected to a continuous infusion into their medial basal hypothalamus of either saline (RC Veh, n=13 and HFD Veh n=17) or dexamethasone (RC DEX) (n=29, black circle or bar) *P<0.05 for HFD Veh and RC DEX versus RC Veh.

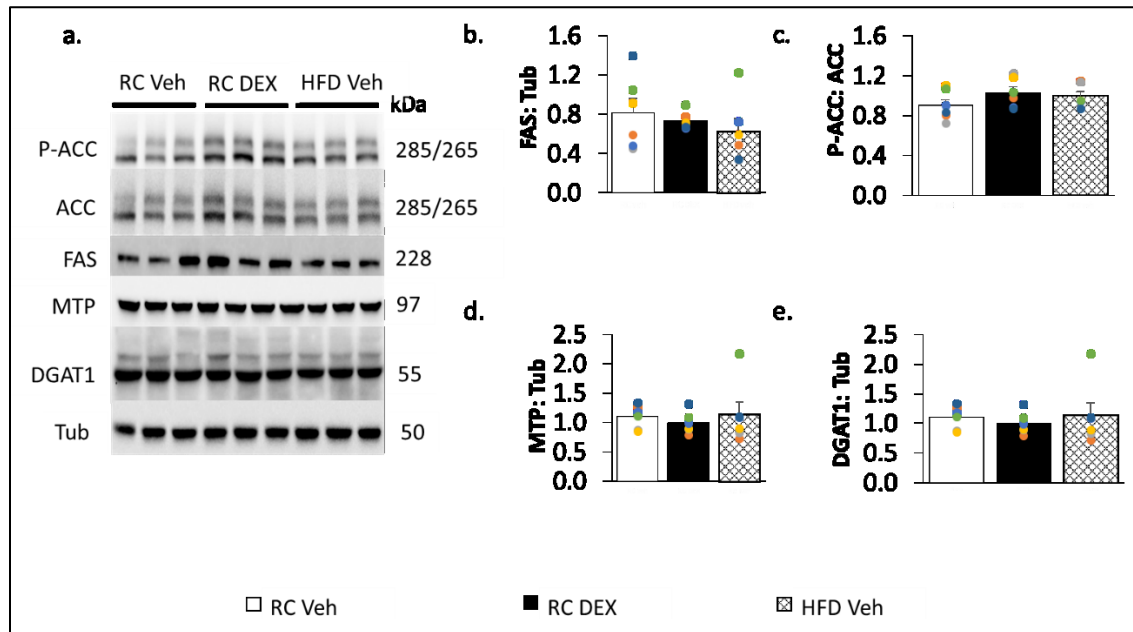


Figure 3.17- Three-day high fat feeding does not alter hepatic FAS, P-ACC:ACC, MTP, or DGAT1. Liver samples were obtained following experimentation from rats that were either on a regular-chow (RC) diet or a 3-day high fat diet (HFD) and were subjected to an acute, continuous infusion of either saline (RC Veh, n=6, white bar, HFD Veh, n=6, hashed bar) or dexamethasone (RC DEX, n=6, black bar) into the medial basal hypothalamus. (a) Protein levels of assessed using a western blot technique, as shown with the representative western blot. Proteins of interest include: (b) fatty acid synthase (FAS) relative to tubulin (Tub), (c) phosphorylated-acetyl CoA carboxylase (P-ACC) to total acetyl-CoA carboxylase (ACC), (d) microsomal triglyceride transfer protein (MTP) relative to Tub, and (e) diacylglycerol acyltransferase 1 (DGAT1) relative to Tub.

3.6. Chronic (13-day) inhibition of the medial basal hypothalamic glucocorticoid receptor lowers hepatic triglyceride-rich very low-density lipoprotein secretion in 3-day high fat diet fed rats

As GCs can act directly in the MBH to stimulate hepatic TG secretion in a similar fashion as a 3-d HFD, and that chronic (13-day) GR knockdown was able to negate the lipostimulatory effects of GC stimulation in the RC model, it was anticipated that chronic loss-of-function of MBH GRs would lead to improved lipid profiles in the 3-d HFD-fed SD rats. These experiments

would test whether MBH GC action contributes to increased plasma TGs observed in HFD-feeding.

As assessed in the RC model, after MBH cannulation, a subset of SD rats were subjected to a MBH specific lentivirus containing GRshRNA, or a MM sequence as a control. HFD MM rats had a plasma TG and VLDL-TG secretion rate similar to that of the HFD Veh. Strikingly, HFD MBH GRshRNA had significantly lower plasma TGs (Figure 3.18a), VLDL-TG secretion rate (Figure 3.18b), and hepatic TG content (Figure 3.19) compared to HFD MM rats, indicating that chronic GR knockdown, selectively in the MBH, was able to lower hepatic VLDL-TG secretion that was elevated via HFD-feeding. This data supports the hypothesis that elevated GCs, as observed in metabolic disease states, act in the MBH to contribute to hyperlipidemia, and this lipid profile can be normalized via chronic MBH GR knockdown.

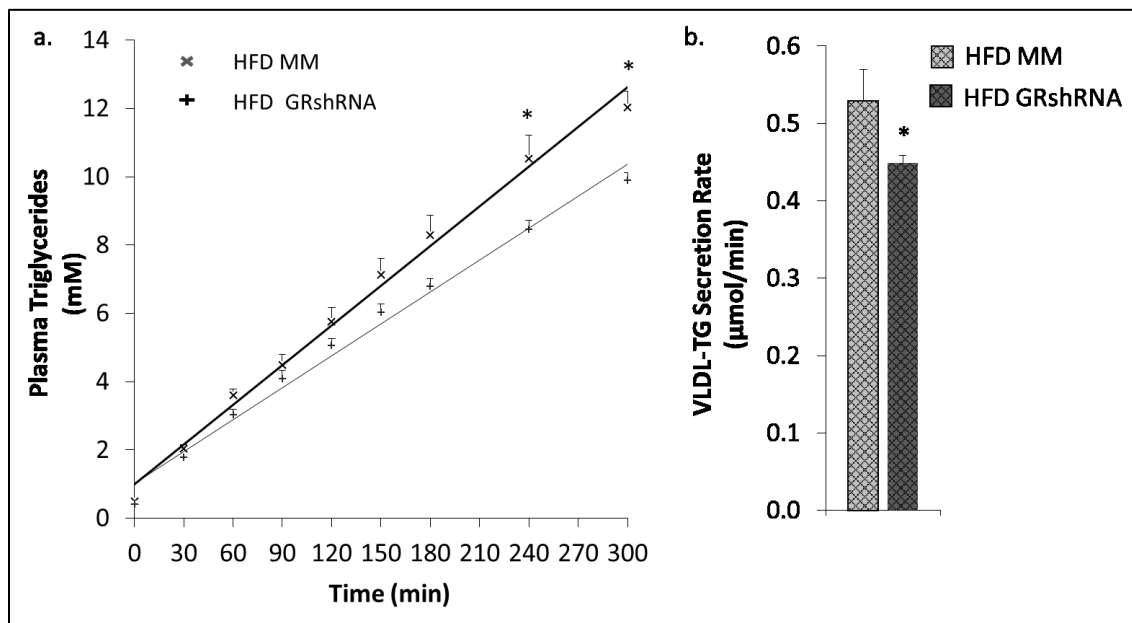


Figure 3.18- Chronic medial basal hypothalamus targeted glucocorticoid receptor knockdown lowers hepatic triglyceride-rich very-low density lipoprotein production and secretion in 3-day high fat diet fed rats. Rats were subjected to a medial basal hypothalamic targeted injection containing a mismatch sequence (MM/control) or a lentivirus containing a glucocorticoid receptor knockdown (GRshRNA) approximately 13 days prior to experimentation. The rats then underwent a vascular surgery, followed by a 3-day high fat diet (HFD) feeding regimen. Following a poloxamer injection, (a) plasma

triglycerides (TG) and (b) TG-rich very-low density lipoprotein secretion (VLDL-TG) rate was assessed in HFD MM (n=6, light grey 'x' or hashed bar) and HFD GRshRNA (n=13, dark grey cross or hashed bar). *P<0.05 for HFD GRshRNA versus HFD MM.

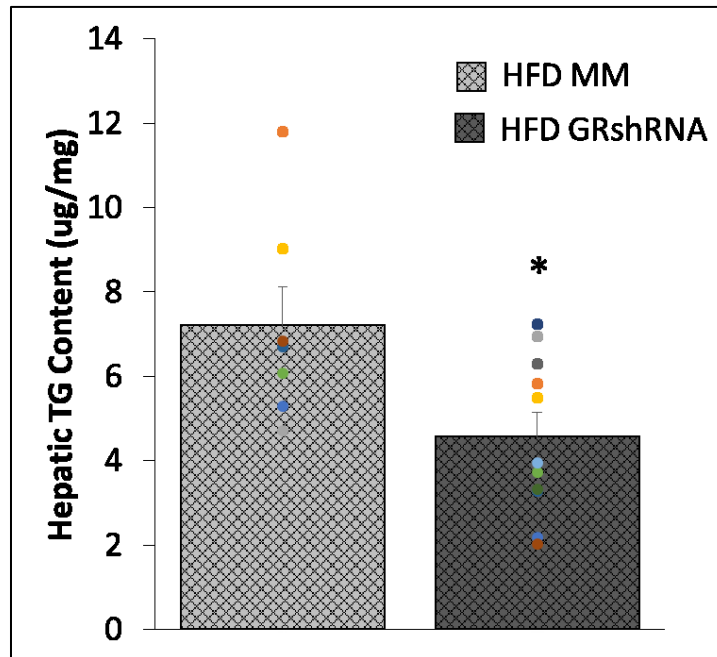


Figure 3.19- Chronic medial basal hypothalamus targeted glucocorticoid receptor knockdown lowers hepatic triglyceride content in 3-day high fat diet fed rats. Rats were subjected to a medial basal hypothalamic targeted injection containing a mismatch sequence (MM) or a lentivirus containing a glucocorticoid receptor knockdown (GRshRNA) approximately 13 days prior to experimentation. The rats then underwent a vascular surgery, followed by a 3-day high fat diet (HFD) feeding regimen. Following poloxamer experimentation, livers were harvested. Hepatic triglyceride (TG) content is reported between HFD MM (n=7, light grey hashed bars) and HFD GRshRNA (n=11, dark grey hashed bars). *P<0.05 for HFD GRshRNA versus HFD MM. Hepatic TG content is reported in ug of TG per mg of liver weight.

The observed decrease in plasma TGs as a result of chronic MBH GR inhibition in HFD-fed rats occurred independent of changes in plasma glucose and FFAs at t=0 mins (basal) and t=300 mins (end of experiment) (Figure 3.20a-b). Further, both HFD MM and HFD GRshRNA groups had a significant increase in plasma apoB-48 and apoB-100 compared to basal values

(Figure 3.21a-c), but there was no difference in plasma apoB levels between the HFD MM group and the HFD GRshRNA group (Figure 3.21a-c). Whereas there was no change between the HFD MM and HFD GRshRNA plasma TG to plasma apoB-48 ratio at t=300 mins, there was a trend (P=0.08) for a decrease in the plasma TG to apoB-100 ratio at t=300 mins for the HFD GRshRNA compared to the HFD MM group (Figure 3.21d-e). This may suggest that the HFD GRshRNA group have less TGs per apoB particle compared to the HFD MM group.

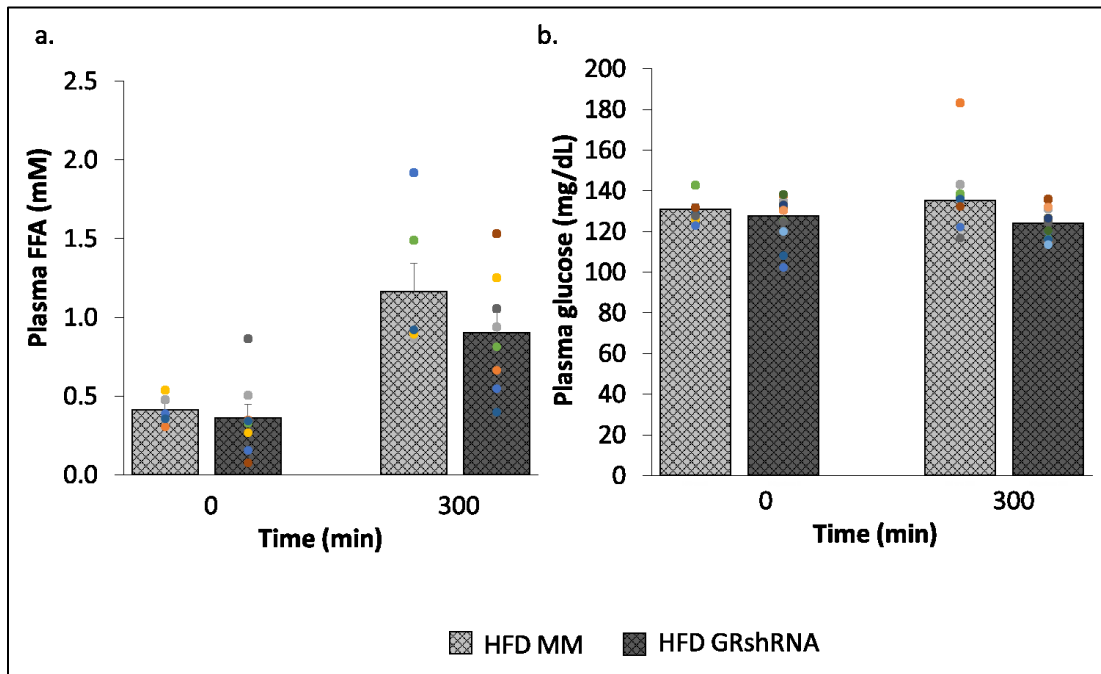


Figure 3.20- Decreased plasma triglycerides as a result of chronic medial basal hypothalamic glucocorticoid receptor inhibition in high fat diet fed rats occurred independently of changes in plasma substrates. Plasma samples at time (t) =0 mins and t=300 mins were obtained from rats that were on a 3-day high fat diet (HFD) and received medial basal hypothalamic targeted injections of a mismatch sequence (MM, light grey hashed bar) or a lentivirus containing a glucocorticoid receptor knockdown (GRshRNA, dark grey hashed bar) during experimentation.(a) Plasma free fatty acids (FFAs) were assessed in HFD MM (n=5 at t=0 mins, n=6 at t=300 mins) and HFD GRshRNA (n=8 at t=0 mins and t=300 mins). (b) Plasma was also assessed for glucose concentration in HFD MM (n=9 at t=0 mins and t=300 mins) and HFD GRshRNA (n=13 at t=0 mins and t=300 mins).

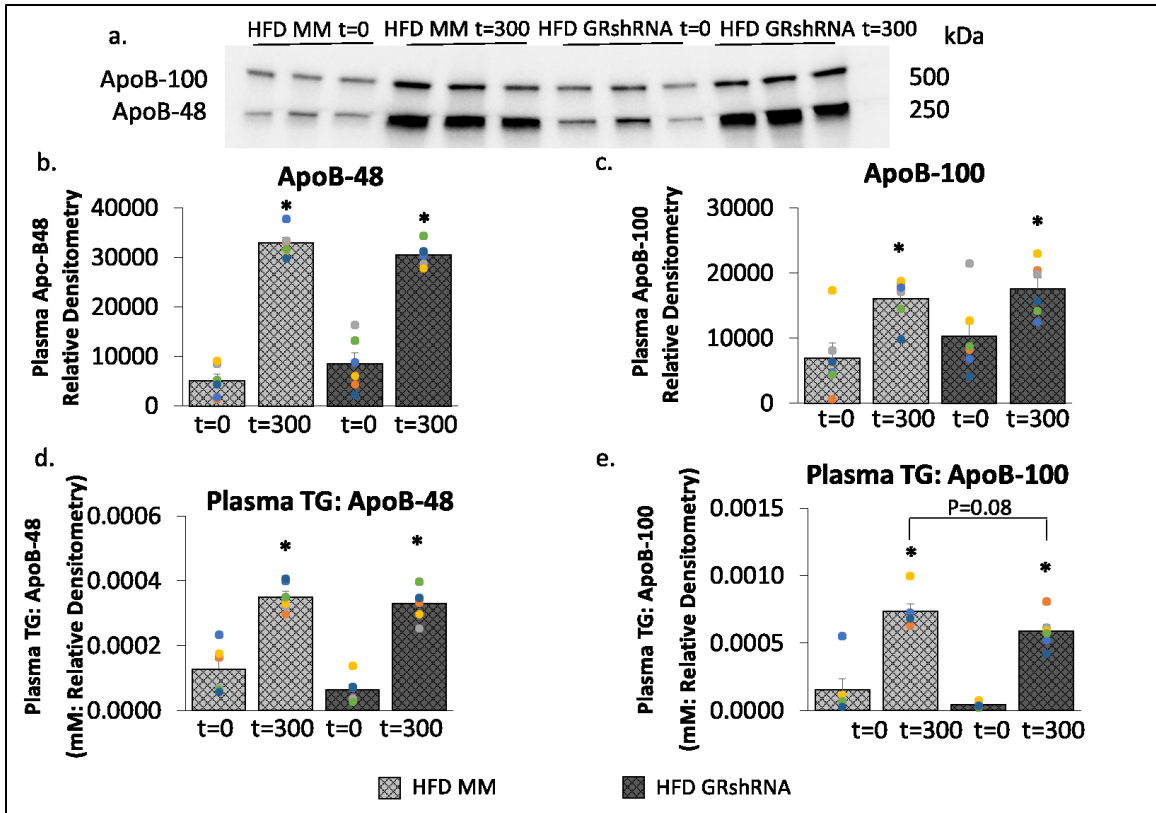


Figure 3.21- Medial basal hypothalamic targeted glucocorticoid knockdown did not change plasma apoB in high fat diet fed rats. Plasma samples from the beginning of the experiment (t=0 mins) and after experiment (t=300 mins) were obtained from rats fed a 3-day high fat diet (HFD) and were subjected to a medial basal hypothalamic targeted lentivirus containing a mismatch (MM, n=6, light grey hashed bar) or a glucocorticoid receptor knockdown (GRshRNA, n=6 dark grey hashed bar) approximately 13 days before experimentation. Following experimentation rats were assessed for plasma apoB-48 or apoB-100. (a) A representative western blot of the plasma samples from t=0 mins and t=300 mins assessing protein levels of apoB-100 and apoB-48 via relative densitometry. (b) Plasma apoB-48 and (c) plasma apoB-100 were assessed. The average ratio of plasma triglycerides (TGs) to (d) apoB-48 or (e) apoB-100 for each sample for each time was also assessed. *P<0.05 for t=300 mins versus t=0 mins within each treatment group.

To investigate some of the liporegulatory mechanisms that underlie the observed changes in HFD rats, the expression of some hepatic liporegulatory proteins were assessed. There was no

change in hepatic FAS, MTP, or P-ACC:ACC protein levels between HFD GRshRNA rats and HFD MM rats (Figure 3.22a-d). This effect is similar to that of the RC model.

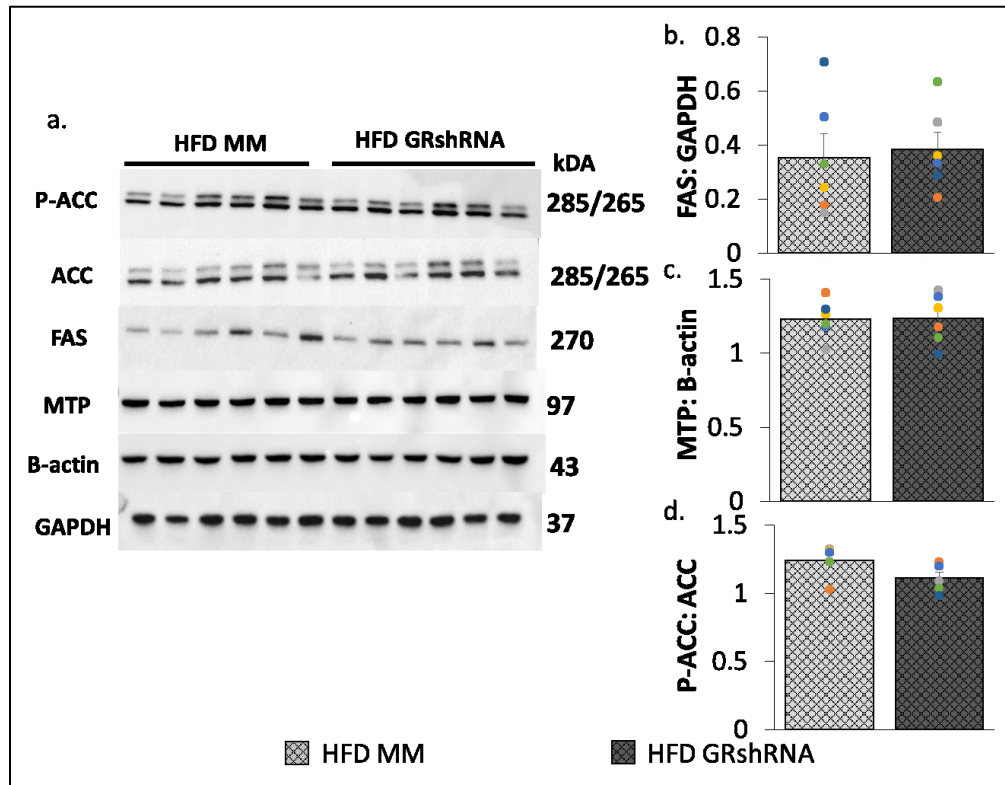


Figure 3.22- Medial basal hypothalamic glucocorticoid receptor knockdown does not change hepatic FAS, MTP, or P-ACC: ACC protein levels. Liver samples were obtained from rats that were on a 3-day high fat diet (HFD) and were subjected to medial basal hypothalamic targeted injection of a lentivirus containing a mismatch (MM, light grey hashed bar) sequence or a glucocorticoid receptor knockdown (GRshRNA, dark grey hashed bar). (a) Representative western blots from liver samples used to assess protein levels of proteins of interest. Proteins of interest include: (b) fatty acid synthase (FAS) relative to glyceraldehyde 3-phosphate dehydrogenase (GAPDH) (HFD MM n=6, HFD GRshRNA n=6), (c) microsomal triglyceride transfer protein (MTP) relative to β-actin (HFD MM n=6, HFD GRshRNA n=6), and (d) phosphorylated-acetyl CoA carboxylase (P-ACC) to total acetyl-CoA carboxylase (ACC) (HFD MM n=5, HFD GRshRNA n=5).

3.7. Both acute and pharmacological inhibition of heat shock protein 90 in the medial basal hypothalamus negates the hyperlipidemic effects of a 3-day high fat diet

Given that Hsp90 inhibition in the MBH was able to lower the lipostimulatory effects of MBH DEX in a RC model, and that blocking the GR in the MBH was able to lower VLDL-TG secretion in the HFD model, it was anticipated that blocking MBH GR function with the inhibition of Hsp90 should also negate the effects of MBH GC action in 3-d HFD rats. Therefore, these experiments were conducted to further implicate the necessity of MBH GRs in HFD-induced hyperlipidemic rats, as Hsp90 is required for the biological function and stability of the GR. Accordingly, both pharmacological inhibition (using Hsp90i) (Figure 3.23a-b) and genetic Hsp90 inhibition (using Hsp90 shRNA) (Figure 3.24a-b) in the MBH was able to lower VLDL-TG in hyperlipidemic rats fed with a 3-d HFD. Thus, this data additionally provides evidence that inhibition of MBH GC action (via GRshRNA or inhibition of Hsp90) lowers VLDL-TG secretion in HFD-induced hyperlipidemic rats.

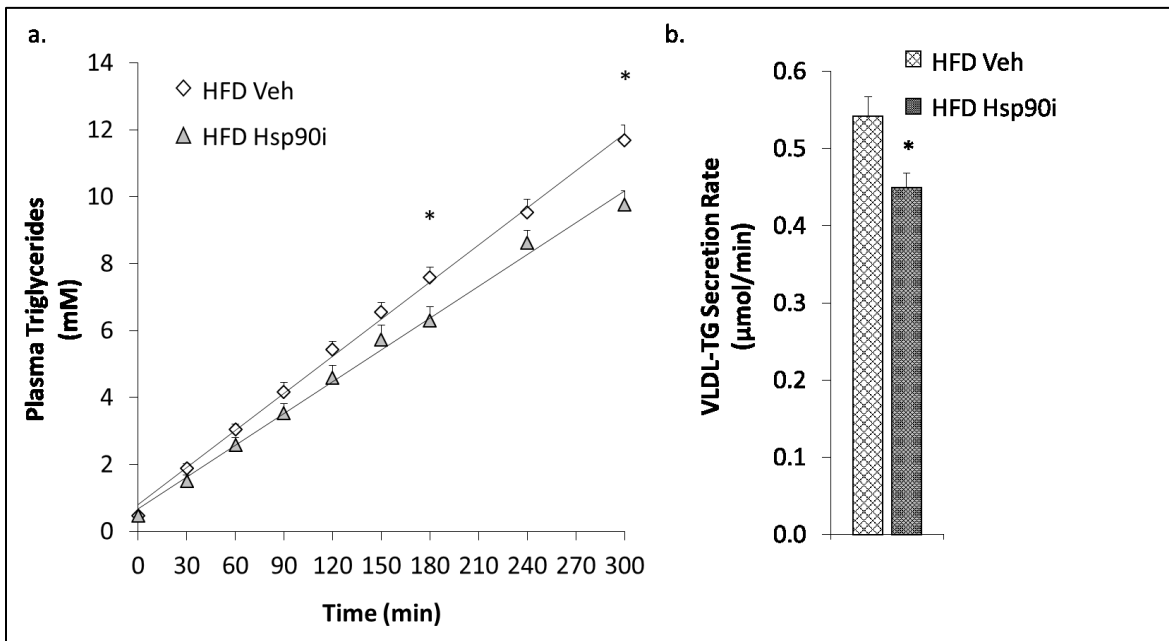


Figure 3.23- Acute inhibition of heat shock protein 90 in the medial basal hypothalamus lowers triglyceride-rich very-low density lipoprotein secretion in diet-induced hyperlipidemic rats. (a) Plasma triglycerides (TG) and (b) TG-rich very-low density lipoprotein secretion (VLDL-TG) secretion rate of rats fed a 3-day high fat diet (HFD) that were subjected to acute, continuous medial basal hypothalamic infusions of

saline (HFD Veh) (n=17, white diamond or black and white hashed bar) and heat shock protein 90 inhibitor (HFD Hsp90i) (n=11, grey triangle or grey hashed bar). *P<0.05 for HFD Hsp90i versus HFD Veh.

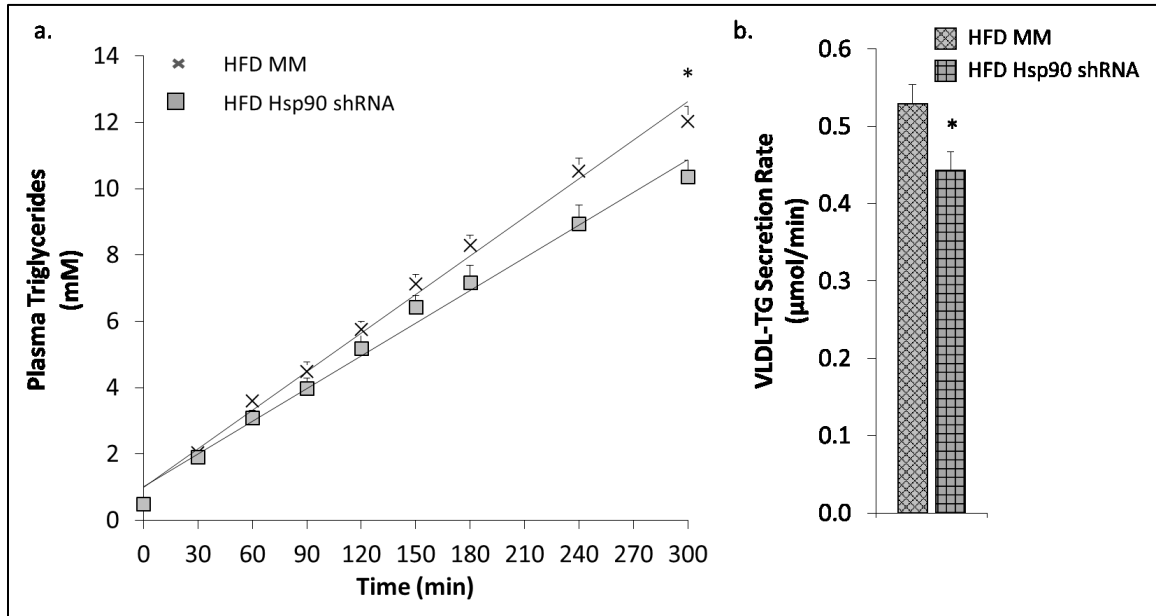


Figure 3.24- Chronic knockdown of heat shock protein 90 in the medial basal hypothalamus lowers triglyceride-rich, very-low density lipoprotein secretion in rats fed a 3-day high fat diet. (a) Plasma triglycerides (TGs) and (b) TG-rich, very-low density lipoprotein (VLDL-TG) secretion rate of rats fed a 3-day high fat diet (HFD) that were subjected to medial basal hypothalamic targeted injects of either a mismatch (HFD MM) (n=6, light grey ‘x’ or hashed bar) sequence or a lentivirus containing a heat shock protein 90 knockdown (HFD Hsp90 shRNA) (n=7, dark grey square or checkered bar). *P<0.05 for HFD Hsp90 shRNA versus HFD MM.

Whereas there was no change in plasma FFAs and glucose between HFD Veh and HFD Hsp90i treated rats (Figure 3.25 a-b), the chronic inhibition of Hsp90 in the MBH of 3-d HFD rats led to a significant reduction in both basal (t=0 mins) and end of experiment (t=300 mins) plasma FFAs (Figure 3.26a), and no change in plasma glucose compared to HFD MM rats (Figure 3.26b). This may indicate that chronic Hsp90 inhibition could be reducing FFA secretion into the periphery, or increasing FFA utilization. Similar to other TG-lowering treatments,

chronic inhibition of Hsp90 in the MBH did not alter hepatic MTP, FAS, or P-ACC:ACC (Figure 3.27a-d).

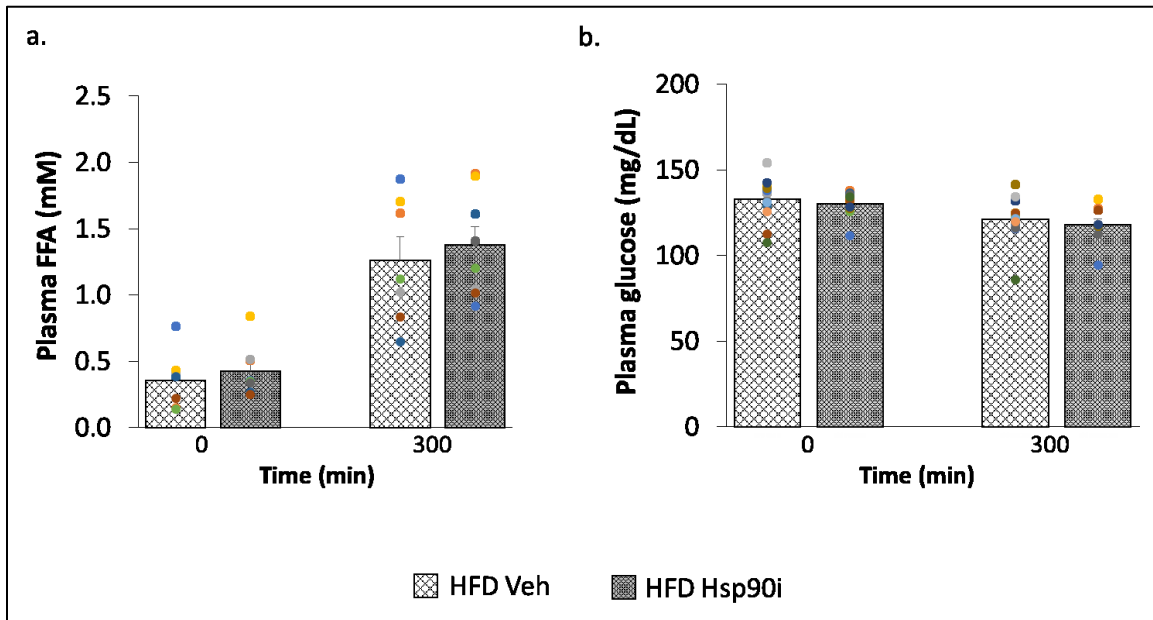


Figure 3.25- The decrease in triglyceride-rich very-low density lipoprotein secretion in diet-induced hyperlipidemic rats subjected to acute inhibition of heat shock protein 90 in the medial basal occurs independently of changes in plasma free fatty acids and plasma glucose. Plasma samples from the beginning of the experiment (t=0 mins) and the end of the experiment (t=300 mins) were obtained from rats that were on a 3-day high fat diet (HFD) that were subjected to an acute, continuous medial basal hypothalamic infusion of either saline (HFD Veh, black and white hashed bar) or a heat shock protein 90 inhibitor (HFD Hsp90i, dark grey hashed bar). (a) Plasma free fatty acids (FFA) (HFD Veh, n=7, HFD Hsp90i n=8) and (b) plasma glucose (HFD Veh, n=14, HFD Hsp90i, n=11) concentrations were assessed.

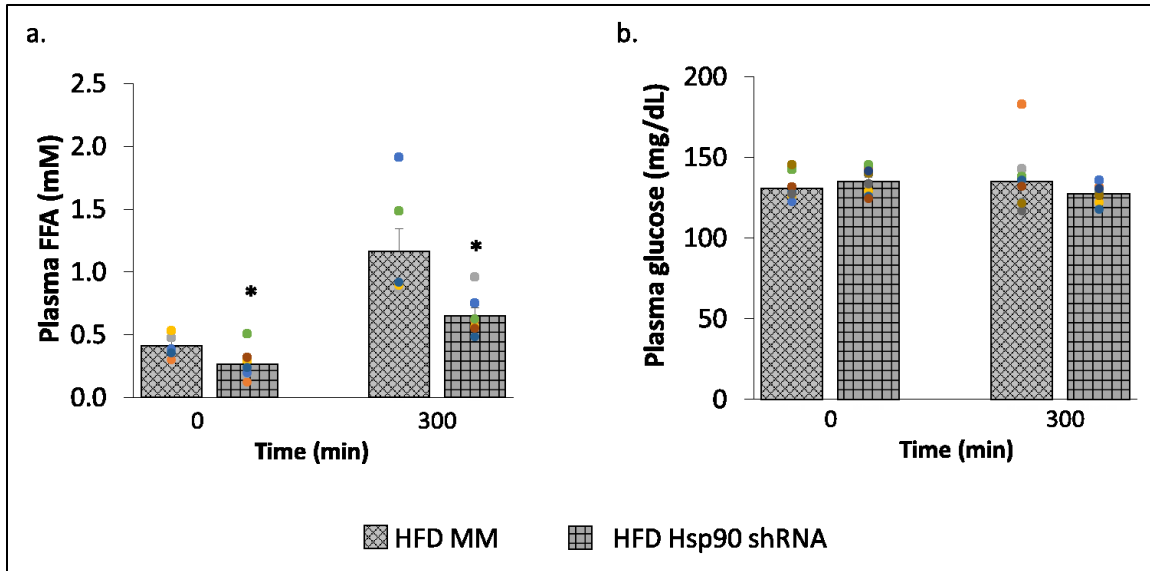


Figure 3.26- Chronic inhibition of medial basal hypothalamic heat shock protein 90 is associated with significantly lower plasma free fatty acids but not plasma glucose in rats fed a 3-day high fat diet. Plasma samples obtained from rats that were on a 3-day high fat diet (HFD) that were subjected to medial basal hypothalamus specific injections of either a mismatch sequence (HFD MM, light grey hashed bars) or a lentivirus containing a heat shock protein 90 knockdown (HFD Hsp90 shRNA, dark grey checkered bars) at the beginning of experimentation (t=0 mins) and after experimentation (t=300 mins) were assessed for (a) plasma free fatty acids (FFA) (HFD MM n=5 at t=0 mins, n=6 at t=300 mins, HFD Hsp90 shRNA n=7 for t=0 mins and t=300 mins) and (b) plasma glucose (HFD MM n=9 at t=0 mins and t=300 mins, HFD Hsp90 shRNA n=10 at t=0 mins and t=300 mins). *P<0.05 for HFD Hsp90 shRNA versus HFD MM.

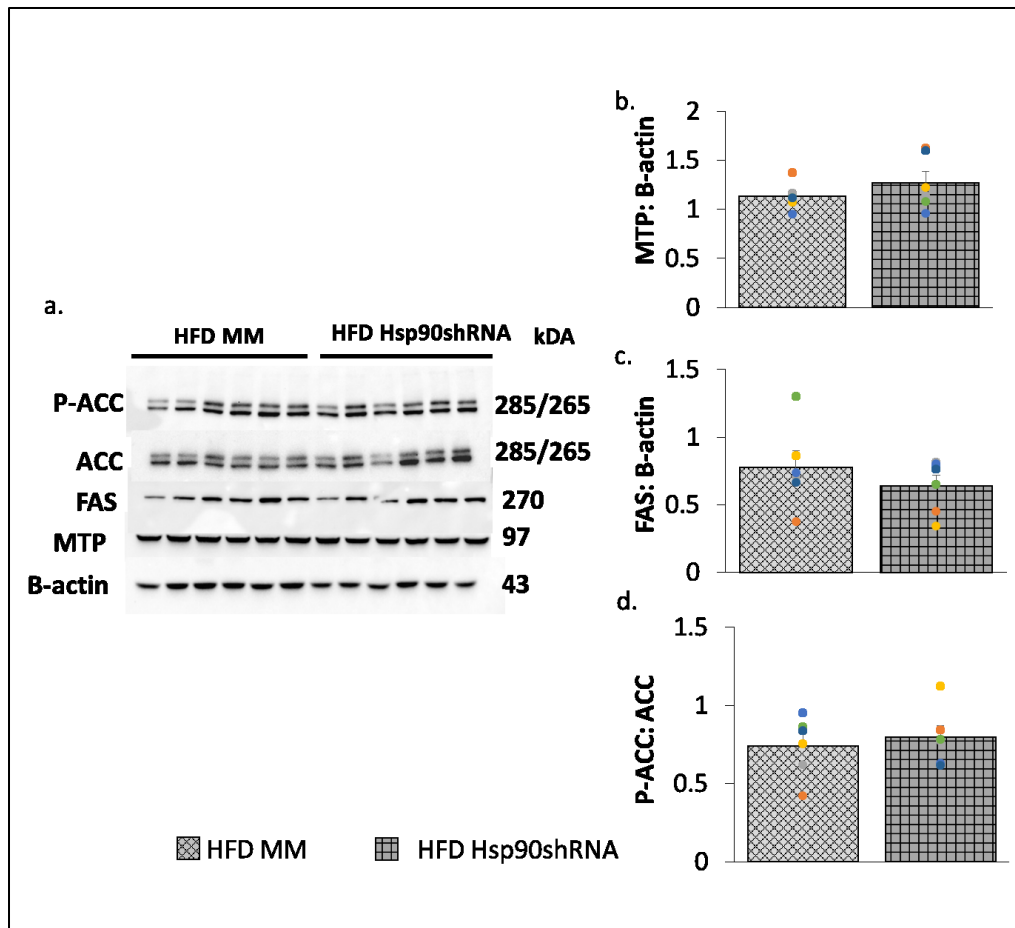


Figure 57- Chronic inhibition of heat shock protein 90 in the medial basal hypothalamus does not alter hepatic MTP, FAS, or P-ACC: ACC protein levels in rats fed a 3-day high fat diet. Liver samples were obtained from rats that were on a 3-day high fat diet (HFD) and were subjected to medial basal hypothalamic targeted injection of a lentivirus containing a mismatch (MM, light grey hashed bar) sequence or a heat shock protein 90 knockdown (Hsp90 shRNA, dark grey checkered bars). (a) Representative western blots from liver samples used to assess protein levels of proteins of interest. Proteins of interest include: (b) microsomal triglyceride transfer protein (MTP) relative to β -actin (HFD MM n=6, HFD Hsp90 shRNA n=6), (c) fatty acid synthase (FAS) relative to β -actin (HFD MM n=6, HFD Hsp90 shRNA n=6), and (d) phosphorylated-acetyl CoA carboxylase (P-ACC) to total acetyl-CoA carboxylase (ACC) (HFD MM n=6, HFD GRshRNA n=6).

Chapter 4: Discussion

4.1. Significance of results

The metabolic disease state is an enormous public health issue, and overproduction and secretion of hepatic triglyceride (TG) rich, very-low density lipoproteins (VLDL-TGs) is one of the main underlying problems for these individuals which contributes to the various physiological and economic issues¹⁻⁵. For example, approximately 2 billion adults are affected by overweight or obesity, and 80% of individuals with diabetes are also affected by excess body weight or obesity^{14,346}. In Canada alone the estimated annual economic burden of obesity is between \$4.6 billion to \$7.1 billion³⁴⁷. The underlying mechanisms that contribute to dyslipidemia remain elusive. Here, we report for the first time to our knowledge, that GC action directly in the medial basal hypothalamus (MBH) on glucocorticoid (GC) receptors (GRs), promotes hepatic VLDL-TG secretion, and that the inhibition of the MBH GR in diet-induced hyperlipidemic rats lowers VLDL-TG secretion. These significance new findings suggest that excessive hypothalamic GC action may contribute to VLDL-TG overproduction and dysregulation of lipid homeostasis in diet-induced hyperlipidemia.

Not only does this research contribute to the understanding of some of the mechanisms involved in the dysregulation of lipid homeostasis, but it also further implicates the importance of the brain in not only sensing peripheral nutrients and hormones, but eliciting a peripheral response. Previous literature has shown that the brain, and in particular the hypothalamus, can sense and respond to fluctuations in glucose^{261,278,281}, fatty acids^{112,282-285}, insulin^{260,289-296}, glucagon^{297,298}, glucagon-like peptide-1²⁹⁹⁻³⁰², leptin^{307-317,341}, and neuropeptide-Y (NPY)^{263,318-322} to lead to changes in metabolic homeostasis. Additionally, it has been shown that impairments in the sensing of these nutrients and hormones are associated with dysregulations in metabolic homeostasis, which has been suggested to contribute to the development of various metabolic disease states^{265,267,287}. Thus, the ability of the brain to effectively detect and respond to these nutrients and hormones is essential in regulating whole-body homeostasis. Importantly, metabolic disease states, such as diabetes and obesity, which are often characterized by dyslipidemia, are also characterized by elevated levels and/or action of GCs⁶⁻¹³. Despite the vast knowledge of the peripheral effects of GCs on regulating various physiological systems, the central effects of GCs with reference to modulating metabolism remains largely unknown. Here, we demonstrate that GCs can act directly in hypothalamus, and importantly, provide evidence that excessive peripheral GCs, which are elevated due to diet-induced hyperlipidemia, can act in

the MBH, to contribute elevated VLDL-TG secretion. Therefore, this research contributes to the understanding of mechanisms that contribute to dyslipidemia, demonstrates the importance of the brain in regulating lipid homeostasis, as well as contributes to the understanding of the central effects of GCs with reference to modulating lipid metabolism.

4.2. Discussion of results

4.2.1. Glucocorticoids can act on glucocorticoid receptors in the medial basal hypothalamus to modulate liver lipid homeostasis in regular chow-fed rats.

Here we show that a direct, acute infusion of GCs into the MBH in conscious, freely moving, SD rats on a RC diet stimulates hepatic VLDL-TG secretion. This data parallels previous findings that chronic (3-day) intracerebroventricular (ICV) dexamethasone (DEX) (5µg/day) infusions targeting the third ventricle increases plasma TGs, though it should be noted that VLDL-TG secretion was not assessed³²⁶. Importantly, we show that the lipostimulatory effect of hypothalamic GCs is negated via acute and chronic GR antagonism in the MBH. Additionally, inhibiting heat shock protein 90 (Hsp90), which is essential for the biological stability and function of the GR, in the MBH, both acutely and chronically, also negates the lipostimulatory effects of GCs. Together, this suggests that MBH GC action, which is mediated by MBH GRs, stimulates hepatic VLDL-TG secretion. Complimentary to this data, the Yue laboratory has demonstrated that acute MBH GC action impairs glucose tolerance and increases hepatic glucose production, and this effect can be negated via GR inhibition in healthy and pre-obese rats^{333,334}, demonstrating that MBH GC action contributes to both glucose and lipid homeostasis, and this effect is mediated by MBH GC-GR action.

The increase in VLDL-TG secretion as a result of MBH GC-GR action occurred independently of changes in hepatic TG content. Further, there was no significant change in plasma glucose or free fatty acids (FFAs). Stored TGs in the liver can undergo hydrolysis and re-esterification to TGs to contribute FFAs for the synthesis of the VLDL-TG particle¹³⁷. Glucose can be used as a substrate for *de novo* lipogenesis²⁹, and FFAs can be taken up by the liver and re-esterified to contribute to the fatty acyl-CoA pool for TG synthesis and VLDL-TG production and secretion^{140,141,348}. Thus, acute MBH DEX does not seem to affect the availability of substrates for VLDL-TG secretion in this model, therefore VLDL-TG secretion is increased without an increase in the mobilization of stored FFAs, which is consistent to acute ICV NPY

studies, which have similarly shown that direct administration of NPY into the hypothalamus stimulates hepatic VLDL-TG secretion^{263,320}.

Furthermore, hypothalamic GC-GR action in a regular chow (RC) model was not associated with any changes in hepatic liporegulatory protein levels (fatty acid synthase (FAS), microsomal triglyceride transfer protein (MTP), phosphorylated-acetyl CoA carboxylase to total acetyl CoA carboxylase (P-ACC: ACC), diacylglycerol acyltransferase 1 (DGAT1), and ADP-ribosylation factor 1 (Arf1)). Previous findings of increased VLDL-TG secretion as a result of hypothalamic NPY action also reported no significant change in hepatic FAS, MTP, or P-ACC: ACC protein levels^{263,320}. Additionally, no changes in hepatic sterol regulatory element binding protein 1c (*Srebf1c*), liver x receptor α (*Nr1h3*), liver x receptor β (*Nr1h2*), stearoyl-CoA desaturase 1 (*Scd1*), diacylglycerol acyltransferase 1 (*Dgat1*), *Dgat2*, fatty acid synthase (*Fasn*), lipin-2 (*Lpin2*), cell death-inducing DFF4-like effector B (*Cideb*), ADP-ribosylation factor 1 (*Arf1*), carnitine palmitoyltransferase 1a (*Cpt1a*), peroxisome proliferator-activated receptor α (*Ppara*), or AMP-activated protein kinase (*Ampk*) mRNA expression were observed. In contrast to our results, previous ICV NPY studies, that have reported similar increases in VLDL-TG secretion^{263,318–320}, also reported increased hepatic SCD1 and Arf1 protein levels and mRNA expression^{263,318–320}. However, this does not suggest SCD1 and/or Arf1 are not implicated in the observed GC-induced VLDL-TG secretory changes. For example, although there was no significant change in *Scd1* mRNA expression, this may not be indicative of SCD1 activity. Therefore, a SCD1 activity assay could be performed in the future to evaluate if MBH DEX affects SCD1 activity, in which 1-[¹⁴C]-stearoyl-CoA is used as a substrate, followed by the extraction and fractionation of long chain fatty acid-CoAs via reverse phase high performance liquid chromatography, and the ratio of oleic acid to stearic acid would then be assessed to determine SCD1 activity^{261,284,316}. However, it should be noted that SCD1 is the rate limiting step of the *de novo* synthesis of monounsaturated fatty acids, which are readily obtainable from diets^{29,63,67–70}. Given that in this model the Sprague Dawley rats are not entirely fasted, the significance of the SCD1 data may be diminished. In harmony with other hypothalamic mediated increase in hepatic VLDL-TG secretion, no significant changes were observed in hepatic MTP protein levels^{263,320}. However, there was an increase in hepatic *Mttp* mRNA expression as a result of ICV NPY infusions^{263,320}, thus, a future gene of interest for this study would be to investigate hepatic *Mttp* mRNA to compare our findings to those of the ICV NPY

infusions, which similarly have an increase in VLDL-TG secretion. Further, the investigated proteins and genes is not an exhaustive list in reference to hepatic lipid metabolism. Many other proteins and genes have yet to be investigated. For example, an ICV infusion of NPY targeting the third ventricle, which similarly increases VLDL-TG secretion^{263,318-320}, led to an increase in hepatic lipin-1 protein levels and mRNA expression³¹⁹. Lipin-1, one of the members of the lipin protein family, is expressed in the liver and has been shown to play a role in TG biosynthesis, by dephosphorylating phosphatidic acid to form diglycerides (DGs), a precursor for TGs and VLDL-TG synthesis¹⁰⁷. As increased hypothalamic NPY and GC action both contribute to increased VLDL-TG secretion^{263,318-320}, and hypothalamic NPY increases hepatic lipin-1³¹⁹, which has also been shown to be regulated by GCs in rodent hepatocytes²⁵⁵⁻²⁵⁷, lipin-1 could be altered via hypothalamic GC action. Thus, an increase in lipin-1 could contribute to an increase in TG synthesis, which would drive VLDL-TG production and secretion.

Recall, the primary apolipoproteins of VLDLs are apoBs, with apoB-48 being the predominant apolipoprotein for VLDLs in rats^{92,108,111-113}. In this study, plasma apoB-48 and plasma apoB-100 remained unchanged after experimentation between MBH Veh and MBH DEX RC-fed rats. However, MBH DEX RC-fed rats had a significantly higher basal apoB-100, which suggests that with just a 90-minute pre-infusion of DEX significantly increased plasma apoB-100. However, the ratios of plasma TGs to apoBs at t=0 mins and t=300 mins shows no significant difference between MBH Veh and MBH DEX RC-fed rats, which suggests there is no significant change of TGs per apoB particle. Together this data suggests that MBH DEX significantly increases hepatic VLDL-TG secretion but does not increase the TG content of the VLDL-TG particles. Though, it should be highlighted that this method of quantifying the TG content per apoB particle is not as accurate as other methods. A more precise method would be to fractionate the plasma samples to obtain lipoprotein fractions via various techniques, such as ultracentrifugation³⁴⁹⁻³⁵¹, high-performance liquid chromatography³⁵², gas chromatography³⁵³, fast-protein liquid chromatography³⁴⁹, and nuclear magnetic resonance spectroscopy³⁵⁴. Using these techniques, concentration of lipid particles, particle size, and lipidation of lipid particles can be determined. Thus, a future direction of this study would be to isolate the VLDL-TG fraction of the plasma samples, and isolate the apoBs from these fractions, to get a more reliable read on lipidation of the VLDL-TG particle.

No molecular analysis of liver samples was assessed for rats that received a MBH specific GR knockdown, acute Hsp90 inhibition, or chronic Hsp90 knockdown on a RC diet. However, all models revealed the same trend; GC action in the MBH stimulates VLDL-TG secretion, and this lipostimulatory effect of DEX can be negated via pharmacological or genetic inhibition of the GR within the MBH. Importantly for the chronic MBH GR knockdown models (MBH GRshRNA and Hsp90 shRNA), no changes in plasma TGs or VLDL-TG secretion were revealed relative to the RC MM control, which suggests that inhibition of the GR alone in RC rats, or Hsp90 (which is required for the stability and biological function of the GR), in the MBH does not alter lipid homeostasis. Additional molecular analysis is required to confirm that there were no liver molecular changes as a result of chronic MBH GR knockdown.

4.2.2. Comparison of the physiological effects of a 3-day high fat diet feeding regimen to regular chow feeding with acute hypothalamic glucocorticoid infusions.

As we have shown that GCs can act in the MBH to stimulate VLDL-TG secretion, the next step was to investigate if in a pre-obese model GC action in the MBH contributes to the hyperlipidemic profile of these rodents. It is known that excessive plasma concentrations and/or actions of GCs are associated with obesity and diabetes^{6-10,12,159} and GCs can cross the blood-brain barrier and act on GRs³⁵⁵⁻³⁵⁹. Further, since the inhibition of the GR and Hsp90 in the MBH negated the lipostimulatory effect of DEX in the RC, we postulated that the inhibition of MBH GC action should lower VLDL-TG secretion in the diet-induced hyperlipidemic rats. To do this we used a model where rats were fed a (high fat diet) for 3 days. Consistent with previously reported data, a 3-day HFD is capable of changing the metabolic profile via inducing mild hyperglycemia, mild hyperinsulinemia, as well as increased basal plasma TG and hepatic VLDL-TG secretion^{112,264,297,340,341}. Importantly, this 3-day HFD model has been shown to significantly increase plasma corticosterone (CORT)^{333,334}. Additionally, here we show that 3-day HFD feeding has a very similar plasma TG secretion and VLDL-TG secretion rate compared to MBH DEX RC-fed rodents, such that there is a significant increase relative to RC Veh. Similarly, HFD Veh and RC DEX did not alter hepatic FAS, P-ACC: ACC, MTP, or DGAT1 protein levels relative to RC Veh liver samples. Furthermore, when comparing RC Veh plasma samples to HFD Veh plasma samples, rats fed a 3-day HFD had elevated plasma apoB values, but both RC Veh and HFD Veh rats had a similar increase in plasma apoB-48 and apoB-100 after experimentation, but no change between the two groups. This effect was similar to the

effect of MBH DEX RC-fed rats relative to Veh-RC fed rats. Despite the decreased change between t=300 mins and t=0 mins plasma apoB values for the HFD, the ratio of plasma TGs to plasma apoBs was not changed between the two samples after experimentation, suggesting that there is no significant change in the amount of TGs per apoB particle following experimentation, which again is a trend similar to what was observed with the RC DEX model. Thus, with the increase plasma CORT concentration, as well as similar trends between RC DEX and HFD Veh, I hypothesized that the elevated GCs that arise from HFD feeding, can act in the MBH to contribute to the hyperlipidemic profile, and this effect can be negated, via the inhibition of the GR, or its downstream target Hsp90, in the MBH of HFD-induced hyperlipidemic rats.

When directly comparing the diet-induced hyperlipidemic model used in this study to other studies, the data is comparable. Previous literature using Sprague Dawley (SD) rats that were fed a 3-day HFD also demonstrated similarly elevated plasma glucose, plasma TGs and VLDL-TG secretion rates compared to the RC-fed controls, independent of changes in bodyweight^{112,261,264,340}. Importantly, the Yue laboratory has previously demonstrated that this 3-day HFD feeding model is associated with elevated plasma CORT levels^{333,334}. Moreover, long-term (12 weeks) HFD-feeding is associated with altered HPA activity and increased basal plasma GCs as well¹⁹⁸. Note, from these studies, no direct measures of plasma apoB-48 or apoB-100 were measured when comparing the RC-fed control rats to the 3-day HFD-fed rats. Additionally, no measures of hepatic molecular mechanisms were assessed to explain the dyslipidemia between the two groups in these studies. Though, in one study, it was shown that an ICV infusion of glucose, targeting the MBH, decreased hepatic VLDL-TG secretion, reducing the activity of SCD1, and this effect of hypothalamic glucose to mediate hepatic VLDL-TG secretion was lost in rats fed a 3-day HFD suggested that a defect in central nutrient sensing could contribute to altered hepatic lipid metabolism²⁶¹. Importantly, the ability of hypothalamus to detect and respond to peripheral nutrients is disrupted in acute HFD models, further disrupting whole body energy homeostasis^{112,261,341}.

Notably, short-term HFD feeding has been shown to increase inflammation in the MBH, which may contribute to insulin resistance within the hypothalamus^{360,361}, in-turn disrupting the hypothalamic regulation of hepatic glucose production leading to hepatic insulin resistance^{289,294,360-364}. Additionally, consistent with our observed data, a hallmark of the 3-day

HFD feeding model on SD rats is hyperglycemia, hyperinsulinemia and hepatic insulin resistance^{112,261,264,297,334,340,341,365-368}. Recall, hyperinsulinemia is associated with increased *de novo* lipogenesis, due in part by the activation of SREBP-1C, which stimulates TG production and subsequent VLDL-TG production and secretion^{23,25,27,28}. Additionally, insulin regulates FFA release from white adipose tissue (WAT) by suppressing lipolysis directly on adipocytes, but also by indirectly reducing sympathetic nervous system outflow to WAT³⁶⁸. However, in insulin resistance states, insulin can no longer suppress lipolysis in the adipose tissue, there is an increased flux of free fatty acids (FFAs) to the liver to stimulate VLDL-TG secretion and hepatic TG accumulation²²⁻²⁶. Importantly, in rats fed a 3-day HFD, insulin signaling within the MBH was impaired leading to disrupted sympathetic nervous system outflow to the WAT, resulting in unrestrained WAT lipolysis³⁶⁸. Note, the HFD did not impair insulin signaling in WAT in this model³⁶⁸. The Yue laboratory has previously shown that GC-GR action in SD rats fed a RC-diet, directly in the MBH impairs glucose homeostasis to a similar extent as a 3-day HFD, and importantly, the inhibition of GRs in the MBH in these rats fed a 3-day HFD led to a decrease in hepatic glucose production and an increase in hepatic insulin sensitivity^{333,334}. This suggests that the elevated plasma CORT that is a result of a 3-day HFD, could cross the blood-brain barrier, act specifically on MBH GRs, and contribute to the impaired hepatic insulin sensitivity and importantly, hepatic insulin sensitivity is improved via the inhibition of MBH GRs^{333,334}.

Thus, given that the 3-day HFD model is characterized by increase plasma CORT concentrations, that there are similar trends between MBH DEX treated rats fed a RC-diet and rats fed a 3-day HFD, and that MBH GR inhibition improved hepatic insulin sensitivity in these 3-day HFD fed rats, I hypothesized that the elevated GCs that arise from HFD feeding, can act in the MBH to contribute to the hyperlipidemic profile, and this effect can be negated, via the inhibition of the GR, or its downstream target Hsp90, in the MBH of HFD-induced hyperlipidemic rats.

4.2.3. Inhibition of the glucocorticoid receptor, specifically within the medial basal hypothalamus, lowers plasma triglycerides in diet induced hyperlipidemic rodents.

With correlating metabolic profiles between the HFD group and the RC DEX group with reference to lipid metabolism, and increased peripheral CORT in the HFD-fed rats, which could act in the MBH, chronic GR inhibition was assessed on rats fed a 3-day HFD. We show, for the first time to our understanding, that indeed, the inhibition of the GR, as shown with genetic inhibition of the GR in the MBH, or acute and chronic inhibition of Hsp90, lowers VLDL-TG secretion in 3-day HFD fed rats. Recall, in the RC model, rats that were subjected to MBH GRshRNA or MBH Hsp90 shRNA alone did not alter plasma TGs or hepatic VLDL-TG secretion. Additionally, note that it is known that peripheral CORT can pass through the blood-brain barrier and act on GRs³⁵⁵⁻³⁵⁹. This suggests increased plasma GCs pass through the blood-brain barrier, act in the MBH, and contribute to diet-induced dyslipidemia, and this effect can be negated via the inhibition of the GR and its downstream target, Hsp90 in the MBH. This data provides additional support to previous literature which demonstrated that chronically increased peripheral CORT, via administration in the drinking water of rodents, can act specifically on GRs in the MBH (confirmed by conducting liquid chromatography dual tandem mass spectrometry or RNA-seq on arcuate nucleus of these rodents), to contribute to obesity and hyperinsulinemia³³⁰⁻³³². Further, 3 day ICV GC infusions similarly increase basal plasma TGs in non-fasted rats, as well as increased food intake, body weight, and hyperinsulinemia, which contributed to the development of obesity, implicating the role of GCs in the hypothalamus³²⁶. Interestingly, chronic inhibition of the GR in the MBH of these hyperlipidemic rats lowers hepatic TG content relative to HFD MM controls. Previous literature has reported that an acute HFD-feeding regimen is capable of increasing hepatic TG stores^{144,369-376}. Interestingly, many of these findings were found to be associated with hepatic, but not peripheral insulin resistance^{144,370,375,376}. The Yue laboratory has also demonstrated that this 3-day HFD model is characterized by hepatic insulin resistance, and importantly, chronic inhibition of the GR in the MBH in 3-day HFD model rodents improved hepatic insulin sensitivity^{333,334}. Targeting hepatic *de novo* lipogenesis proteins, such as ACC and FAS has been shown to lower hepatic TG content in rodents fed an acute HFD^{375,377,378}. However, the decrease in hepatic TG content in HFD GR shRNA rats occurred independently of changes in plasma FFAs and glucose, as well as changes in hepatic FAS, MTP and P-ACC: ACC protein levels. Though, previous reports have detailed

changes in hepatic TG content independent of changes in FFAs and plasma glucose^{371,372,375,376}. Furthermore, the inhibition of the GR, selectively in the MBH, of diet-induced hyperlipidemic rats did not alter plasma apoB-48 or apoB-100 values relative to HFD MM controls, yet there was a strong trend for the HFD GRshRNA treated rats to have a lower plasma TG to apoB-100 ratio following experimentation. The increase in both plasma apoB-48 and apoB-100 following poloxamer administration was expected due to the increase in plasma VLDL-TG secretion relative to basal plasma TGs, and expectedly, plasma apoB-48 was the predominant form of apoB lipoprotein derived from the liver in rats^{92,108,111-113}. Consistent to these findings, previous literature using 10- hour fasted SD rats fed a RC diet that demonstrated a MBH-mediated decrease in hepatic VLDL-TG secretion had no change in in plasma apoB-48 or apoB-100 between the vehicle group and the VLDL-TG lowering group¹¹². However, there was no change in plasma apoB-100 following experimentation (t=150 mins) for either group¹¹². Though this data does provide additional support that apoB-48 is the predominant apoB derived from the liver in rats, the absence of an increase in plasma apoB-100 may be due to a shorter duration of experimentation (t=300 mins versus t=150 mins). Together, with the decrease plasma TGs following experimentation, comparable plasma apoB particles to HFD MM rats, yet a decrease in plasma TGs per apoB-100 particle ratio, the VLDL particles of the HFD GRshRNA rats may potentially have less TGs by t=300 mins. However, again, a future avenue for this study would be to fractionate the plasma samples, obtain the VLDL-TG fraction, and quantify VLDL-TG particle sizes and apoB content. A future direction of this project would also including investing hepatic proteins, such as CPT1, involved in fatty acid oxidation, as improved fatty oxidation has been associated with improved hepatic TG content^{144,377,379,380}.

Alternatively, both acute and chronic inhibition of the Hsp90 in the MBH negates the hyperlipidemic profile in a diet-induced hyperlipidemic model. Whereas there was no change in plasma FFAs and glucose for in the acute model (HFD Veh vs HFD Hsp90i), there was a significant reduction in both basal and end-of-experiment plasma FFAs for HFD Hsp90 shRNA rats compared to HFD MM rats. This may indicate that chronic Hsp90 inhibition could be reducing FFA secretion into the periphery from peripheral stores, or, increasing FFA uptake by the liver. Thus, chronic inhibition of Hsp90, selectively in the MBH, of 3-day HFD fed rats, decreases plasma TGs and plasma FFAs, therefore improving the dyslipidemic profile compared to HFD controls. However, this does not correlate with previously mentioned treatments groups

of this thesis that lower VLDL-TG secretion. This may be due to the variability of the individual data points from the FFA assay. However, future perspectives for this study would be to assess hepatic content of HFD Hsp90 shRNA rats to determine if there is an increase in FFA uptake and storage, or, alternatively, proteins levels and mRNA expression of genes involved in TG hydrolysis in WAT, such as ATGL, hormone sensitive lipase, and comparative gene identification 58, could be assessed. Chronic ICV GC infusions into rats have shown that GC action in the hypothalamus alters adipose tissue lipid metabolism, specifically by increasing expression of genes involved in lipogenesis (*Fasn* and *Acc*) and decreasing genes involved in lipolysis (*Lipe*), but does not increase plasma FFAs³²⁸. This would suggest that not only does GC action in the hypothalamus directly modulate hepatic lipid metabolism, but also is involved in adipose tissue lipid metabolism, providing further support that hypothalamic GCs modulate whole body lipid homeostasis. As previously stated, in rats fed a 3-day HFD, insulin signaling within the MBH was impaired leading to disrupted sympathetic nervous system outflow to the WAT, resulting in unrestrained WAT lipolysis independent of WAT insulin sensitivity³⁶⁸. Similar to other TG-lowering brain treatments presented in this thesis, there was no significant change in hepatic FAS, MTP, and P-ACC: ACC between HFD controls and HFD Hsp90 shRNA rats, suggesting that the mechanisms involved in lowering VLDL-TG secretion is not due to changes in hepatic *de novo* lipogenesis or MTP action. This trend is consistent for all VLDL-TG lowering models that were assessed (RC MIF+DEX vs RC DEX, HFD GRshRNA vs HFD MM, and HFD Hsp90shRNA vs HFD MM). Plasma apoB analysis was not completed for these treatment groups, but it is anticipated that similar to the chronic inhibition of the GR in the MBH in HFD GRshRNA plasma samples, no change of plasma apoB concentrations would be observed following experimentation, but a potential decrease in the ratio of plasma TGs to plasma apoBs would be observed, suggesting again a decrease in the number of TGs per VLDL particle, relative to HFD controls. Again, analysis of plasma apoB concentration, as well as a more accurate quantification of lipidation of the VLDL-TG particles can be alternatively and more accurately attained via analysis of lipid fractions.

4.3. Future directions

4.3.1. Further delineating mechanisms that underlie the lipostimulatory effects of glucocorticoid action in the medial basal hypothalamus.

Some future directions have been outlined above. These include investigating more proteins and genes that are involved in TG synthesis and VLDL-TG production and secretion. Some of these aforementioned proteins include SCD1 (SCD1 activity assay), lipin-1, and *Mtp* mRNA expression. However, given that in this model the SD rats are not entirely fasted, the significance of the SCD1 data may be diminished. An additional hepatic protein of interest would be TGH, which is involved in the hydrolysis of stored TGs to contribute to TG packaging during VLDL-TG production, and has been shown to be negatively regulated by peripheral GCs^{122,138,139,251}. Additionally, as mentioned prior, lipid fractions of the plasma samples should be assessed. This will enable for better analysis of the plasma samples, in particular lipidation of the VLDL-particles and a more accurate quantification of apoB particle concentration.

In this project, MBH specific GC stimulation promoted hepatic VLDL-TG secretion, and for all models, except for chronic MBH Hsp90 inhibition in the HFD model, these changes occurred independently of changes in peripheral FFAs. However, this does not suggest that FFA secretion and/or absorption doesn't play a role. Recall that peripheral GCs have a dichotomous effect on WAT lipid metabolism as GCs can promote both lipolysis²³⁷⁻²⁴⁰ and lipogenesis^{238,243}. Peripheral GCs have been shown to stimulate lipolysis in adipose tissue²³⁷⁻²⁴⁰, which contributes to an increase in FFAs which in turn can increase hepatic VLDL-TG flux^{140,141}. Additionally, hypercorticoesteronemia has been shown to promote lipolysis in the WAT, subsequently increasing peripheral FFAs²³⁹. However, chronic ICV infusion of GCs targeting the third ventricle into rats increases expression of genes involved in adipose tissues lipogenesis (*Fasn* and *Acc*) and decreasing genes involved in adipose tissue lipolysis (*Lipe*), independent of increases in plasma FFAs³²⁸. Though, with ICV infusions precise sites of GC action cannot be specified. Additionally, WAT dysfunction, characterized by impaired lipid deposition and unrestrained lipolysis leading to increased FFA flux in the nonfasted state has been linked to metabolic disease states, such as diabetes and obesity³⁸¹⁻³⁸⁴, and can contribute to hepatic insulin resistance³⁸⁵⁻³⁸⁷. Previous literature has revealed that using a 3-day HFD feeding regimen on SD rats led to increased basal FFAs and unrestrained WAT lipolysis due in part to impaired MBH sympathetic nervous system insulin mediated signaling to the WAT to restrict lipolysis

independent of WAT insulin sensitivity³⁶⁸. The Yue laboratory has previously demonstrated that hypothalamic GR inhibition improved hyperglycemia and hepatic insulin sensitivity in these 3-day HFD-fed rodents that have elevated basal CORT^{333,334}. Therefore, with evidence implicating GCs in regulating adipose tissue lipid metabolism, hypothalamic GCs having a role in glucose and lipid homeostasis, and the MBH being a regulatory site for WAT lipid homeostasis, a future direction of this study could be to investigate the effects of hypothalamic GCs in WAT lipid metabolism.

4.3.2. Neural populations in hypothalamus that may be modulated by glucocorticoids

Though this research clearly demonstrates that GCs act on GRs in the MBH to stimulate hepatic VLDL-TG secretion, the specific neural population(s) has yet to be investigated. As outlined previously, GRs are expressed on almost every tissue type of the body, and the brain is no different. GRs have been shown to be expressed on neurons and glial cells^{388,389}. The MBH, specifically the ARC, has been shown to have high levels of GR expression¹⁸². Within the ARC, there are two functionally opposed neural populations that are critical for regulating feeding and whole body energy metabolism; agouti-related protein (AgRP)/ NPY and pro-opiomelanocortin (POMC) neurons^{268,390–392}. These neurons stimulate and inhibit feeding, respectively²⁶⁸. As reported previously, ICV infusions of NPY into the third ventricle stimulates hepatic VLDL-TG secretion^{263,318–320}. In addition to this, hypothalamic *Npy* mRNA expression is upregulated by acute GC action^{332,393–396}, and NPY fibers found in the MBH innervate preautonomic neurons in the PVN and spinal column, which provides sympathetic nervous system output to the peripheral tissues^{397–399}. Importantly, a GC infusion directly into the MBH has been shown to decrease hepatic insulin sensitivity, but this effect is negated via hypothalamic NPY inhibition, suggesting that the hypothalamic effects of GCs to modulate peripheral energy metabolism is mediated by NPY signaling³²⁹. Furthermore, POMC signaling has been shown to be decreased in diet-induced obese mice⁴⁰⁰ and increased hypothalamic NPY tone is associated with obesity and diabetes^{291,401–403}. Thus, with differential roles of AgRP/NPY and POMC neuronal activity in whole body energy homeostasis, yet the similar lipostimulatory effect of both hypothalamic GCs and NPY, but evidence suggesting that hypothalamic GC action to alter metabolic changes is mediated NPY, future studies are required to not only identify if MBH GCs are acting on these neuronal populations, but also to identify if this interaction is required for the lipostimulatory effects of hypothalamic GCs.

4.3.3. Brain-liver neurocircuitry.

Although we show that direct GC action in the MBH stimulates a peripheral, hepatic change in lipid metabolism, we have yet to show direct mechanism by which the brain is able to communicate with the liver. It is known that the brain can directly communicate to the liver to alter lipid metabolism via the central nervous system, either via the hepatic vagal (parasympathetic) nerve, or the hepatic sympathetic nerve^{112,315,318}. There seems to be conflicting data as to whether MBH GC action is mediated via sympathetic or parasympathetic signals to the liver. For example, one group has suggested that the metabolic effects of 2-day ICV DEX, (hyperphagia, increased body weight, basal hyperinsulinemia, decreased insulin-stimulated total rate of glucose disappearance, and no change in glucose production) were mediated by the hepatic vagal nerve, as a vagotomy, negated the observed effects³²⁷. Other studies illustrated that MBH oleic acid, which lowers hepatic VLDL-TG secretion¹¹², or ICV leptin, which increases hepatic VLDL-TG secretion³¹⁵, required an intact hepatic vagal nerve to alter hepatic VLDL-TG secretion, and importantly, a sympathectomy did not alter ICV leptin's ability to increase VLDL-TG secretion³¹⁵. Conversely, infusion of DEX directly into the ARC, which was shown to alter hepatic insulin sensitivity was mediated by the sympathetic nerve, not the vagal nerve³²⁹. In support of this claim, various ICV NPY studies have also demonstrated that the metabolic effects of hypothalamic NPY, which increases VLDL-TG to a similar extent as hypothalamic GCs, is inhibited by hepatic sympathetic denervation^{318,319,404}. Therefore, hepatic sympathetic and/or parasympathetic denervation surgeries on our SD rats could provide us with understanding of the direct brain-liver neurocircuitry that mediates the lipostimulatory effects of MBH GC action.

4.4. Limitations of the study.

4.4.1. Medial basal hypothalamic glucocorticoid action was only investigated under fasted conditions

Although the effects of hypothalamic GC action have now clearly been demonstrated to alter hepatic lipid metabolism, these effects were only under fasted conditions. A 10-hour fast was implemented for these rats to minimize the production and secretion of gut-derived TG-rich lipoproteins^{112,263}. Although this model not only provides critical evidence that hypothalamic GC excess may contribute to dyslipidemia, but also helps delineate some of the central effects of GCs, it is not a true representation of all physiological relevant conditions (i.e., both fasted and fed states). Thus, to mitigate this limitation, the same poloxamer studies could be performed in

the post-prandial condition to investigate if hypothalamic GCs contribute to not just VLDL-TG production and secretion, but also chylomicron production and secretion. Additionally, VLDL-TG secretion could also be investigated in the fed state, without the contribution of chylomicrons via the use of a glucose gavage administration in fasted rats with a poloxamer infusion, as a glucose gavage mimics the postprandial state (increased insulin, which facilitates the diffusion of plasma glucose into fat and muscle cells as well as activates glycolysis and protein and fatty acid synthesis) without contributing dietary lipids to the gut⁴⁰⁵⁻⁴⁰⁷.

4.4.2. Limitations of pharmaceuticals used for medial basal hypothalamic treatments

In this study DEX was utilized as a synthetic GC rather than CORT, which is the main biologically active natural GC. DEX has been shown to bind to the GR with higher affinity and potency compared to CORT and is cleared from the circulation at a slower rate^{408,409}. Additionally, the structures of DEX and CORT differ, in-part by a C1-C2 double bond in the DEX structure, which facilitates the hydrogen groups to form a hydrogen bond network with the GR, which increases its binding affinity^{409,410}. Importantly, DEX almost exclusively binds to GRs, as it has been shown to have a minimal effect on MR activity, while CORT binds to both GRs and MRs⁴¹¹. Therefore, to not only mimic natural conditions, but also to investigate the role of GC action on MRs in relation to lipid homeostasis, MBH CORT infusions should be tested in the future to verify the above conditions.

Furthermore, MIF, which was used as a GR antagonist in this study, is also widely used as an abortion drug due to its ability to antagonize the progesterone receptor⁴¹²⁻⁴¹⁴. In addition to progesterone receptors and GRs, MIF also antagonizes androgen receptors to a much lesser extent compared to the other two receptors (IC_{50} : PR<GR<AR)⁴¹⁵⁻⁴¹⁷. Though, it should be noted that MIF does not have an effect on MRs or estrogen receptors⁴¹⁶. In reference to the GR, MIF competitively binds to the GR and is able to bind to the human GR with approximately a 4 times higher affinity than DEX⁴¹⁸. However, progesterone receptors and androgen receptors are found in the hypothalamus⁴¹⁹⁻⁴²⁴, and there is evidence that GCs can bind to progesterone and androgen receptors⁴²⁵⁻⁴²⁷. Thus, since both MIF and GCs are capable of binding onto various nuclear receptors, future research is needed to investigate the involvement of hypothalamic progesterone and androgen receptors in mediating GC signaling to alter hepatic lipid metabolism. Though, it should be noted that in this study we were able to illustrate that MBH MIF inhibited the

lipostimulatory effects of MBH DEX presumably by acting on the GR in the MBH, as both the pharmacological inhibition, as well as the genetic loss-of-function technique, using GRshRNA, negated the effects of DEX in a similar fashion.

The Hsp90 inhibitor used in this study (17-AAG) is a class of benzoquinone ansamycins that inhibit Hsp90 by binding to the N-terminal ATP binding pocket of Hsp90 to block ATPase activity, as well as inhibiting the association of Hsp90 with heat shock factor-1, which leads to the transcription of chaperones such as Hsp70 and Hsp40, which facilitate the degradation of the misfolded protein⁴²⁸⁻⁴³¹. Although Hsp90 is required for the biological function and stability of the GR¹⁸⁵⁻¹⁸⁷, it is also required for the biological function of the androgen and progesterone receptors^{432,433}. Additionally, Hsp90 is one of the most abundant and highly conserved molecular chaperones in eukaryotes, as it is involved in numerous different physiological pathways due to its housekeeping function and involvement in protein folding, stability, and transport⁴³⁴. In light of the diverse actions of Hsp90, Hsp90 inhibition in various tissues has been considered a therapeutic prospective in the treatment of cancer⁴³⁵, obesity⁴³⁶, diabetes⁴³⁶⁻⁴³⁸, and Alzheimer's disease^{337,439}. Thus, with Hsp90s being implicated in cellular and physiological mechanisms, the effects of Hsp90 inhibition in this study may have not been specific to just the GRs. To mitigate this issue, future studies should identify if MBH GR activity is decreased as a result of Hsp90 inhibition. However, we were able to illustrate that MBH Hsp90i and MBH Hsp90 shRNA were able to negate the lipostimulatory effects of hypothalamic GC action in a similar fashion in both the RC and HFD model, which suggests that Hsp90 inhibition was indeed mediating MBH GR function.

4.4.3. High fat diet feeding studies

The 3-day HFD feeding model implemented in this study was used to investigate the effects of GR inhibition in the MBH to modulate lipid homeostasis in a pre-obese model with hypercorticosteronemia. However, the effects of GR inhibition should also be assessed in other metabolic disease models, such as models of obesity and diabetes, to not only contribute to our understanding of these diseases, but to further implicate the physiological relevance of GC excess acting in the brain. For example, the same set of poloxamer VLDL-TG secretion studies can be performed in SD rats subjected to longer HFD feeding (12-weeks), which has also been demonstrated to alter HPA activity and have increased basal GCs and increase GR

immunoreactivity in the hypothalamus¹⁹⁸. Additionally, MBH GC action could be investigated in diet-induced obese rats subjected to a low-dose streptozotocin-nicotinamide injection to induce type 2 diabetes^{367,440–443}.

4.4.4. ApoB assessments

As mentioned prior, the methodology used in this thesis to assess plasma apoB concentrations, as well as the estimate of plasma TGs per apoBs, was a proxy evaluation. A more accurate and precise method would be to obtain the VLDL-TG lipid fraction from the plasma sample, then isolate the apoBs from the VLDL-TG fraction. This can be attained via various techniques, such as ultracentrifugation^{349–351}, high-performance liquid chromatography³⁵², gas chromatography³⁵³, fast-protein liquid chromatography³⁴⁹, and nuclear magnetic resonance spectroscopy³⁵⁴. Though, using these more precise techniques, the same effect would be expected, such that following the administration of poloxamer, and the subsequent rise in VLDL-TG secretion, an increase in plasma apoB-48 and apoB-100 would follow, with apoB-48 being the predominant apoB particle^{92,108,111–113}. Additionally, using these techniques various other important lipid readouts can be attained, such as: concentration of lipid particles, particle size, and lipidation of lipid particles. Further, this study is based on the assumption that in the fasted state gut derived chylomicrons do not significantly play a role in the rate of appearance of TG-rich lipoproteins^{112,263}, thus we present the rate of TG appearance as VLDL-TG secretion rate, assuming all TGs are bound to liver derived VLDLs. Lipid fractionation would confirm the contribution of each TG-rich lipoprotein in TG accumulation. However a reason why these particular techniques were not implemented was because they require far more plasma compared to the western blot technique used in this thesis (2µl versus 100µl-2ml). Thus, a future direction of this study could be to isolate the VLDL-TG fraction of the plasma samples, and isolate the apoBs from these fractions, to get a more reliable read on lipidation of the VLDL-TG particle.

4.4.5. Measurements of brain physiological concentrations of corticosterone

Although it is known that GCs cross the blood-brain barrier and act on GRs^{355–359}, the extracellular levels of CORT within the MBH of rats *in vivo* has yet to be determined in this study. For example, in studies where peripheral CORT levels were increased in mice via exogenous CORT treatment there was a similar trend in circulating CORT levels and hypothalamic CORT levels, as after 4 weeks of exogenous CORT treatment, peripheral CORT

increased 9-fold and hypothalamic CORT increased 4-fold³³⁰. Thus, to assess the local physiological increase in CORT in the MBH following 3-day HFD feeding, which is known to increase peripheral CORT, future experiments could conduct a microdialysis assessment in RC and 3-day HFD fed rats⁴⁴⁴.

4.5. Conclusion

In summary, here we report, for the first time, that hypothalamic GC action alters hepatic lipid metabolism, and provide novel evidence that excessive hypothalamic GC action may contribute to VLDL-TG overproduction and dysregulation of lipid homeostasis in diet-induced hyperlipidemia. In the RC model we show that MBH GC action, which is mediated by MBH GRs, stimulates hepatic VLDL-TG overproduction. Additionally, in the HFD model, which has elevated VLDL-TG secretion as well as elevated basal plasma CORT levels, the inhibition of GC action, either genetically with GR shRNA, or by targeting Hsp90 which is required for the biological function and stability of the GR, lowers VLDL-TG secretion, thus improving the lipid profile of these rats. Excessive levels and/ or levels of GCs are associated with metabolic disease states characterized by dyslipidemia, such as diabetes and obesity⁶⁻¹³. Thus, this research provides a clear link with increased GCs action, which is associated with metabolic disease states, which can act in the MBH, to contribute to VLDL-TG overproduction, and this hyperlipidemia can be improved via selective MBH GR inhibition.

Not only does this research contribute to the understanding of GC action in the brain in regulating peripheral metabolism, and implicate the role of hypothalamic GC excess in the metabolic disease states, but it also could lead to future therapeutics involving MBH GC action to modulate lipid metabolism in disease states. A growing body of evidence in animal studies supports that brain pathways play a role in energy homeostasis^{266,445-448}. In light of this, pharmaceuticals have been developed to target brain pathways in efforts to improve the metabolic profiles of those with metabolic diseases. For example, Wegovy (semaglutide) is a glucagon-like peptide-1 receptor agonist that received FDA approval in 2021⁴⁴⁹. Wegovy works by either directly acting on the hypothalamus or hindbrain, or, by indirect activation via the vagus nerve⁴⁴⁹. Activation of the glucagon-like peptide-1 receptor induces anorectic effects and decreases body weight in obese individuals with and without diabetes⁴⁴⁹. Additionally, lorcaserin, which was FDA approved until 2020 due to increased risk of malignancies, was an

anti-obesity drug that acts as a serotonin 5-HT_{2C} receptor agonist in the hypothalamus to reduce feeding behaviour⁴⁵⁰. Furthermore, hypercortisolemia is implicated in depression, neurodegeneration, and age-related disorders, which further broadens the implications of this research for future clinical applications targeting MBH-GC mediated signaling^{160,173,451}.

References

1. Reaven, G. M., Chen, Y.-D. I., Jeppesen, J., Maheux, P. & Krauss, R. M. Insulin resistance and hyperinsulinemia in individuals with small, dense, low density lipoprotein particles. *J. Clin. Invest.* **92**, 141–146 (1993).
2. Ginsberg, H. N. New perspectives on atherogenesis. *Circulation* **106**, 2137–2142 (2002).
3. Sparks, J. D., Sparks, C. E. & Adeli, K. Selective hepatic insulin resistance, VLDL overproduction, and hypertriglyceridemia. *Arterioscler. Thromb. Vasc. Biol.* **32**, 2104–2112 (2012).
4. Nelson, A. J., Rochelau, S. K. & Nicholls, S. J. Managing dyslipidemia in type 2 diabetes. *Endocrinol. Metab. Clin. North Am.* **47**, 153–173 (2018).
5. Sherling, D. H., Perumareddi, P. & Hennekens, C. H. Metabolic Syndrome: Clinical and Policy Implications of the New Silent Killer. *J. Cardiovasc. Pharmacol. Ther.* **22**, 365–367 (2017).
6. Bjorntorp, P. & Rosmond, R. Hypothalamic origin of the metabolic syndrome x. *Ann. N. Y. Acad. Sci.* **892**, 297–307 (1999).
7. Nashel, D. J. Is atherosclerosis a complication of long-term corticosteroid treatment? *Am. J. Med.* **80**, 925–929 (1986).
8. Pivonello, R. *et al.* Metabolic alterations and cardiovascular outcomes of cortisol excess. *Front. Horm. Res.* **46**, 54–65 (2016).
9. Roy, M., Collier, B. & Roy, A. Hypothalamic-pituitary-adrenal axis dysregulation among diabetic outpatients. *Psychiatry Res.* **31**, 31–37 (1990).
10. Chan, O., Inouye, K., Vranic, M. & Matthews, S. G. Hyperactivation of the Hypothalamo-Pituitary-Adrenocortical Axis in Streptozotocin-Diabetes Is Associated with Reduced Stress Responsiveness and Decreased Pituitary and Adrenal Sensitivity. *Endocrinology* **143**, 1761–1768 (2002).
11. Roy, M. S., Roy, A. & Brown, S. Increased urinary-free cortisol outputs in diabetic patients. *J. Diabetes Complications* **12**, 24–27 (1998).
12. Hewagalamulage, S. D., Lee, T. K., Clarke, I. J. & Henry, B. A. Stress, cortisol, and obesity: a role for cortisol responsiveness in identifying individuals prone to obesity. *Domestic Animal Endocrinology* **56**, S112–S120 (2016).
13. Hudson, J. I. *et al.* Abnormal Results of Dexamethasone Suppression Tests in Nondepressed Patients With Diabetes Mellitus. *Arch. Gen. Psychiatry* **41**, 1086–1089 (1984).
14. World Health Organization. Obesity and overweight. (2021). Available at: <https://www.who.int/en/news-room/fact-sheets/detail/obesity-and-overweight>. (Accessed: 22nd November 2021)
15. Statistics Canada. Overweight and obese adults, 2018. *Health Fact Sheets* (2019). Available at: <https://www150.statcan.gc.ca/n1/pub/82-625-x/2019001/article/00005-eng.htm>. (Accessed: 22nd November 2021)
16. González-Muniesa, P. *et al.* Obesity. *Nat. Rev. Dis. Prim.* **2017 31 3**, 1–18 (2017).
17. Blüher, M. Obesity: global epidemiology and pathogenesis. *Nat. Rev. Endocrinol.* **2019 155 15**, 288–298 (2019).
18. World Health Organization. *Global Report on Diabetes*. (2016).
19. Statistics Canada. Diabetes, 2017. *Health Fact Sheets* (2018). Available at: <https://www150.statcan.gc.ca/n1/pub/82-625-x/2018001/article/54982-eng.htm>.

- (Accessed: 22nd November 2021)
20. Aras, M., Tchang, B. G. & Pape, J. Obesity and Diabetes. *Nurs. Clin. North Am.* **56**, 527–541 (2021).
 21. World Health Organization. Diabetes. (2021). Available at: <https://www.who.int/news-room/fact-sheets/detail/diabetes>. (Accessed: 22nd November 2021)
 22. Mili, N. *et al.* Obesity, metabolic syndrome, and cancer: pathophysiological and therapeutic associations. *Endocr. 2021 743* **74**, 478–497 (2021).
 23. Klop, B., Elte, J. W. F. & Cabezas, M. C. Dyslipidemia in Obesity: Mechanisms and Potential Targets. *Nutrients* **5**, 1218 (2013).
 24. Choi, S. H. & Ginsberg, H. N. Increased very low density lipoprotein (VLDL) secretion, hepatic steatosis, and insulin resistance. *Trends Endocrinol. Metab.* **22**, 353–363 (2011).
 25. Ye, J. Mechanisms of insulin resistance in obesity. *Front. Med. 2013 71* **7**, 14–24 (2013).
 26. Monteiro, R. & Azevedo, I. Chronic inflammation in obesity and the metabolic syndrome. *Mediators Inflamm.* **2010**, (2010).
 27. Choi, S. H. & Ginsberg, H. N. Increased Very Low Density Lipoprotein Secretion, Hepatic Steatosis, and Insulin Resistance. *Trends Endocrinol. Metab.* **22**, 353 (2011).
 28. Brown, M. S. & Goldstein, J. L. Selective versus Total Insulin Resistance: A Pathogenic Paradox. *Cell Metab.* **7**, 95–96 (2008).
 29. Rui, L. Energy metabolism in the liver. *Compr. Physiol.* **4**, 177–97 (2014).
 30. Shimomura, I. *et al.* Decreased IRS-2 and Increased SREBP-1c Lead to Mixed Insulin Resistance and Sensitivity in Livers of Lipodystrophic and ob/ob Mice. *Mol. Cell* **6**, 77–86 (2000).
 31. DeFronzo, R. A. & Tripathy, D. Skeletal Muscle Insulin Resistance Is the Primary Defect in Type 2 Diabetes. *Diabetes Care* **32**, S157 (2009).
 32. Robertson, R. P. Beta-cell deterioration during diabetes: what's in the gun? *Trends Endocrinol. Metab.* **20**, 388–393 (2009).
 33. Mu, H. & Høy, C. E. The digestion of dietary triacylglycerols. *Prog. Lipid Res.* **43**, 105–133 (2004).
 34. Ko, C.-W., Qu, J., Black, D. D. & Tso, P. Regulation of intestinal lipid metabolism: current concepts and relevance to disease. *Nat. Rev. Gastroenterol. Hepatol.* **2020 173** **17**, 169–183 (2020).
 35. DeNigris, S. J., Hamosh, M., Kasbekar, D. K., Lee, T. C. & Hamosh, P. Lingual and gastric lipases: species differences in the origin of prepancreatic digestive lipases and in the localization of gastric lipase. *Biochim. Biophys. Acta - Lipids Lipid Metab.* **959**, 38–45 (1988).
 36. Field, R. B. & Scow, R. O. Purification and characterization of rat lingual lipase. *J. Biol. Chem.* **258**, 14563–14569 (1983).
 37. Hamosh, M., Ganot, D. & Hamosh, P. Rat lingual lipase. Characteristics of enzyme activity. *J. Biol. Chem.* **254**, 12121–12125 (1979).
 38. Liao, T. H., Hamosh, P. & Hamosh, M. Fat digestion by lingual lipase: Mechanism of lipolysis in the stomach and upper small intestine. *Pediatr. Res.* **18**, (1984).
 39. Bernbäck, S., Bläckberg, L. & Hernell, O. Fatty acids generated by gastric lipase promote human milk triacylglycerol digestion by pancreatic colipase-dependent lipase. *Biochim. Biophys. Acta - Lipids Lipid Metab.* **1001**, 286–293 (1989).
 40. Hamosh, M. *et al.* Fat Digestion in the Newborn: Characterization of lipase in gastric aspirates of premature and term infants. *J. Clin. Invest.* **67**, 838–846 (1981).

41. Zeng, Q., Ou, L., Wang, W. & Guo, D.-Y. Gastrin, Cholecystokinin, Signaling, and Biological Activities in Cellular Processes. *Front. Endocrinol. (Lausanne)*. **11**, 112 (2020).
42. Watanabe, S., Lee, K. Y., Chang, T. M., Berger-Ornstein, L. & Chey, W. Y. Role of pancreatic enzymes on release of cholecystokinin-pancreozymin in response to fat. <https://doi.org/10.1152/ajpgi.1988.254.6.G837> **254**, (1988).
43. Mattson, F. H. & Volpenhein, R. A. The Digestion and Absorption of Triglycerides. *J. Biol. Chem.* **239**, 2772–2777 (1964).
44. Gallo, L. L., Bennett Clark, S., Myers, S. & Vahouny, G. V. Cholesterol absorption in rat intestine: role of cholesterol esterase and acyl coenzyme A:cholesterol acyltransferase. *J. Lipid Res.* **25**, 604–612 (1984).
45. Lobo, M. V. T. *et al.* Localization of the lipid receptors CD36 and CLA-1/SR-BI in the human gastrointestinal tract: Towards the identification of receptors mediating the intestinal absorption of dietary lipids. *J. Histochem. Cytochem.* **49**, (2001).
46. Nauli, A. M. *et al.* CD36 Is Important for Chylomicron Formation and Secretion and May Mediate Cholesterol Uptake in the Proximal Intestine. *Gastroenterology* **131**, 1197–1207 (2006).
47. Nassir, F., Wilson, B., Han, X., Gross, R. W. & Abumrad, N. A. CD36 Is Important for Fatty Acid and Cholesterol Uptake by the Proximal but Not Distal Intestine. *J. Biol. Chem.* **282**, 19493–19501 (2007).
48. Drover, V. A. *et al.* CD36 deficiency impairs intestinal lipid secretion and clearance of chylomicrons from the blood. *J. Clin. Invest.* **115**, 1290–1297 (2005).
49. Hajri, T., Han, X., Bonen, A. & Abumrad, N. Defective fatty acid uptake modulates insulin responsiveness and metabolic responses to diet in CD36-null mice. *J. Clin. Invest.* **109**, 1381–1389 (2002).
50. Goldberg, I., Eckel, R. & Abumrad, N. Regulation of fatty acid uptake into tissues: lipoprotein lipase- and CD36-mediated pathways. *J. Lipid Res.* **50 Suppl**, (2009).
51. Hames, K., Vella, A., Kemp, B. & Jensen, M. Free fatty acid uptake in humans with CD36 deficiency. *Diabetes* **63**, 3606–3614 (2014).
52. Bass, N. M. *et al.* Regulation of the biosynthesis of two distinct fatty acid-binding proteins in rat liver and intestine. Influences of sex difference and of clofibrate. *J. Biol. Chem.* **260**, 1432–1436 (1985).
53. Kayden, H. J., Senior, J. R. & Mattson, F. H. The monoglyceride pathway of fat absorption in man. *J. Clin. Invest.* **46**, (1967).
54. Demignot, S., Beilstein, F. & Morel, E. Triglyceride-rich lipoproteins and cytosolic lipid droplets in enterocytes: Key players in intestinal physiology and metabolic disorders. *Biochimie* **96**, 48–55 (2014).
55. Tso, P. & Balint, J. A. Formation and transport of chylomicrons by enterocytes to the lymphatics. <https://doi.org/10.1152/ajpgi.1986.250.6.G715> **250**, (1986).
56. Sabesin, S. M. & Frase, S. Electron microscopic studies of the assembly, intracellular transport, and secretion of chylomicrons by rat intestine. *J. Lipid Res.* **18**, 496–511 (1977).
57. Dallinga-Thie, G. M. *et al.* The metabolism of triglyceride-rich lipoproteins revisited: New players, new insight. *Atherosclerosis* **211**, 1–8 (2010).
58. Olivecrona, G. Role of lipoprotein lipase in lipid metabolism. *Curr. Opin. Lipidol.* **27**, 233–241 (2016).
59. Babayan, V. K. Medium chain triglycerides and structured lipids. *Lipids* **22**, 417–420

- (1987).
60. Schönfeld, P. & Wojtczak, L. Short- and medium-chain fatty acids in energy metabolism: The cellular perspective. *Journal of Lipid Research* **57**, (2016).
 61. Ameer, F., ScandiuZZi, L., Hasnain, S., Kalbacher, H. & Zaidi, N. De novo lipogenesis in health and disease. *Metabolism* **63**, 895–902 (2014).
 62. Hellerstein, M. K. De novo lipogenesis in humans: Metabolic and regulatory aspects. *Eur. J. Clin. Nutr.* **53**, (1999).
 63. Lehner, R. & Quiroga, A. D. Fatty Acid Handling in Mammalian Cells. in *Biochemistry of Lipids, Lipoproteins and Membranes* (eds. Ridgway, N. & McLeod, R. S.) 149–184 (Elsevier, 2016).
 64. Tong, L. Structure and function of biotin-dependent carboxylases. *Cellular and Molecular Life Sciences* **70**, (2013).
 65. Hunkeler, M. *et al.* Structural basis for regulation of human acetyl-CoA carboxylase. *Nat.* *2018 5587710* **558**, 470–474 (2018).
 66. Ha, J., Daniel, S., Broyles, S. S. & Kim, K. H. Critical phosphorylation sites for acetyl-CoA carboxylase activity. *J. Biol. Chem.* **269**, 22162–22168 (1994).
 67. Ntambi, J. M. & Miyazaki, M. Regulation of stearoyl-CoA desaturases and role in metabolism. *Prog. Lipid Res.* **43**, 91–104 (2004).
 68. Weng, C. M., Miyazaki, M., Chu, K. & Ntambi, J. Colocalization of SCD1 and DGAT2: Implying preference for endogenous monounsaturated fatty acids in triglyceride synthesis. *J. Lipid Res.* **47**, (2006).
 69. Enoch, H. G., Catala, A. & Strittmatter, P. Mechanism of rat liver microsomal stearyl-CoA desaturase. Studies of the substrate specificity, enzyme-substrate interactions, and the function of lipid. *J. Biol. Chem.* **251**, 5095–5103 (1976).
 70. Miyazaki, M. *et al.* Stearoyl-CoA desaturase 1 gene expression is necessary for fructose-mediated induction of lipogenic gene expression by sterol regulatory element-binding protein-1c-dependent and independent mechanisms. *J. Biol. Chem.* **279**, (2004).
 71. Iizuka, K., Bruick, R. K., Liang, G., Horton, J. D. & Uyeda, K. Deficiency of carbohydrate response element-binding protein (ChREBP) reduces lipogenesis as well as glycolysis. *Proc. Natl. Acad. Sci. U. S. A.* **101**, 7281–7286 (2004).
 72. Yamashita, H. *et al.* A glucose-responsive transcription factor that regulates carbohydrate metabolism in the liver. *Proc. Natl. Acad. Sci. U. S. A.* **98**, (2001).
 73. Denechaud, P. D. *et al.* ChREBP, but not LXRs, is required for the induction of glucose-regulated genes in mouse liver. *J. Clin. Invest.* **118**, 956–964 (2008).
 74. Kawaguchi, T., Osatomi, K., Yamashita, H., Kabashima, T. & Uyeda, K. Mechanism for fatty acid ‘sparing’ effect on glucose-induced transcription: regulation of carbohydrate-responsive element-binding protein by AMP-activated protein kinase. *J. Biol. Chem.* **277**, 3829–3835 (2002).
 75. Kawaguchi, T., Takenoshita, M., Kabashima, T. & Uyeda, K. Glucose and cAMP regulate the L-type pyruvate kinase gene by phosphorylation/dephosphorylation of the carbohydrate response element binding protein. *Proc. Natl. Acad. Sci. U. S. A.* **98**, 13710–13715 (2001).
 76. Horton, J. D., Goldstein, J. L. & Brown, M. S. SREBPs: activators of the complete program of cholesterol and fatty acid synthesis in the liver. *J. Clin. Invest.* **109**, 1125–31 (2002).
 77. Shimomura, I., Shimano, H., Korn, B. S., Bashmakov, Y. & Horton, J. D. Nuclear sterol

- regulatory element-binding proteins activate genes responsible for the entire program of unsaturated fatty acid biosynthesis in transgenic mouse liver. *J. Biol. Chem.* **273**, (1998).
78. Norton, J. D. *et al.* Activation of cholesterol synthesis in preference to fatty acid synthesis in liver and adipose tissue of transgenic mice overproducing sterol regulatory element-binding protein-2. *J. Clin. Invest.* **101**, (1998).
 79. Oh, S. Y. *et al.* Acetyl-CoA Carboxylase β Gene Is Regulated by Sterol Regulatory Element-binding Protein-1 in Liver *. *J. Biol. Chem.* **278**, 28410–28417 (2003).
 80. Li, Y. *et al.* AMPK phosphorylates and inhibits SREBP activity to attenuate hepatic steatosis and atherosclerosis in diet-induced insulin-resistant mice. *Cell Metab.* **13**, 376–388 (2011).
 81. Repa, J. J. *et al.* Regulation of mouse sterol regulatory element-binding protein-1c gene (SREBP-1c) by oxysterol receptors, LXRalpha and LXRbeta. *Genes Dev.* **14**, 2819–2830 (2000).
 82. Seol, W., Choi, H. S. & Moore, D. D. Isolation of proteins that interact specifically with the retinoid X receptor: two novel orphan receptors. *Mol. Endocrinol.* **9**, 72–85 (1995).
 83. Wang, B. & Tontonoz, P. Liver X receptors in lipid signalling and membrane homeostasis. *Nat. Rev. Endocrinol.* *2018 148* **14**, 452–463 (2018).
 84. Joseph, S. B. *et al.* Direct and Indirect Mechanisms for Regulation of Fatty Acid Synthase Gene Expression by Liver X Receptors . *J. Biol. Chem.* **277**, 11019–11025 (2002).
 85. Chu, K., Miyazaki, M., Man, W. C. & Ntambi, J. M. Stearoyl-Coenzyme A Desaturase 1 Deficiency Protects against Hypertriglyceridemia and Increases Plasma High-Density Lipoprotein Cholesterol Induced by Liver X Receptor Activation. *Mol. Cell. Biol.* **26**, (2006).
 86. Cha, J. Y. & Repa, J. J. The Liver X Receptor (LXR) and hepatic lipogenesis: The carbohydrate-response element-binding protein is a target gene of LXR. *J. Biol. Chem.* **282**, (2007).
 87. Diraison, F., Dusserre, E., Vidal, H., Sothier, M. & Beylot, M. Increased hepatic lipogenesis but decreased expression of lipogenic gene in adipose tissue in human obesity. *Am. J. Physiol. - Endocrinol. Metab.* **282**, (2002).
 88. Kennedy, E. P. Metabolism of lipides. *Annu. Rev. Biochem.* **26**, 119–148 (1957).
 89. Coleman, R. A. & Lee, D. P. Enzymes of triacylglycerol synthesis and their regulation. *Prog. Lipid Res.* **43**, 134–176 (2004).
 90. Lehner, R. & Kuksis, A. Biosynthesis of triacylglycerols. *Prog. Lipid Res.* **35**, 169–201 (1996).
 91. Bell, R. M. & Coleman, R. A. Enzymes of glycerolipid synthesis in eukaryotes. *Annual review of biochemistry* **49**, (1980).
 92. McLeod, R. S. & Yao, Z. Assembly and Secretion of Triglyceride-Rich Lipoproteins. in *Biochemistry of Lipids, Lipoproteins and Membranes* (eds. Ridgway, N. & McLeod, R.) 459–488 (Elsevier, 2016).
 93. Yen, C.-L. E., Nelson, D. W. & Yen, M.-I. Intestinal triacylglycerol synthesis in fat absorption and systemic energy metabolism. *J. Lipid Res.* **56**, 489–501 (2015).
 94. Yen, C.-L. E., Stone, S. J., Koliwad, S., Harris, C. & Farese, R. V. Thematic Review Series: Glycerolipids. DGAT enzymes and triacylglycerol biosynthesis. *J. Lipid Res.* **49**, (2008).
 95. Cases, S. *et al.* Identification of a gene encoding an acyl CoA:diacylglycerol acyltransferase, a key enzyme in triacylglycerol synthesis. *Proc. Natl. Acad. Sci.* **95**,

- 13018–13023 (1998).
96. Cases, S. *et al.* Cloning of DGAT2, a Second Mammalian Diacylglycerol Acyltransferase, and Related Family Members *. *J. Biol. Chem.* **276**, 38870–38876 (2001).
 97. Gobbi, P. G. *et al.* The prognostic role of time to diagnosis and presenting symptoms in patients with pancreatic cancer. *Cancer Epidemiol.* **37**, 186–90 (2013).
 98. Stone, S. J. *et al.* Lipopenia and Skin Barrier Abnormalities in DGAT2-deficient Mice . *J. Biol. Chem.* **279**, 11767–11776 (2004).
 99. Meegalla, R. L., Billheimer, J. T. & Cheng, D. Concerted elevation of acyl-coenzyme A:diacylglycerol acyltransferase (DGAT) activity through independent stimulation of mRNA expression of DGAT1 and DGAT2 by carbohydrate and insulin. *Biochem. Biophys. Res. Commun.* **298**, 317–323 (2002).
 100. Heden, T. D. *et al.* Differential effects of low-fat and high-fat diets on fed-state hepatic triacylglycerol secretion, hepatic fatty acid profiles, and DGAT-1 protein expression in obese-prone Sprague-Dawley rats. *Appl. Physiol. Nutr. Metab.* **39**, (2014).
 101. Suzuki, R. *et al.* Expression of DGAT2 in white adipose tissue is regulated by central leptin action. *J. Biol. Chem.* **280**, (2005).
 102. Chitraju, C. *et al.* Triglyceride Synthesis by DGAT1 Protects Adipocytes from Lipid-Induced ER Stress during Lipolysis. *Cell Metab.* **26**, 407-418.e3 (2017).
 103. Manganaro, F. & Kuksis, A. Purification and preliminary characterization of 2-monoacylglycerol acyltransferase from rat intestinal villus cells. <https://doi-org.login.ezproxy.library.ualberta.ca/10.1139/o85-050> **63**, 341–347 (2011).
 104. Weiss, S. B., Kennedy, E. P. & Kiyasu, J. Y. The enzymatic synthesis of triglycerides. *J. Biol. Chem.* **235**, (1960).
 105. Weiss, S. B. & Kennedy, E. P. The Enzymatic Synthesis of Triglycerides. *J. Am. Chem. Soc.* **78**, (1956).
 106. Reue, K. The Lipin Family: Mutations and Metabolism. *Curr. Opin. Lipidol.* **20**, 165 (2009).
 107. Reue, K. & Zhang, P. The lipin protein family: Dual roles in lipid biosynthesis and gene expression. *FEBS Lett.* **582**, 90–96 (2008).
 108. Vance, J. & Vance, D. The assembly of lipids into lipoproteins during secretion. *Experientia* **46**, 560–569 (1990).
 109. Mahley, R. W., Innerarity, T. L., Rall, S. C. & Weisgraber, K. H. Plasma lipoproteins: apolipoprotein structure and function. *J. Lipid Res.* **25**, 1277–1294 (1984).
 110. Breslow, J. L. Human apolipoprotein molecular biology and genetic variation. *Annu. Rev. Biochem.* **54**, 699–727 (1985).
 111. Segrest, J. P., Jones, M. K., De Loof, H. & Dashti, N. Structure of apolipoprotein B-100 in low density lipoproteins. *J. Lipid Res.* **42**, 1346–1367 (2001).
 112. Yue, J. T. Y. *et al.* A fatty acid-dependent hypothalamic–DVC neurocircuitry that regulates hepatic secretion of triglyceride-rich lipoproteins. *Nat. Commun.* **6**, 5970 (2015).
 113. Cartwright, I. J. & Higgins, J. A. Quantification of apolipoprotein B-48 and B-100 in rat liver endoplasmic reticulum and Golgi fractions. *Biochem. J.* **285**, 159 (1992).
 114. Sparks, C. E., Hnatiuk, O. & Marsh, J. B. Hepatic and intestinal contribution of two forms of apolipoprotein B to plasma lipoprotein fractions in the rat. *Can. J. Biochem.* **59**, (1981).
 115. Fisher, E. A. & McLeod, R. S. Assembly and secretion of triacylglycerol-rich lipoproteins. *Biochem. Lipids, Lipoproteins Membr.* 515–546 (2021). doi:10.1016/B978-0-12-824048-9.00003-1

116. Sirwi, A. & Mahmood Hussain, M. Lipid transfer proteins in the assembly of apoB-containing lipoproteins. *J. Lipid Res.* **59**, 1094–1102 (2018).
117. Wetterau, J. R. *et al.* Absence of Microsomal Triglyceride Transfer Protein in Individuals with Abetalipoproteinemia. *Science (80-.)*. **258**, 999–1001 (1992).
118. Hussain, M. M., Shi, J. & Dreizen, P. Microsomal triglyceride transfer protein and its role in apoB-lipoprotein assembly. *J. Lipid Res.* **44**, 22–32 (2003).
119. Olofsson, S. O. & Boren, J. Apolipoprotein B: a clinically important apolipoprotein which assembles atherogenic lipoproteins and promotes the development of atherosclerosis. *J. Intern. Med.* **258**, 395–410 (2005).
120. Rustaeus, S. *et al.* Assembly of Very Low Density Lipoprotein: A Two-Step Process of Apolipoprotein B Core Lipidation. *J. Nutr.* **129**, 463S-466S (1999).
121. Sundaram, M. & Yao, Z. Recent progress in understanding protein and lipid factors affecting hepatic VLDL assembly and secretion. *Nutr. Metab. (Lond)*. **7**, 35 (2010).
122. Wang, H., Gilham, D. & Lehner, R. Proteomic and Lipid Characterization of Apolipoprotein B-free Luminal Lipid Droplets from Mouse Liver Microsomes: Implications for very low density lipoprotein assembly. *J. Biol. Chem.* **282**, 33218–33226 (2007).
123. Asp, L. *et al.* Role of ADP ribosylation factor 1 in the assembly and secretion of apoB-100-containing lipoproteins. *Arterioscler. Thromb. Vasc. Biol.* **25**, (2005).
124. Asp, L., Claesson, C., Borén, J. & Olofsson, S. O. ADP-ribosylation factor 1 and its activation of phospholipase D are important for the assembly of very low density lipoproteins. *J. Biol. Chem.* **275**, (2000).
125. Gibbons, G. F., Wiggins, D., Brown, A. M. & Hebbachi, A. M. Synthesis and function of hepatic very-low-density lipoprotein. *Biochem. Soc. Trans.* **32**, 59–64 (2004).
126. Ye, J. *et al.* Cideb, an ER- and Lipid Droplet-Associated Protein, Mediates VLDL Lipidation and Maturation by Interacting with Apolipoprotein B. *Cell Metab.* **9**, 177–190 (2009).
127. Valyi-Nagy, K., Harris, C. & Swift, L. L. The assembly of hepatic very low density lipoproteins: Evidence of a role for the Golgi apparatus. *Lipids* **37**, (2002).
128. Gusarova, V., Brodsky, J. L. & Fisher, E. A. Apolipoprotein B100 Exit from the Endoplasmic Reticulum (ER) Is COPII-dependent, and Its Lipidation to Very Low Density Lipoprotein Occurs Post-ER. *J. Biol. Chem.* **278**, 48051–48058 (2003).
129. Lehner, R., Lian, J. & Quiroga, A. D. Luminal lipid metabolism: Implications for lipoprotein assembly. *Arterioscler. Thromb. Vasc. Biol.* **32**, 1087–1093 (2012).
130. D’Souza-Schorey, C. & Chavrier, P. ARF proteins: Roles in membrane traffic and beyond. *Nat. Rev. Mol. Cell Biol.* **7**, 347–358 (2006).
131. Bennett, M. J. Pathophysiology of fatty acid oxidation disorders. *J. Inherit. Metab. Dis.* **2009 335** **33**, 533–537 (2009).
132. Kerner, J. & Hoppel, C. Fatty acid import into mitochondria. *Biochim. Biophys. Acta - Mol. Cell Biol. Lipids* **1486**, 1–17 (2000).
133. Brindle, N. P. J., Zammit, V. A. & Pogson, C. I. Regulation of carnitine palmitoyltransferase activity by malonyl-CoA in mitochondria from sheep liver, a tissue with a low capacity for fatty acid synthesis. *Biochem. J.* **232**, 177–182 (1985).
134. Tyagi, S., Gupta, P., Saini, A., Kaushal, C. & Sharma, S. The peroxisome proliferator-activated receptor: A family of nuclear receptors role in various diseases. *J. Adv. Pharm. Technol. Res.* **2**, 236 (2011).

135. Pawlak, M., Lefebvre, P. & Staels, B. Molecular mechanism of PPAR α action and its impact on lipid metabolism, inflammation and fibrosis in non-alcoholic fatty liver disease. *J. Hepatol.* **62**, 720–733 (2015).
136. Olzmann, J. A. & Carvalho, P. Dynamics and functions of lipid droplets. *Nat. Rev. Mol. Cell Biol.* **2018** *203* **20**, 137–155 (2018).
137. Mashek, D. G. Hepatic lipid droplets: A balancing act between energy storage and metabolic dysfunction in NAFLD. *Mol. Metab.* **50**, 101115 (2021).
138. Dolinsky, V. W., Gilham, D., Alam, M., Vance, D. E. & Lehner, R. Triacylglycerol hydrolase: role in intracellular lipid metabolism. *Cell. Mol. Life Sci. C. 2004* *6113* **61**, 1633–1651 (2004).
139. Gilham, D. *et al.* Inhibitors of hepatic microsomal triacylglycerol hydrolase decrease very low density lipoprotein secretion. *FASEB J.* **17**, 1685–1687 (2003).
140. Duez, H. *et al.* Both intestinal and hepatic lipoprotein production are stimulated by an acute elevation of plasma free fatty acids in humans. *Circulation* **117**, 2369–2376 (2008).
141. Zhang, Y. L. *et al.* Regulation of Hepatic Apolipoprotein B-lipoprotein Assembly and Secretion by the Availability of Fatty Acids: I. Differential response to the delivery of fatty acids via albumin or remnant-like emulsion particles. *J. Biol. Chem.* **279**, 19362–19374 (2004).
142. Lewis, G. F., Carpentier, A., Adeli, K. & Giacca, A. Disordered Fat Storage and Mobilization in the Pathogenesis of Insulin Resistance and Type 2 Diabetes. *Endocr. Rev.* **23**, 201–229 (2002).
143. Kovacs, P. & Stumvoll, M. Fatty acids and insulin resistance in muscle and liver. *Best Pract. Res. Clin. Endocrinol. Metab.* **19**, 625–635 (2005).
144. Meex, R. C. R. & Watt, M. J. Hepatokines: Linking nonalcoholic fatty liver disease and insulin resistance. *Nature Reviews Endocrinology* **13**, 509–520 (2017).
145. Donnelly, K. L. *et al.* Sources of fatty acids stored in liver and secreted via lipoproteins in patients with nonalcoholic fatty liver disease. *J. Clin. Invest.* **115**, 1343–1351 (2005).
146. Fabbrini, E. *et al.* Alterations in Adipose Tissue and Hepatic Lipid Kinetics in Obese Men and Women With Nonalcoholic Fatty Liver Disease. *Gastroenterology* **134**, 424–431 (2008).
147. Younossi, Z. *et al.* Global burden of NAFLD and NASH: Trends, predictions, risk factors and prevention. *Nature Reviews Gastroenterology and Hepatology* **15**, 11–20 (2018).
148. Younossi, Z. M. *et al.* Global epidemiology of nonalcoholic fatty liver disease—Meta-analytic assessment of prevalence, incidence, and outcomes. *Hepatology* **64**, 73–84 (2016).
149. Leite, N. C., Salles, G. F., Araujo, A. L. E., Villela-Nogueira, C. A. & Cardoso, C. R. L. Prevalence and associated factors of non-alcoholic fatty liver disease in patients with type-2 diabetes mellitus. *Liver Int.* **29**, 113–119 (2009).
150. Wicklow, B. A. *et al.* Metabolic Consequences of Hepatic Steatosis in Overweight and Obese Adolescents. *Diabetes Care* **35**, 905–910 (2012).
151. Rafiq, N. *et al.* Long-Term Follow-Up of Patients With Nonalcoholic Fatty Liver. *Clin. Gastroenterol. Hepatol.* **7**, 234–238 (2009).
152. Anstee, Q. M., Targher, G. & Day, C. P. Progression of NAFLD to diabetes mellitus, cardiovascular disease or cirrhosis. *Nat. Rev. Gastroenterol. Hepatol.* **2013** *106* **10**, 330–344 (2013).
153. Eslam, M. *et al.* MAFLD: A Consensus-Driven Proposed Nomenclature for Metabolic

- Associated Fatty Liver Disease. *Gastroenterology* **158**, 1999-2014.e1 (2020).
154. Saponaro, C., Gaggini, M., Carli, F. & Gastaldelli, A. The Subtle Balance between Lipolysis and Lipogenesis: A Critical Point in Metabolic Homeostasis. *Nutr. 2015, Vol. 7, Pages 9453-9474* **7**, 9453–9474 (2015).
 155. Kadmiel, M. & Cidlowski, J. A. Glucocorticoid receptor signaling in health and disease. *Trends Pharmacol. Sci.* **34**, 518–530 (2013).
 156. Timmermans, S., Souffriau, J. & Libert, C. A general introduction to glucocorticoid biology. *Front. Immunol.* **10**, 1545 (2019).
 157. Coutinho, A. E. & Chapman, K. E. The anti-inflammatory and immunosuppressive effects of glucocorticoids, recent developments and mechanistic insights. *Mol. Cell. Endocrinol.* **335**, 2–13 (2011).
 158. Wu, T. *et al.* Chronic glucocorticoid treatment induced circadian clock disorder leads to lipid metabolism and gut microbiota alterations in rats. *Life Sci.* **192**, 173–182 (2018).
 159. Tsigos, C. & Chrousos, G. P. Stress, Obesity, and the Metabolic Syndrome: Soul and Metabolism. *Ann. N. Y. Acad. Sci.* **1083**, xi–xiii (2006).
 160. de Kloet, E. R., Joëls, M. & Holsboer, F. Stress and the brain: from adaptation to disease. *Nat. Rev. Neurosci.* **6**, 463–475 (2005).
 161. Ulrich-Lai, Y. M. & Herman, J. P. Neural regulation of endocrine and autonomic stress responses. *Nat. Rev. Neurosci.* **10**, 397–409 (2009).
 162. Miller, W. L. & Auchus, R. J. The molecular biology, biochemistry, and physiology of human steroidogenesis and its disorders. *Endocr. Rev.* **32**, (2011).
 163. Stocco, D. M. Clinical disorders associated with abnormal cholesterol transport: mutations in the steroidogenic acute regulatory protein. *Mol. Cell. Endocrinol.* **191**, 19–25 (2002).
 164. Miller, W. L. Steroidogenesis: Unanswered Questions. *Trends in Endocrinology and Metabolism* **28**, (2017).
 165. Hanukoglu, I. Steroidogenic enzymes: Structure, function, and role in regulation of steroid hormone biosynthesis. *J. Steroid Biochem. Mol. Biol.* **43**, 779–804 (1992).
 166. Bremer, A. A. & Miller, W. L. Regulation of Steroidogenesis. *Cell. Endocrinol. Heal. Dis.* 207–227 (2014). doi:10.1016/B978-0-12-408134-5.00013-5
 167. Oakley, R. H. & Cidlowski, J. A. The biology of the glucocorticoid receptor: New signaling mechanisms in health and disease. *J. Allergy Clin. Immunol.* **132**, 1033–1044 (2013).
 168. Seckl, J. R. 11 β -hydroxysteroid dehydrogenases: Changing glucocorticoid action. *Current Opinion in Pharmacology* **4**, (2004).
 169. Chapman, K., Holmes, M. & Seckl, J. 11 β -hydroxysteroid dehydrogenases intracellular gate-keepers of tissue glucocorticoid action. *Physiol. Rev.* **93**, (2013).
 170. Stewart, P. M. & Krozowski, Z. S. 11 β -Hydroxysteroid Dehydrogenase. *Vitam. Horm.* **57**, 249–324 (1997).
 171. Morgan, S. A. *et al.* Glucocorticoids and 11 β -HSD1 are major regulators of intramyocellular protein metabolism. *J. Endocrinol.* **229**, (2016).
 172. Walker, E. A. & Stewart, P. M. 11 β -hydroxysteroid dehydrogenase: Unexpected connections. *Trends in Endocrinology and Metabolism* **14**, (2003).
 173. De Kloet, E. R., Vreugdenhil, E., Oitzl, M. S., Joëls, M. & Joëls, J. Brain Corticosteroid Receptor Balance in Health and Disease. *Endocr. Rev.* **19**, 269–301 (1998).
 174. Herman, J. P. *et al.* Regulation of the hypothalamic-pituitary- adrenocortical stress response. *Compr. Physiol.* **6**, (2016).

175. Reul, J. M. H. M. & De Kloet, E. R. Two Receptor Systems for Corticosterone in Rat Brain: Microdistribution and Differential Occupation. *Endocrinology* **117**, 2505–2511 (1985).
176. Arriza, J. L., Simerly, R. B., Swanson, L. W. & Evans, R. M. The neuronal mineralocorticoid receptor as a mediator of glucocorticoid response. *Neuron* **1**, (1988).
177. Young, E. A., Abelson, J. & Lightman, S. L. Cortisol pulsatility and its role in stress regulation and health. *Frontiers in Neuroendocrinology* **25**, (2004).
178. De Kloet, E. R. & Reul, J. M. H. M. Feedback action and tonic influence of corticosteroids on brain function: A concept arising from the heterogeneity of brain receptor systems. *Psychoneuroendocrinology* **12**, (1987).
179. Weikum, E. R., Knuesel, M. T., Ortlund, E. A. & Yamamoto, K. R. Glucocorticoid receptor control of transcription: precision and plasticity via allostery. *Nat. Rev. Mol. Cell Biol.* **18**, 159–174 (2017).
180. Reul, J. M. H. M. & De Kloet, E. R. Anatomical resolution of two types of corticosterone receptor sites in rat brain with in vitro autoradiography and computerized image analysis. *J. Steroid Biochem.* **24**, 269–272 (1986).
181. Morimoto, M., Morita, N., Ozawa, H., Yokoyama, K. & Kawata, M. Distribution of glucocorticoid receptor immunoreactivity and mRNA in the rat brain: an immunohistochemical and in situ hybridization study. *Neurosci. Res.* **26**, 235–269 (1996).
182. Aronsson, M. *et al.* Localization of glucocorticoid receptor mRNA in the male rat brain by in situ hybridization. *Proc. Natl. Acad. Sci. U. S. A.* **85**, 9331–9335 (1988).
183. Cintra, A. *et al.* Presence of glucocorticoid receptor immunoreactivity in corticotrophin releasing factor and in growth hormone releasing factor immunoreactive neurons of the rat di- and telencephalon. *Neurosci. Lett.* **77**, 25–30 (1987).
184. Stahn, C. & Buttgerit, F. Genomic and nongenomic effects of glucocorticoids. *Nat. Clin. Pract. Rheumatol.* **4**, 525–533 (2008).
185. Picard, D. *et al.* Reduced levels of hsp90 compromise steroid receptor action in vivo. *Nature* **348**, 166–168 (1990).
186. Kirschke, E., Goswami, D., Southworth, D., Griffin, P. R. & Agard, D. A. Glucocorticoid Receptor Function Regulated by Coordinated Action of the Hsp90 and Hsp70 Chaperone Cycles. *Cell* **157**, 1685–1697 (2014).
187. Ricketson, D., Hostick, U., Fang, L., Yamamoto, K. R. & Darimont, B. D. A Conformational Switch in the Ligand-binding Domain Regulates the Dependence of the Glucocorticoid Receptor on Hsp90. *J. Mol. Biol.* **368**, 729–741 (2007).
188. Stankiewicz, M., Nikolay, R., Rybin, V. & Mayer, M. P. CHIP participates in protein triage decisions by preferentially ubiquitinating Hsp70-bound substrates. *FEBS J.* **277**, 3353–3367 (2010).
189. Agyeman, A. S. *et al.* Hsp90 Inhibition Results in Glucocorticoid Receptor Degradation in Association with Increased Sensitivity to Paclitaxel in Triple-Negative Breast Cancer. *Horm. Cancer* **7**, 114–126 (2016).
190. Hadley, M. E. & Haskell-Luevano, C. The Proopiomelanocortin System. *Ann. N. Y. Acad. Sci.* **885**, 1–21 (1999).
191. Simpson, E. R. & Waterman, M. R. Regulation of the Synthesis of Steroidogenic Enzymes in Adrenal Cortical Cells by ACTH. <http://dx.doi.org/10.1146/annurev.ph.50.030188.002235> **50**, 427–440 (2003).
192. Rhen, T. & Cidlowski, J. A. Antiinflammatory Action of Glucocorticoids — New

- Mechanisms for Old Drugs. *N. Engl. J. Med.* **353**, 1711–1723 (2005).
193. Nicolaidis, N. C., Charmandari, E., Kino, T. & Chrousos, G. P. Stress-related and circadian secretion and target tissue actions of glucocorticoids: Impact on health. *Front. Endocrinol. (Lausanne)*. **8**, 70 (2017).
 194. Qian, X., Droste, S. K., Lightman, S. L., Reul, J. M. H. M. & Linthorst, A. C. E. Circadian and Ultradian Rhythms of Free Glucocorticoid Hormone Are Highly Synchronized between the Blood, the Subcutaneous Tissue, and the Brain. *Endocrinology* **153**, 4346–4353 (2012).
 195. Dickmeis, T. Glucocorticoids and the circadian clock. *J. Endocrinol.* **200**, 3–22 (2009).
 196. Gjerstad, J. K., Lightman, S. L. & Spiga, F. Role of glucocorticoid negative feedback in the regulation of HPA axis pulsatility. <https://doi.org/10.1080/10253890.2018.1470238> **21**, 403–416 (2018).
 197. Weitzman, E. D. *et al.* Twenty-four Hour Pattern of the Episodic Secretion of Cortisol in Normal Subjects. *J. Clin. Endocrinol. Metab.* **33**, 14–22 (1971).
 198. McNeilly, A. D., Stewart, C. A., Sutherland, C. & Balfour, D. J. K. High fat feeding is associated with stimulation of the hypothalamic-pituitary-adrenal axis and reduced anxiety in the rat. *Psychoneuroendocrinology* **52**, 272–280 (2015).
 199. Hryhorczuk, C. *et al.* Saturated high-fat feeding independent of obesity alters hypothalamus-pituitary-adrenal axis function but not anxiety-like behaviour. *Psychoneuroendocrinology* **83**, 142–149 (2017).
 200. Walker, C. D., Scribner, K. A., Stern, J. S. & Dallman, M. F. Obese Zucker (Fa/fa) rats exhibit normal target sensitivity to corticosterone and increased drive to adrenocorticotropin during the diurnal trough. *Endocrinology* **131**, (1992).
 201. Ahima, R. S., Prabakaran, D. & Flier, J. S. Postnatal leptin surge and regulation of circadian rhythm of leptin by feeding. Implications for energy homeostasis and neuroendocrine function. *J. Clin. Invest.* **101**, 1020–1027 (1998).
 202. Nader, N., Chrousos, G. P. & Kino, T. Interactions of the circadian CLOCK system and the HPA axis. *Trends Endocrinol. Metab.* **21**, 277–286 (2010).
 203. Oakley, R. H. & Cidlowski, J. A. Cellular processing of the glucocorticoid receptor gene and protein: new mechanisms for generating tissue-specific actions of glucocorticoids. *J. Biol. Chem.* **286**, 3177–84 (2011).
 204. Zen, M. *et al.* The kaleidoscope of glucocorticoid effects on immune system. *Autoimmun. Rev.* **10**, 305–310 (2011).
 205. Heck, S. *et al.* A distinct modulating domain in glucocorticoid receptor monomers in the repression of activity of the transcription factor AP-1. *EMBO J.* **13**, 4087–4095 (1994).
 206. Mukaida, N. *et al.* Novel mechanism of glucocorticoid-mediated gene repression. Nuclear factor-kappa B is target for glucocorticoid-mediated interleukin 8 gene repression. *J. Biol. Chem.* **269**, 13289–13295 (1994).
 207. Caldenhoven, E. *et al.* Negative cross-talk between RelA and the glucocorticoid receptor: a possible mechanism for the antiinflammatory action of glucocorticoids. *Mol. Endocrinol.* **9**, 401–412 (1995).
 208. Heck, S. *et al.* I κ B α -independent downregulation of NF- κ B activity by glucocorticoid receptor. *EMBO J.* **16**, 4698–4707 (1997).
 209. Oakley, R. H. *et al.* Essential role of stress hormone signaling in cardiomyocytes for the prevention of heart disease. *Proc. Natl. Acad. Sci. U. S. A.* **110**, 17035–17040 (2013).
 210. Cruz-Topete, D., Myers, P. H., Foley, J. F., Willis, M. S. & Cidlowski, J. A.

- Corticosteroids Are Essential for Maintaining Cardiovascular Function in Male Mice. *Endocrinology* **157**, 2759–2771 (2016).
211. Goodwin, J. E. Glucocorticoids and the Cardiovascular System. *Adv. Exp. Med. Biol.* **872**, 299–314 (2015).
 212. Nussinovitch, U., Freire de Carvalho, J., Maria R. Pereira, R. & Shoenfeld, Y. Glucocorticoids and the Cardiovascular System: State of the Art. *Curr. Pharm. Des.* **16**, 3574–3585 (2010).
 213. Pimenta, E., Wolley, M. & Stowasser, M. Adverse Cardiovascular Outcomes of Corticosteroid Excess. *Endocrinology* **153**, 5137–5142 (2012).
 214. Patschan, D., Loddenkemper, K. & Buttgereit, F. Molecular mechanisms of glucocorticoid-induced osteoporosis. *Bone* **29**, 498–505 (2001).
 215. Baschant, U., Lane, N. E. & Tuckermann, J. The multiple facets of glucocorticoid action in rheumatoid arthritis. *Nat. Rev. Rheumatol.* **2012** *811* **8**, 645–655 (2012).
 216. Magomedova, L. & Cummins, C. L. Glucocorticoids and Metabolic Control. *Handb. Exp. Pharmacol.* **233**, 73–93 (2015).
 217. Kuo, T., Harris, C. A. & Wang, J. C. Metabolic functions of glucocorticoid receptor in skeletal muscle. *Mol. Cell. Endocrinol.* **380**, 79–88 (2013).
 218. Long, W., Barrett, E. J., Wei, L. & Liu, Z. Adrenalectomy enhances the insulin sensitivity of muscle protein synthesis. *Am. J. Physiol. - Endocrinol. Metab.* **284**, 102–109 (2003).
 219. Sandri, M. *et al.* Foxo Transcription Factors Induce the Atrophy-Related Ubiquitin Ligase Atrogin-1 and Cause Skeletal Muscle Atrophy. *Cell* **117**, 399–412 (2004).
 220. Giorgino, F., Almahfouz, A., Goodyear, L. J. & Smith, R. J. Glucocorticoid regulation of insulin receptor and substrate IRS-1 tyrosine phosphorylation in rat skeletal muscle in vivo. *J. Clin. Invest.* **91**, 2020–2030 (1993).
 221. Saad, M. J. A., Folli, F., Kahn, J. A. & Kahn, C. R. Modulation of insulin receptor, insulin receptor substrate-1, and phosphatidylinositol 3-kinase in liver and muscle of dexamethasone-treated rats. *J. Clin. Invest.* **92**, 2065–2072 (1993).
 222. Weinstein, S. P., Wilson, C. M., Pritsker, A. & Cushman, S. W. Dexamethasone inhibits insulin-stimulated recruitment of GLUT4 to the cell surface in rat skeletal muscle. *Metabolism* **47**, 3–6 (1998).
 223. Weinstein, S. P., Paquin, T., Pritsker, A. & Haber, R. S. Glucocorticoid-Induced Insulin Resistance: Dexamethasone Inhibits the Activation of Glucose Transport in Rat Skeletal Muscle by Both Insulin- and Non-Insulin-Related Stimuli. *Diabetes* **44**, 441–445 (1995).
 224. Haber, R. S. & Weinstein, S. P. Role of Glucose Transporters in Glucocorticoid-Induced Insulin Resistance: GLUT4 Isoform in Rat Skeletal Muscle is Not Decreased by Dexamethasone. *Diabetes* **41**, 728–735 (1992).
 225. Dimitriadis, G. *et al.* Effects of glucocorticoid excess on the sensitivity of glucose transport and metabolism to insulin in rat skeletal muscle. *Biochem. J.* **321**, 707–712 (1997).
 226. Morgan, S. A. *et al.* 11 β -Hydroxysteroid Dehydrogenase Type 1 Regulates Glucocorticoid-Induced Insulin Resistance in Skeletal Muscle. *Diabetes* **58**, 2506–2515 (2009).
 227. Ruzzin, J., Wagman, A. S. & Jensen, J. Glucocorticoid-induced insulin resistance in skeletal muscles: Defects in insulin signalling and the effects of a selective glycogen synthase kinase-3 inhibitor. *Diabetologia* **48**, 2119–2130 (2005).
 228. Coderre, L., Srivastava, A. K. & Chiasson, J. L. Role of glucocorticoid in the regulation of

- glycogen metabolism in skeletal muscle.
<https://doi.org/10.1152/ajpendo.1991.260.6.E927> **260**, (1991).
229. Coderre, L., Srivastava, A. K. & Chiasson, J. L. Effect of hypercorticism on regulation of skeletal muscle glycogen metabolism by insulin.
<https://doi.org/10.1152/ajpendo.1992.262.4.E427> **262**, (1992).
 230. Gounarides, J. S. *et al.* Effect of Dexamethasone on Glucose Tolerance and Fat Metabolism in a Diet-Induced Obesity Mouse Model. *Endocrinology* **149**, 758–766 (2008).
 231. Wang, X. Juan, Wei, D. lin, Song, Z. gang, Jiao, H. chao & Lin, H. Effects of Fatty Acid Treatments on the Dexamethasone-Induced Intramuscular Lipid Accumulation in Chickens. *PLoS One* **7**, e36663 (2012).
 232. Christ-Crain, M. *et al.* AMP-activated protein kinase mediates glucocorticoid- induced metabolic changes: a novel mechanism in Cushing’s syndrome. *FASEB J.* **22**, 1672–1683 (2008).
 233. Nathan Nakken, G., Jacobs, D. L., Thomson, D. M., Fillmore, N. & Winder, W. W. Effects of excess corticosterone on LKB1 and AMPK signaling in rat skeletal muscle. *J. Appl. Physiol.* **108**, 298–305 (2010).
 234. Sakoda, H. *et al.* Dexamethasone-induced insulin resistance in 3T3-L1 adipocytes is due to inhibition of glucose transport rather than insulin signal transduction. *Diabetes* **49**, 1700–1708 (2000).
 235. Olefsky, J. M. Effect of dexamethasone on insulin binding, glucose transport, and glucose oxidation of isolated rat adipocytes. *J. Clin. Invest.* **56**, 1499–1508 (1975).
 236. Caperuto, L. C. *et al.* Distinct regulation of IRS proteins in adipose tissue from obese aged and dexamethasone-treated rats. *Endocr. 2006 293* **29**, 391–398 (2006).
 237. Campbell, J. E., Peckett, A. J., D’souza, A. M., Hawke, T. J. & Riddell, M. C. Adipogenic and lipolytic effects of chronic glucocorticoid exposure. *Am. J. Physiol. Physiol.* **300**, C198–C209 (2011).
 238. Peckett, A. J., Wright, D. C. & Riddell, M. C. The effects of glucocorticoids on adipose tissue lipid metabolism. *Metabolism* **60**, 1500–1510 (2011).
 239. Divertie, G. D., Jensen, M. D. & Miles, J. M. Stimulation of lipolysis in humans by physiological hypercortisolemia. *Diabetes* **40**, 1228–1232 (1991).
 240. Slavin, B. G., Ong, J. M. & Kern, P. A. Hormonal regulation of hormone-sensitive lipase activity and mRNA levels in isolated rat adipocytes. *J. Lipid Res.* **35**, 1535–1541 (1994).
 241. Xu, C. *et al.* Direct Effect of Glucocorticoids on Lipolysis in Adipocytes. *Mol. Endocrinol.* **23**, 1161–1170 (2009).
 242. Gao, Z. *et al.* Inhibition of insulin sensitivity by free fatty acids requires activation of multiple serine kinases in 3T3-L1 adipocytes. *Mol. Endocrinol.* **18**, 2024–2034 (2004).
 243. Bujalska, I. J., Kumar, S., Hewison, M. & Stewart, P. M. Differentiation of Adipose Stromal Cells: The Roles of Glucocorticoids and 11 β -Hydroxysteroid Dehydrogenase. *Endocrinology* **140**, 3188–3196 (1999).
 244. Fardet, L. & Fève, B. Systemic Glucocorticoid Therapy: a Review of its Metabolic and Cardiovascular Adverse Events. *Drugs* **74**, 1731–1745 (2014).
 245. Ishida-Takahashi, R. *et al.* Rapid Inhibition of Leptin Signaling by Glucocorticoids in Vitro and in Vivo*. *J. Biol. Chem.* **279**, 19658–19664 (2004).
 246. Uddén, J. *et al.* Effects of glucocorticoids on leptin levels and eating behaviour in women. *J. Intern. Med.* **253**, 225–231 (2003).

247. Solano, J. M. & Jacobson, L. Glucocorticoids reverse leptin effects on food intake and body fat in mice without increasing NPY mRNA. *Am. J. Physiol. - Endocrinol. Metab.* **277**, (1999).
248. Perry, R. J. *et al.* Leptin's hunger-suppressing effects are mediated by the hypothalamic–pituitary–adrenocortical axis in rodents. *Proc. Natl. Acad. Sci. U. S. A.* **116**, 13670–13679 (2019).
249. Reaven, E. P., Kolterman, O. G. & Reaven, G. M. Ultrastructural and physiological evidence for corticosteroid-induced alterations in hepatic production of very low density lipoprotein particles. *J. Lipid Res.* **15**, 74–83 (1974).
250. Bagdade, J. D., Yee, E., Albers, J. & Pykalisto, O. J. Glucocorticoids and triglyceride transport: Effects on triglyceride secretion rates, lipoprotein lipase, and plasma lipoproteins in the rat. *Metabolism* **25**, 533–542 (1976).
251. Dolinsky, V. W., Douglas, D. N., Lehner, R. & Vance, D. E. Regulation of the enzymes of hepatic microsomal triacylglycerol lipolysis and re-esterification by the glucocorticoid dexamethasone. *Biochem. J* **378**, 967–974 (2004).
252. Du, K., Herzig, S., Kulkarni, R. N. & Montminy, M. TRB3: A tribbles homolog that inhibits Akt/PKB activation by insulin in liver. *Science (80-.)*. **300**, 1574–1577 (2003).
253. Zhao, L. F. *et al.* Hormonal regulation of acetyl-CoA carboxylase isoenzyme gene transcription. *Endocr. J.* **57**, 317–324 (2010).
254. Diamant, S. & Shafrir, E. Modulation of the Activity of Insulin-Dependent Enzymes of Lipogenesis by Glucocorticoids. *Eur. J. Biochem.* **53**, 541–546 (1975).
255. Manmontri, B. *et al.* Glucocorticoids and cyclic AMP selectively increase hepatic lipin-1 expression, and insulin acts antagonistically *. *J. Lipid Res.* **49**, 1056–1067 (2008).
256. Pittner, R. A., Fears, R. & Brindley, D. N. Interactions of insulin, glucagon and dexamethasone in controlling the activity of glycerol phosphate acyltransferase and the activity and subcellular distribution of phosphatidate phosphohydrolase in cultured rat hepatocytes. *Biochem. J.* **230**, 525–534 (1985).
257. Pittner, R. A., Fears, R. & Brindley, D. N. Effects of cyclic AMP, glucocorticoids and insulin on the activities of phosphatidate phosphohydrolase, tyrosine aminotransferase and glycerol kinase in isolated rat hepatocytes in relation to the control of triacylglycerol synthesis and gluconeogenesis. *Biochem. J.* **225**, 455–462 (1985).
258. Mangiapane, E. H. & Brindley, D. N. Effects of dexamethasone and insulin on the synthesis of triacylglycerols and phosphatidylcholine and the secretion of very-low-density lipoproteins and lysophosphatidylcholine by monolayer cultures of rat hepatocytes. *Biochem. J.* **233**, 151–160 (1986).
259. Wang, C. N., McLeod, R. S., Yao, Z. & Brindley, D. N. Effects of dexamethasone on the synthesis, degradation, and secretion of apolipoprotein B in cultured rat hepatocytes. *Arterioscler. Thromb. Vasc. Biol.* **15**, 1481–1491 (1995).
260. Koch, L. *et al.* Central insulin action regulates peripheral glucose and fat metabolism in mice. *J. Clin. Invest.* **118**, 2132–2147 (2008).
261. Lam, T. K. T. *et al.* Brain glucose metabolism controls the hepatic secretion of triglyceride-rich lipoproteins. *Nat. Med.* **13**, 171–180 (2007).
262. Nogueiras, R. *et al.* The central melanocortin system directly controls peripheral lipid metabolism. *J. Clin. Invest.* **117**, 3475–3488 (2007).
263. Stafford, J. M. *et al.* Central Nervous System Neuropeptide Y Signaling Modulates VLDL Triglyceride Secretion. *Diabetes* **57**, 1482–1490 (2008).

264. Yue, J. T. Y., Mighiu, P. I., Naples, M., Adeli, K. & Lam, T. K. T. Glycine normalizes hepatic triglyceride-rich VLDL secretion by triggering the CNS in high-fat fed rats. *Circ. Res.* **110**, 1345–1354 (2012).
265. Yue, J. T. Y. & Lam, T. K. T. Lipid Sensing and Insulin Resistance in the Brain. *Cell Metab.* **15**, 646–655 (2012).
266. Taher, J., Farr, S. & Adeli, K. Central nervous system regulation of hepatic lipid and lipoprotein metabolism. *Curr. Opin. Lipidol.* **28**, 32–38 (2016).
267. Lam, T. K. T., Schwartz, G. J. & Rossetti, L. Hypothalamic sensing of fatty acids. *Nat. Neurosci.* **8**, 579–584 (2005).
268. Kim, K. S., Seeley, R. J. & Sandoval, D. A. Signalling from the periphery to the brain that regulates energy homeostasis. *Nat. Rev. Neurosci.* *2018 194* **19**, 185–196 (2018).
269. Belgardt, B. F., Okamura, T. & Brüning, J. C. Hormone and glucose signalling in POMC and AgRP neurons. *J. Physiol.* **587**, 5305–5314 (2009).
270. Paxinos, G. & Charles Watson. *The Rat Brain in Stereotaxic Coordinates Sixth Edition.* Elsevier Academic Press **170**, (2007).
271. Jais, A. & Brüning, J. C. Hypothalamic inflammation in obesity and metabolic disease. *J. Clin. Invest.* **127**, 24–32 (2017).
272. Bernard, C. *Lecons de Physiologie Experimentale Appliquee a la Medicine Faites au College de France. Bailere et Fils* (1855).
273. Morton, G. J., Meek, T. H. & Schwartz, M. W. Neurobiology of food intake in health and disease. *Nat. Rev. Neurosci.* *2014 156* **15**, 367–378 (2014).
274. Deem, J. D., Muta, K., Scarlett, J. M., Morton, G. J. & Schwartz, M. W. How Should We Think About the Role of the Brain in Glucose Homeostasis and Diabetes? *Diabetes* **66**, 1758–1765 (2017).
275. Lundqvist, M. H., Almby, K., Abrahamsson, N. & Eriksson, J. W. Is the brain a key player in glucose regulation and development of type 2 diabetes? *Front. Physiol.* **10**, 457 (2019).
276. Morton, G. J., Cummings, D. E., Baskin, D. G., Barsh, G. S. & Schwartz, M. W. Central nervous system control of food intake and body weight. *Nat.* *2006 4437109* **443**, 289–295 (2006).
277. Lam, T. K. T. Neuronal regulation of homeostasis by nutrient sensing. *Nat. Med.* *2010 164* **16**, 392–395 (2010).
278. Lam, T. K. T., Gutierrez-Juarez, R., Poci, A. & Rossetti, L. Regulation of blood glucose by hypothalamic pyruvate metabolism. *Science (80-.)*. **309**, 943–947 (2005).
279. Anand, B. K., Chhina, G. S., Sharma, K. N., Dua, S. & Singh, B. Activity of single neurons in the hypothalamic feeding centers: effect of glucose. <https://doi.org/10.1152/ajplegacy.1964.207.5.1146> **207**, 1146–1154 (1964).
280. Woods, S. C. & McKay, L. D. Intraventricular Alloxan Eliminates Feeding Elicited by 2-Deoxyglucose. *Science (80-.)*. **202**, 1209–1211 (1978).
281. Davis, J. D., Wirtshafter, D., Asin, K. E. & Brief, D. Sustained Intracerebroventricular Infusion of Brain Fuels Reduces Body Weight and Food Intake in Rats. *Science (80-.)*. **212**, 81–83 (1981).
282. Obici, S. *et al.* Central Administration of Oleic Acid Inhibits Glucose Production and Food Intake. *Diabetes* **51**, 271–275 (2002).
283. Obici, S., Feng, Z., Arduini, A., Conti, R. & Rossetti, L. Inhibition of hypothalamic carnitine palmitoyltransferase-1 decreases food intake and glucose production. *Nat. Med.*

- 2003 96 **9**, 756–761 (2003).
284. Lam, T. K. T. *et al.* Hypothalamic sensing of circulating fatty acids is required for glucose homeostasis. *Nat. Med.* 2005 113 **11**, 320–327 (2005).
 285. Pocai, A. *et al.* Restoration of hypothalamic lipid sensing normalizes energy and glucose homeostasis in overfed rats. *J. Clin. Invest.* **116**, 1081–1091 (2006).
 286. Morgan, K., Obici, S. & Rossetti, L. Hypothalamic Responses to Long-chain Fatty Acids Are Nutritionally Regulated *. *J. Biol. Chem.* **279**, 31139–31148 (2004).
 287. He, W., Lam, T. K. T., Obici, S. & Rossetti, L. Molecular disruption of hypothalamic nutrient sensing induces obesity. *Nat. Neurosci.* **9**, 227–233 (2006).
 288. Hu, Z., Dai, Y., Prentki, M., Chohnan, S. & Lane, M. D. A Role for Hypothalamic Malonyl-CoA in the Control of Food Intake *. *J. Biol. Chem.* **280**, 39681–39683 (2005).
 289. Obici, S., Zhang, B. B., Karkanias, G. & Rossetti, L. Hypothalamic insulin signaling is required for inhibition of glucose production. *Nat. Med.* **8**, 1376–1382 (2002).
 290. Woods, S. C., Lotter, E. C., McKay, L. D. & Porte, D. Chronic intracerebroventricular infusion of insulin reduces food intake and body weight of baboons. *Nat.* 1979 2825738 **282**, 503–505 (1979).
 291. Sipols, A. J., Baskin, D. G. & Schwartz, M. W. Effect of Intracerebroventricular Insulin Infusion on Diabetic Hyperphagia and Hypothalamic Neuropeptide Gene Expression. *Diabetes* **44**, 147–151 (1995).
 292. Wang, J. & Leibowitz, K. L. Central insulin inhibits hypothalamic galanin and neuropeptide Y gene expression and peptide release in intact rats. *Brain Res.* **777**, 231–236 (1997).
 293. Schwartz, M. W. *et al.* Inhibition of hypothalamic neuropeptide Y gene expression by insulin. *Endocrinology* **130**, 3608–3616 (1992).
 294. Inoue, H. *et al.* Role of hepatic STAT3 in brain-insulin action on hepatic glucose production. *Cell Metab.* **3**, 267–275 (2006).
 295. Ramnanan, C. J. *et al.* Brain insulin action augments hepatic glycogen synthesis without suppressing glucose production or gluconeogenesis in dogs. *J. Clin. Invest.* **121**, 3713–3723 (2011).
 296. Scherer, T. *et al.* Insulin regulates hepatic triglyceride secretion and lipid content via signaling in the brain. *Diabetes* **65**, 1511–1520 (2016).
 297. Mighiu, P. I. *et al.* Hypothalamic glucagon signaling inhibits hepatic glucose production. *Nat. Med.* **19**, 766–772 (2013).
 298. Abraham, M. A. *et al.* Hypothalamic glucagon signals through the KATP channels to regulate glucose production. *Mol. Metab.* **3**, 202–208 (2014).
 299. Sandoval, D. A., Bagnol, D., Woods, S. C., D'Alessio, D. A. & Seeley, R. J. Arcuate glucagon-like peptide 1 receptors regulate glucose homeostasis but not food intake. *Diabetes* **57**, 2046–2054 (2008).
 300. Perez-Tilve, D. *et al.* Melanocortin signaling in the CNS directly regulates circulating cholesterol. *Nat. Neurosci.* 2010 137 **13**, 877–882 (2010).
 301. Panjwani, N. *et al.* GLP-1 Receptor Activation Indirectly Reduces Hepatic Lipid Accumulation But Does Not Attenuate Development of Atherosclerosis in Diabetic Male ApoE^{-/-} Mice. *Endocrinology* **154**, 127–139 (2013).
 302. Taher, J. *et al.* GLP-1 receptor agonism ameliorates hepatic VLDL overproduction and de novo lipogenesis in insulin resistance. *Mol. Metab.* **3**, 823–833 (2014).
 303. Caron, A., Lee, S., Elmquist, J. K. & Gautron, L. Leptin and brain–adipose crosstalks.

- Nat. Rev. Neurosci.* 2018 193 **19**, 153–165 (2018).
304. Friedman, J. The long road to leptin. *J. Clin. Invest.* **126**, 4727–4734 (2016).
 305. Friedman, J. M. A tale of two hormones. *Nat. Med.* 2010 1610 **16**, 1100–1106 (2010).
 306. Williams, K. W., Scott, M. M. & Elmquist, J. K. From observation to experimentation: leptin action in the mediobasal hypothalamus. *Am. J. Clin. Nutr.* **89**, 985S-990S (2009).
 307. Pocai, A. *et al.* Central Leptin Acutely Reverses Diet-Induced Hepatic Insulin Resistance. *Diabetes* **54**, 3182–3189 (2005).
 308. Gutiérrez-Juárez, R., Obici, S. & Rossetti, L. Melanocortin-independent Effects of Leptin on Hepatic Glucose Fluxes *. *J. Biol. Chem.* **279**, 49704–49715 (2004).
 309. Liu, L. Sen *et al.* Intracerebroventricular leptin regulates hepatic but not peripheral glucose fluxes. *J. Biol. Chem.* **273**, 31160–31167 (1998).
 310. Da Silva, A. A., Tallam, L. S., Liu, J. & Hall, J. E. Chronic antidiabetic and cardiovascular actions of leptin: Role of CNS and increased adrenergic activity. *Am. J. Physiol. - Regul. Integr. Comp. Physiol.* **291**, 1275–1282 (2006).
 311. German, J. P. *et al.* Leptin Activates a Novel CNS Mechanism for Insulin-Independent Normalization of Severe Diabetic Hyperglycemia. *Endocrinology* **152**, 394–404 (2011).
 312. Hidaka, S. *et al.* Chronic central leptin infusion restores hyperglycemia independent of food intake and insulin level in streptozotocin-induced diabetic rats. *FASEB J.* **16**, 509–518 (2002).
 313. Lin, C. Y., Allan Higginbotham, D., Judd, R. L. & Douglas White, B. Central leptin increases insulin sensitivity in streptozotocin-induced diabetic rats. *Am. J. Physiol. - Endocrinol. Metab.* **282**, 1084–1091 (2002).
 314. Buettner, C. *et al.* Leptin controls adipose tissue lipogenesis via central, STAT3-independent mechanisms. *Nat. Med.* **14**, 667–675 (2008).
 315. Hackl, M. T. *et al.* Brain leptin reduces liver lipids by increasing hepatic triglyceride secretion and lowering lipogenesis. *Nat. Commun.* **10**, 2717 (2019).
 316. Cohen, P. *et al.* Role for stearoyl-CoA desaturase-1 in leptin-mediated weight loss. *Science (80-.)*. **297**, 240–243 (2002).
 317. Lin, J. *et al.* CNS melanocortin and leptin effects on stearoyl-CoA desaturase-1 and resistin expression. *Biochem. Biophys. Res. Commun.* **311**, 324–328 (2003).
 318. Bruinstroop, E. *et al.* Hypothalamic Neuropeptide Y (NPY) Controls Hepatic VLDL-Triglyceride Secretion in Rats via the Sympathetic Nervous System. *Diabetes* **61**, 1043–1050 (2012).
 319. Rojas, J. M. *et al.* Central nervous system neuropeptide Y regulates mediators of hepatic phospholipid remodeling and very low-density lipoprotein triglyceride secretion via sympathetic innervation. *Mol. Metab.* **4**, 210–221 (2015).
 320. Rojas, J. M. *et al.* Central nervous system neuropeptide Y signaling via the Y1 receptor partially dissociates feeding behavior from lipoprotein metabolism in lean rats. *Am. J. Physiol. - Endocrinol. Metab.* **303**, 1479–1488 (2012).
 321. Zarjevski, N., Cusin, I., Vettor, R., Rohner-Jeanrenaud, F. & Jeanrenaud, B. Chronic intracerebroventricular neuropeptide-Y administration to normal rats mimics hormonal and metabolic changes of obesity. *Endocrinology* **133**, 1753–1758 (1993).
 322. van den Hoek, A. M. *et al.* Intracerebroventricular neuropeptide Y infusion precludes inhibition of glucose and VLDL production by insulin. *Diabetes* **53**, 2529–34 (2004).
 323. Chen, H. L. & Romsos, D. R. A Single Intracerebroventricular Injection of Dexamethasone Elevates Food Intake and Plasma Insulin and Depresses Metabolic Rates

- in Adrenalectomized Obese (ob/ob) Mice. *J. Nutr.* **125**, 540–545 (1995).
324. Chen, H. L. & Romsos, D. R. Dexamethasone rapidly increases hypothalamic neuropeptide Y secretion in adrenalectomized ob/ob mice. <https://doi.org/10.1152/ajpendo.1996.271.1.E151> **271**, (1996).
 325. Walker, H. C. & Romsos, D. R. Glucocorticoids in the CNS regulate BAT metabolism and plasma insulin in ob/ob mice. <https://doi.org/10.1152/ajpendo.1992.262.1.E110> **262**, (1992).
 326. Zakrzewska, K. E. *et al.* Induction of obesity and hyperleptinemia by central glucocorticoid infusion in the rat. *Diabetes* **48**, (1999).
 327. Cusin, I., Rouru, J. & Rohner-Jeanrenaud, F. Intracerebroventricular glucocorticoid infusion in normal rats: Induction of parasympathetic-mediated obesity and insulin resistance. *Obes. Res.* **9**, (2001).
 328. Veyrat-Durebex, C. *et al.* Central Glucocorticoid Administration Promotes Weight Gain and Increased 11 β -Hydroxysteroid Dehydrogenase Type 1 Expression in White Adipose Tissue. *PLoS One* **7**, e34002 (2012).
 329. Yi, C. X. *et al.* Glucocorticoid signaling in the arcuate nucleus modulates hepatic insulin sensitivity. *Diabetes* **61**, 339–345 (2012).
 330. Sefton, C. *et al.* Elevated Hypothalamic Glucocorticoid Levels Are Associated With Obesity and Hyperphagia in Male Mice. *Endocrinology* **157**, 4257–4265 (2016).
 331. Sefton, C. *et al.* Metabolic Abnormalities of Chronic High-Dose Glucocorticoids Are Not Mediated by Hypothalamic AgRP in Male Mice. *Endocrinology* **160**, 964–978 (2019).
 332. Wray, J. R. *et al.* Global transcriptomic analysis of the arcuate nucleus following chronic glucocorticoid treatment. *Mol. Metab.* **26**, 5–17 (2019).
 333. Beaulieu-Bayne, E., Cardoso, M., Kim, H., Yang, S. & Yue, J. T. 104-OR: Glucoregulatory Effects of Hypothalamic Glucocorticoid Action In Vivo. *Diabetes* **68**, 104-OR (2019).
 334. Beaulieu-Bayne, E. *Glucocorticoid Action in the Mediobasal Hypothalamus Regulates Glucose Production In Vivo.* (2019). doi:10.7939/R3-EAHB-A894
 335. Lamia, K. A. *et al.* Cryptochromes mediate rhythmic repression of the glucocorticoid receptor. *Nat. 2011 4807378* **480**, 552–556 (2011).
 336. Cuevas-Ramos, D. & Fleseriu, M. Treatment of Cushing’s disease: a mechanistic update. *J. Endocrinol.* **223**, R19–R39 (2014).
 337. Ho, S. W. *et al.* Effects of 17-allylamino-17-demethoxygeldanamycin (17-AAG) in transgenic mouse models of frontotemporal lobar degeneration and Alzheimer’s disease. *Transl. Neurodegener.* **2**, 24 (2013).
 338. Zuo, Y. *et al.* Inhibition of heat shock protein 90 by 17-AAG reduces inflammation via P2X7 receptor/NLRP3 inflammasome pathway and increases neurogenesis after subarachnoid hemorrhage in mice. *Front. Mol. Neurosci.* **11**, 401 (2018).
 339. Wang, H., Lu, M., Yao, M. & Zhu, W. Effects of treatment with an Hsp90 inhibitor in tumors based on 15 phase II clinical trials. *Mol. Clin. Oncol.* **5**, 326–334 (2016).
 340. Li, R. J. W. *et al.* Nutrient infusion in the dorsal vagal complex controls hepatic lipid and glucose metabolism in rats. *iScience* **24**, 102366 (2021).
 341. Abraham, M. A., Rasti, M., Bauer, P. V. & Lam, T. K. T. Leptin enhances hypothalamic lactate dehydrogenase A (LDHA)–dependent glucose sensing to lower glucose production in high-fat–fed rats. *J. Biol. Chem.* **293**, 4159–4166 (2018).
 342. Johnston, T. P. & Palmer, W. K. Mechanism of poloxamer 407-induced

- hypertriglyceridemia in the rat. *Biochem. Pharmacol.* **46**, 1037–1042 (1993).
343. Folch, J., Lees, M. & Sloane Stanley, G. H. A simple method for the isolation and purification of total lipides from animal tissues. *J. Biol. Chem.* **226**, 497–509 (1957).
344. Eggers, L. F. & Schwudke, D. Liquid Extraction: Folch. *Encycl. lipidomics* 1–6 (2016). doi:10.1007/978-94-007-7864-1_89-1
345. Livak, K. J. & Schmittgen, T. D. Analysis of relative gene expression data using real-time quantitative PCR and the 2- $\Delta\Delta$ CT method. *Methods* **25**, 402–408 (2001).
346. Bhupathiraju, S. N. & Hu, F. B. Epidemiology of obesity and diabetes and their cardiovascular complications. *Circ. Res.* **118**, 1723–1735 (2016).
347. Government of Canada. Obesity in Canada – Health and economic implications - Canada.ca. Available at: <https://www.canada.ca/en/public-health/services/health-promotion/healthy-living/obesity-canada/health-economic-implications.html>. (Accessed: 27th January 2022)
348. Diraison, F. & Beylot, M. Role of human liver lipogenesis and reesterification in triglycerides secretion and in FFA reesterification. *Am. J. Physiol. - Endocrinol. Metab.* **274**, (1998).
349. De Silva, H. V., Mas-Oliva, J., Taylor, J. M. & Mahley, R. W. Identification of apolipoprotein B-100 low density lipoproteins, apolipoprotein B-48 remnants, and apolipoprotein E-rich high density lipoproteins in the mouse. *J. Lipid Res.* **35**, 1297–1310 (1994).
350. Lehner, R. & Vance, D. E. Cloning and expression of a cDNA encoding a hepatic microsomal lipase that mobilizes stored triacylglycerol. *Biochem. J.* **343**, 1–10 (1999).
351. Chung, B. H., Wilkinson, T., Geer, J. C. & Segrest, J. P. Preparative and quantitative isolation of plasma lipoproteins: rapid, single discontinuous density gradient ultracentrifugation in a vertical rotor. *J. Lipid Res.* **21**, 284–291 (1980).
352. Hidaka, H. *et al.* Apolipoprotein B-48 analysis by high-performance liquid chromatography in VLDL: a sensitive and rapid method. *Clin. Chim. Acta.* **189**, 287–296 (1990).
353. Beghin, L. *et al.* Measurement of apolipoprotein B concentration in plasma lipoproteins by combining selective precipitation and mass spectrometry. *J. Lipid Res.* **41**, 1172–1176 (2000).
354. Otvos, J. D., Jeyarajah, E. J., Bennett, D. W. & Krauss, R. M. Development of a Proton Nuclear Magnetic Resonance Spectroscopic Method for Determining Plasma Lipoprotein Concentrations and Subspecies Distributions from a Single, Rapid Measurement. *Clin. Chem.* **38**, 1632–1638 (1992).
355. Coutard, M., Duval, D. & Osborne-Pellegrin, M. J. In vivo competitive autoradiographic study of [3H]corticosterone and [3H]aldosterone binding sites within mouse brain hippocampus. *J. Steroid Biochem.* **28**, 29–34 (1987).
356. McEwen, B. S., Weiss, J. M. & Schwartz, L. S. Selective retention of corticosterone by limbic structures in rat brain. *Nature* **220**, 911–912 (1968).
357. McEwen, B. S., Weiss, J. M. & Schwartz, L. S. Uptake of corticosterone by rat brain and its concentration by certain limbic structures. *Brain Res.* **16**, 227–241 (1969).
358. Gerlach, J. L. & McEwen, B. S. Rat brain binds adrenal steroid hormone: radioautography of hippocampus with corticosterone. *Science* **175**, 1133–1136 (1972).
359. de Kloet, R., Wallach, G. & McEwen, B. S. Differences in corticosterone and dexamethasone binding to rat brain and pituitary. *Endocrinology* **96**, 598–609 (1975).

360. Ono, H. *et al.* Activation of hypothalamic S6 kinase mediates diet-induced hepatic insulin resistance in rats. *J. Clin. Invest.* **118**, 2959–2968 (2008).
361. Thaler, J. P. *et al.* Obesity is associated with hypothalamic injury in rodents and humans. *J. Clin. Invest.* **122**, 153–162 (2012).
362. Gelling, R. W. *et al.* Insulin action in the brain contributes to glucose lowering during insulin treatment of diabetes. *Cell Metab.* **3**, 67–73 (2006).
363. Könnner, A. C. *et al.* Insulin Action in AgRP-Expressing Neurons Is Required for Suppression of Hepatic Glucose Production. *Cell Metab.* **5**, 438–449 (2007).
364. Pocal, A. *et al.* Hypothalamic KATP channels control hepatic glucose production. *Nat. 2005 4347036* **434**, 1026–1031 (2005).
365. Wang, J. *et al.* Overfeeding Rapidly Induces Leptin and Insulin Resistance. *Diabetes* **50**, 2786–2791 (2001).
366. Chari, M., Lam, C. K. L., Wang, P. Y. T. & Lam, T. K. T. Activation of Central Lactate Metabolism Lowers Glucose Production in Uncontrolled Diabetes and Diet-Induced Insulin Resistance. *Diabetes* **57**, 836–840 (2008).
367. Cote, C. D. *et al.* Resveratrol activates duodenal Sirt1 to reverse insulin resistance in rats through a neuronal network. *Nat. Med.* **21**, 498–507 (2015).
368. Scherer, T. *et al.* Short Term Voluntary Overfeeding Disrupts Brain Insulin Control of Adipose Tissue Lipolysis *. *J. Biol. Chem.* **287**, 33061–33069 (2012).
369. Jackman, M. R., Kramer, R. E., MacLean, P. S. & Bessesen, D. H. Trafficking of dietary fat in obesity-prone and obesity-resistant rats. *Am. J. Physiol. - Endocrinol. Metab.* **291**, 1083–1091 (2006).
370. Kraegen, E. W. *et al.* Development of muscle insulin resistance after liver insulin resistance in high-fat-fed rats. *Diabetes* **40**, 1397–1403 (1991).
371. Panasevich, M. R. *et al.* Gut microbiota are linked to increased susceptibility to hepatic steatosis in low-aerobic-capacity rats fed an acute high-fat diet. *Am. J. Physiol. - Gastrointest. Liver Physiol.* **311**, G166–G179 (2016).
372. Jin, E. S., Beddow, S. A., Malloy, C. R. & Samuel, V. T. Hepatic glucose production pathways after three days of a high-fat diet. *Metabolism* **62**, 152–162 (2013).
373. Levin, B. E., Triscari, J. & Sullivan, A. C. Altered sympathetic activity during development of diet-induced obesity in rat. <https://doi.org/10.1152/ajpregu.1983.244.3.R347> **13**, (1983).
374. Morris, E. M. *et al.* Intrinsic aerobic capacity impacts susceptibility to acute high-fat diet-induced hepatic steatosis. *Am. J. Physiol. - Endocrinol. Metab.* **307**, 355–364 (2014).
375. Savage, D. B. *et al.* Reversal of diet-induced hepatic steatosis and hepatic insulin resistance by antisense oligonucleotide inhibitors of acetyl-CoA carboxylases 1 and 2. *J. Clin. Invest.* **116**, 817–824 (2006).
376. Samuel, V. T. *et al.* Mechanism of Hepatic Insulin Resistance in Non-alcoholic Fatty Liver Disease *. *J. Biol. Chem.* **279**, 32345–32353 (2004).
377. Yin, Y. *et al.* Vitamin D attenuates high fat diet-induced hepatic steatosis in rats by modulating lipid metabolism. *Eur. J. Clin. Invest.* **42**, 1189–1196 (2012).
378. Harriman, G. *et al.* Acetyl-CoA carboxylase inhibition by ND-630 reduces hepatic steatosis, improves insulin sensitivity, and modulates dyslipidemia in rats. *Proc. Natl. Acad. Sci. U. S. A.* **113**, E1796–E1805 (2016).
379. Berger, J. P., Akiyama, T. E. & Meinke, P. T. PPARs: therapeutic targets for metabolic disease. *Trends Pharmacol. Sci.* **26**, 244–251 (2005).

380. Smith, B. K. *et al.* Treatment of nonalcoholic fatty liver disease: Role of AMPK. *Am. J. Physiol. - Endocrinol. Metab.* **311**, E730–E740 (2016).
381. Groop, L. C. *et al.* Glucose and free fatty acid metabolism in non-insulin-dependent diabetes mellitus. Evidence for multiple sites of insulin resistance. *J. Clin. Invest.* **84**, 205–213 (1989).
382. Groop, L. C. *et al.* The Role of Free Fatty Acid Metabolism in the Pathogenesis of Insulin Resistance in Obesity and Noninsulin-Dependent Diabetes Mellitus. *J. Clin. Endocrinol. Metab.* **72**, 96–107 (1991).
383. Roust, L. R. & Jensen, M. D. Postprandial Free Fatty Acid Kinetics Are Abnormal in Upper Body Obesity. *Diabetes* **42**, 1567–1573 (1993).
384. Mittendorfer, B., Magkos, F., Fabbrini, E., Mohammed, B. S. & Klein, S. Relationship Between Body Fat Mass and Free Fatty Acid Kinetics in Men and Women. *Obesity* **17**, 1872–1877 (2009).
385. Boden, G., Cheung, P., Peter Stein, T., Kresge, K. & Mozzoli, M. FFA cause hepatic insulin resistance by inhibiting insulin suppression of glycogenolysis. *Am. J. Physiol. - Endocrinol. Metab.* **283**, 12–19 (2002).
386. Boden, G., Chen, X., Ruiz, J., White, J. V. & Rossetti, L. Mechanisms of fatty acid-induced inhibition of glucose uptake. *J. Clin. Invest.* **93**, 2438–2446 (1994).
387. Boden, G. Fatty acid-induced inflammation and insulin resistance in skeletal muscle and liver. *Curr. Diab. Rep.* **6**, 177–181 (2006).
388. Meijer, O. C., Buurstede, J. C. & Schaaf, M. J. M. Corticosteroid Receptors in the Brain: Transcriptional Mechanisms for Specificity and Context-Dependent Effects. *Cell. Mol. Neurobiol.* **2018 394** **39**, 539–549 (2018).
389. Madalena, K. M. & Lerch, J. K. The effect of glucocorticoid and glucocorticoid receptor interactions on brain, spinal cord, and glial cell plasticity. *Neural Plast.* **2017**, (2017).
390. Pacák, K. & Palkovits, M. Stressor Specificity of Central Neuroendocrine Responses: Implications for Stress-Related Disorders. *Endocr. Rev.* **22**, 502–548 (2001).
391. Muroya, S., Yada, T., Shioda, S. & Takigawa, M. Glucose-sensitive neurons in the rat arcuate nucleus contain neuropeptide Y. *Neurosci. Lett.* **264**, 113–116 (1999).
392. Fioramonti, X. *et al.* Characterization of Glucosensing Neuron Subpopulations in the Arcuate Nucleus. *Diabetes* **56**, 1219–1227 (2007).
393. Ferenczi, S., Zelei, E., Pintér, B., Szoke, Z. & Kovács, K. J. Differential regulation of hypothalamic neuropeptide Y hnRNA and mRNA during psychological stress and insulin-induced hypoglycemia. *Mol. Cell. Endocrinol.* **321**, 138–145 (2010).
394. Shimizu, H. *et al.* Glucocorticoids increase neuropeptide Y and agouti-related peptide gene expression via adenosine monophosphate-activated protein kinase signaling in the arcuate nucleus of rats. *Endocrinology* **149**, 4544–4553 (2008).
395. Shimizu, H. *et al.* Glucocorticoids increase NPY gene expression in the arcuate nucleus by inhibiting mTOR signaling in rat hypothalamic organotypic cultures. *Peptides* **31**, 145–149 (2010).
396. Corder, R. *et al.* Dexamethasone treatment increases neuropeptide Y levels in rat hypothalamic neurones. *Life Sci.* **43**, 1879–1886 (1988).
397. Winkler, Z. *et al.* Hypoglycemia-activated Hypothalamic Microglia Impairs Glucose Counterregulatory Responses. *Sci. Rep.* **9**, 1–14 (2019).
398. Yi, C. X., la Fleur, S. E., Fliers, E. & Kalsbeek, A. The role of the autonomic nervous liver innervation in the control of energy metabolism. *Biochimica et Biophysica Acta -*

- Molecular Basis of Disease* **1802**, 416–431 (2010).
399. La Fleur, S. E., Kalsbeek, A., Wortel, J. & Buijs, R. M. Polysynaptic neural pathways between the hypothalamus, including the suprachiasmatic nucleus, and the liver. *Brain Res.* **871**, 50–56 (2000).
 400. Paeger, L. *et al.* Energy imbalance alters Ca²⁺ handling and excitability of POMC neurons. *Elife* **6**, (2017).
 401. Wilding, J. P. H. *et al.* Increased neuropeptide Y content in individual hypothalamic nuclei, but not neuropeptide Y mRNA, in diet-induced obesity in rats. *J. Endocrinol.* **132**, 299–304 (1992).
 402. Baranowska, B. *et al.* The role of neuropeptides in the disturbed control of appetite and hormone secretion in eating disorders. *Neuroendocrinol. Lett.* **24**, 240603–240610 (2003).
 403. Sadari, N. *et al.* NPY and VGF Immunoreactivity Increased in the Arcuate Nucleus, but Decreased in the Nucleus of the Tractus Solitarius, of Type-II Diabetic Patients. *PLoS One* **7**, e40070 (2012).
 404. Van Den Hoek, A. M. *et al.* Intracerebroventricular Administration of Neuropeptide Y Induces Hepatic Insulin Resistance via Sympathetic Innervation. *Diabetes* **57**, 2304–2310 (2008).
 405. Schlein, C. *et al.* FGF21 Lowers Plasma Triglycerides by Accelerating Lipoprotein Catabolism in White and Brown Adipose Tissues. *Cell Metab.* **23**, 441–453 (2016).
 406. Nagy, C. & Einwallner, E. Study of In Vivo Glucose Metabolism in High-fat Diet-fed Mice Using Oral Glucose Tolerance Test (OGTT) and Insulin Tolerance Test (ITT). *J. Vis. Exp.* **2018**, 56672 (2018).
 407. Freinkel, N. & Metzger, B. E. Oral Glucose Tolerance Curve and Hypoglycemias in the Fed State. *N. Engl. J. Med.* **280**, 820–828 (1969).
 408. Birrenkott, G. P. & Wiggins, M. E. Determination of Dexamethasone and Corticosterone Half-Lives in Male Broilers. *Poult. Sci.* **63**, 1064–1068 (1984).
 409. He, Y. *et al.* Structures and mechanism for the design of highly potent glucocorticoids. *Cell Res.* **2014** *246* **24**, 713–726 (2014).
 410. Bledsoe, R. K. *et al.* Crystal Structure of the Glucocorticoid Receptor Ligand Binding Domain Reveals a Novel Mode of Receptor Dimerization and Coactivator Recognition. *Cell* **110**, 93–105 (2002).
 411. Cirulli, F., van Oers, H., De Kloet, E. R. & Levine, S. Differential influence of corticosterone and dexamethasone on schedule-induced polydipsia in adrenalectomized rats. *Behav. Brain Res.* **65**, 33–39 (1994).
 412. Cadepond, F., Ulmann, A. & Baulieu, E. E. RU486 (MIFEPRISTONE): Mechanisms of Action and Clinical Uses. *Annu. Rev. Med.* **48**, 129–156 (1997).
 413. Moguilewsky, M. & Philibert, D. RU 38486: Potent antiglucocorticoid activity correlated with strong binding to the cytosolic glucocorticoid receptor followed by an impaired activation. *J. Steroid Biochem.* **20**, 271–276 (1984).
 414. Heikinheimo, O., Kekkonen, R. & Lähteenmäki, P. The pharmacokinetics of mifepristone in humans reveal insights into differential mechanisms of antiprogesterin action. *Contraception* **68**, 421–426 (2003).
 415. Song, L. N., Coghlan, M. & Gelmann, E. P. Antiandrogen Effects of Mifepristone on Coactivator and Corepressor Interactions with the Androgen Receptor. *Mol. Endocrinol.* **18**, 70–85 (2004).
 416. Brogden, R. N., Goa, K. L. & Faulds, D. Mifepristone. *Drugs* **1993** *453* **45**, 384–409

- (1993).
417. National Center for Advancing Translational Sciences. Mifepristone. *Inxight: Drugs* Available at: <https://drugs.ncats.io/drug/320T6RNW1F>. (Accessed: 22nd December 2021)
 418. Oskari, H. *et al.* Plasma concentrations and receptor binding of RU 486 and its metabolites in humans. *J. Steroid Biochem.* **26**, 279–284 (1987).
 419. Romano, G. J., Krust, A. & Pfaff, D. W. Expression and Estrogen Regulation of Progesterone Receptor mRNA in Neurons of the Mediobasal Hypothalamus: An in Situ Hybridization Study. *Mol. Endocrinol.* **3**, 1295–1300 (1989).
 420. Francis, K., Meddle, S. L., Bishop, V. R. & Russell, J. A. Progesterone receptor expression in the pregnant and parturient rat hypothalamus and brainstem. *Brain Res.* **927**, 18–26 (2002).
 421. Walters, K. A. *et al.* The Role of Central Androgen Receptor Actions in Regulating the Hypothalamic-Pituitary-Ovarian Axis. *Neuroendocrinology* **106**, 389–400 (2018).
 422. Wu, D., Lin, G. & Gore, A. C. Age-related changes in hypothalamic androgen receptor and estrogen receptor α in male rats. *J. Comp. Neurol.* **512**, 688–701 (2008).
 423. Olster, D. H. & Blaustein, J. D. Immunocytochemical colocalization of progestin receptors and β -endorphin or enkephalin in the hypothalamus of female guinea pigs. *J. Neurobiol.* **21**, 768–780 (1990).
 424. Warembourg, M. Uptake of 3H labeled synthetic progestin by rat brain and pituitary. A radioautography study. *Neurosci. Lett.* **9**, 329–332 (1978).
 425. Issar, M., Sahasranaman, S., Buchwald, P. & Hochhaus, G. Differences in the glucocorticoid to progesterone receptor selectivity of inhaled glucocorticoids. *Eur. Respir. J.* **27**, 511–516 (2006).
 426. Syms, A. J., Norris, J. S. & Smith, R. G. Androgen stimulated elevation in androgen receptor levels is inhibited by the synthetic glucocorticoid triamcinolone acetonide. *Biochem. Biophys. Res. Commun.* **116**, 1020–1025 (1983).
 427. Maruyama, S. & Sato, S. Binding of glucocorticoid to the androgen receptor of mouse submandibular glands. *J. Endocrinol.* **106**, 329–335 (1985).
 428. Grenert, J. P. *et al.* The amino-terminal domain of heat shock protein 90 (hsp90) that binds geldanamycin is an ATP/ADP switch domain that regulates hsp90 conformation. *J. Biol. Chem.* **272**, 23843–23850 (1997).
 429. Waza, M. *et al.* Modulation of Hsp90 function in neurodegenerative disorders: A molecular-targeted therapy against disease-causing protein. *J. Mol. Med.* **84**, 635–646 (2006).
 430. Bharadwaj, S., Ali, A. & Ovsenek, N. Multiple Components of the HSP90 Chaperone Complex Function in Regulation of Heat Shock Factor 1 In Vivo. *Mol. Cell. Biol.* **19**, 8033–8041 (1999).
 431. Zou, J., Guo, Y., Guettouche, T., Smith, D. F. & Voellmy, R. Repression of Heat Shock Transcription Factor HSF1 Activation by HSP90 (HSP90 Complex) that Forms a Stress-Sensitive Complex with HSF1. *Cell* **94**, 471–480 (1998).
 432. Fang, Y., Fliss, A. E., Robins, D. M. & Caplan, A. J. Hsp90 regulates androgen receptor hormone binding affinity in vivo. *J. Biol. Chem.* **271**, 28697–28702 (1996).
 433. Smith, D. F. *et al.* Progesterone receptor structure and function altered by geldanamycin, an hsp90-binding agent. *Mol. Cell. Biol.* **15**, 6804–6812 (1995).
 434. Picard, D. Heat-shock protein 90, a chaperone for folding and regulation. *Cell. Mol. Life Sci. C. 2002 5910* **59**, 1640–1648 (2002).

435. Tatokoro, M., Koga, F., Yoshida, S. & Kihara, K. Heat shock protein 90 targeting therapy: state of the art and future perspective. *EXCLI J.* **14**, 48 (2015).
436. Henstridge, D. C., Whitham, M. & Febbraio, M. A. Chaperoning to the metabolic party: The emerging therapeutic role of heat-shock proteins in obesity and type 2 diabetes. *Mol. Metab.* **3**, 781–793 (2014).
437. Lee, J. H. *et al.* Heat shock protein 90 (HSP90) inhibitors activate the heat shock factor 1 (HSF1) stress response pathway and improve glucose regulation in diabetic mice. *Biochem. Biophys. Res. Commun.* **430**, 1109–1113 (2013).
438. Jing, E. *et al.* Hsp90 β knockdown in DIO mice reverses insulin resistance and improves glucose tolerance. *Nutr. Metab.* **15**, 1–10 (2018).
439. Ou, J. R., Tan, M. S., Xie, A. M., Yu, J. T. & Tan, L. Heat shock protein 90 in Alzheimer's disease. *Biomed Res. Int.* **2014**, (2014).
440. Kishore, L., Kajal, A. & Kaur, N. Role of Nicotinamide in Streptozotocin Induced Diabetes in Animal Models. *J Endocrinol Thyroid Res* **2**, 1–4 (2017).
441. Szkudelski, T. Minireview Streptozotocin-nicotinamide-induced diabetes in the rat. Characteristics of the experimental model. *Exp. Biol. Med.* **237**, 481–490 (2012).
442. Yue, J. T. Y. *et al.* Inhibition of glycine transporter-1 in the dorsal vagal complex improves metabolic homeostasis in diabetes and obesity. *Nat. Commun.* **7**, 13501 (2016).
443. Duca, F. A. *et al.* Metformin activates a duodenal Ampk-dependent pathway to lower hepatic glucose production in rats. (2015). doi:10.1038/nm.3787
444. Chan, G. N. Y. *et al.* In vivo induction of P-glycoprotein expression at the mouse blood–brain barrier: an intracerebral microdialysis study. *J. Neurochem.* **127**, 342–352 (2013).
445. Carey, M., Kehlenbrink, S. & Hawkins, M. Evidence for Central Regulation of Glucose Metabolism. *J. Biol. Chem.* **288**, 34981–34988 (2013).
446. Kishore, P. *et al.* Activation of K(ATP) channels suppresses glucose production in humans. *J. Clin. Invest.* **121**, 4916–20 (2011).
447. Prigeon, R. L., Quddusi, S., Paty, B. & D'Alessio, D. A. Suppression of glucose production by GLP-1 independent of islet hormones: A novel extrapancreatic effect. *Am. J. Physiol. - Endocrinol. Metab.* **285**, 701–707 (2003).
448. Takahashi, A. & Shimazu, T. Hypothalamic regulation of lipid metabolism in the rat: Effect of hypothalamic stimulation on lipolysis. *J. Auton. Nerv. Syst.* **4**, 195–206 (1981).
449. Singh, G., Krauthamer, M. & Bjälme-Evans, M. Wegovy (semaglutide): a new weight loss drug for chronic weight management. *J. Investig. Med.* **0**, jim-2021-001952 (2021).
450. Brashier, D. B. S., Sharma, A. K., Dahiya, N., Singh, S. K. & Khadka, A. Lorcaserin: A novel antiobesity drug. *J. Pharmacol. Pharmacother.* **5**, 175–178 (2014).
451. Popoli, M., Yan, Z., McEwen, B. S. & Sanacora, G. The stressed synapse: the impact of stress and glucocorticoids on glutamate transmission. *Nat. Rev. Neurosci.* **13**, 22 (2012).